CZECH UNIVERSITY OF LIFE SCIENCES PRAGUE
FACULTY OF ENVIRONMENTAL SCIENCES

DEPARTMENT OF ENVIRONMENTAL GEOSCIENCES

MASTER THESIS

Mobility and biogeochemical cycling of selected major base cations (Mg, K, Ca) and toxic metals (Ni, Cr) in serpentinite-dominated ecosystem: Pluhův Bor, Slavkov Forest, Czech Republic

Author: Mgr. Anna Pereponova
Supervisor: doc. Mgr. Juraj Farkaš, Ph.D.

Co-supervisor: RNDr. Pavel Krám, Ph.D.

Prague 2014

CZECH UNIVERSITY OF LIFE SCIENCES PRAGUE

Department of Environmental Geosciences
Faculty of Environmental Sciences

DIPLOMA THESIS ASSIGNMENT

Pereponova Anna

Thesis title

Mobility and bio-geochemical cycling of nickel (Ni) during weathering processes in sensitive forest ecosystem

Objectives of thesis

This project will focus on the quantification of natural weathering fluxes of toxic Ni and Cr within the sensitive forest ecosystem environment, developed on naturally Ni-rich bedrock composed of serpentinites (i.e. Mg and Ni rich igneous rocks) at the study site of the Slavkov Forest (Pluhuv Bor, CZ). Within the project we will investigate changes in Ni and Cr concentrations as a function of depth, throughout a complete weathering profile (i.e. regolith), using samples of soil profiles but also recently recovered drill core material reaching depths up to 30 meters below the surface. These unique sample materials will allow to study the dynamics of the studied elements release from rocks during weathering and it subsequent uptake by plants and vegetation, and its deposition/mobilization within the organic-rich and mineral soils.

Methodology

In terms of methods, this project will employ state-of-the-art facilities such as the metal-free geochemical laboratories used for sample digestion and preparation (at CGS), and modern analytical instrumentation such as ICP-OES, available at KGEV, CZU. Specifically, we will normalize the concentration of Ni and Cr measured in rock/soil/organic samples to an immobile element such as zirconium (Zr) or titanium (Ti) which will allow us to quantify the rates of release of toxic Ni and Cr to the soil system and vegetation pools at our study site. These results, in turn, will have implications for our understanding of the biogeochemical cycle of Ni and Cr in the environment and the negative effects of their toxicity for the growth and overall health of the local forest ecosystem (composted mostly of Norwegian spruce, and oak species).

Schedule for processing

January - February 2013: Study of references and literature
March - April 2013: Examination of the drill core, and preparation of IGA proposal
May - September 2013: Data collection and laboratory work
October - December 2013: Data analysis, modeling, and Thesis write up
Thesis submission April 2014

The proposed extent of the thesis

Anticipated extent of this Master thesis is set at about 50 pages of the written text.

Keywords

nickel, mobility, biogeochemistry, weathering, forest ecosysetm

Recommended information sources

Krám, P., Oulehle, F., Štedrá V., Hruška, J., Shanley, J.B., Minocha, R., and Traister E. (2008) Geoecology of a forested watershed underlain by serpentinite in Central Europe. Northeastern Naturalist, 16, 309-328.

Burton, K.W., Morgan, E. (1983) The influence of heavy metals upon the growth of sitka-spruce in South Wales forests, I. Upper critical and foliar concentrations. Plant and Soil, Vol. 73, 327-336.

Hruška J. and Krám P. (2003) Modelling long-term changes in stream water and soil chemistry in catchments with contrasting vulnerability to acidification (Lysina and Pluhuv Bor, Czech Republic). Hydrology and Earth System Sciences 7, 525-539.

The Diploma Thesis Supervisor

Farkaš Juraj, doc. Mgr., Ph.D.

Thesis Consultant

Dr. Pavel Kram

Electronic approval: January 21. 2014

Electronic approval: January 22. 2014

Head of the Department

Dean

Declaration

I hereby certify that work presented in this thesis and entitled as "*Mobility and biogeochemical cycling of selected major base cations (Mg, Ca) and toxic metals (Ni, Cr) in serpentinite-dominated ecosystem: Pluhuv Bor, Slavkov Forest, Czech Republic*", is, to the best of my knowledge and belief, original, and that the material has not been submitted, either in whole or in part, for a degree at this or any other university. The literature and other sources, which I used, are stated list of references, which are attached to this work.

Prague, 23th of April   Anna Pereponova

Aknowledgement

I would like to express my deepest gratitude to doc. Mgr. Juraj Farkaš, Ph.D., my research supervisor, and co-supervisor RNDr. Pavel Krám, Ph.D, for their patient guidance, enthusiastic encouragement and useful critiques during my work. I would like to express my great appreciation to Mgr. Veronika Štědrá, Ph.D, for her highly professional help with petrological and mineralogical analysis. My grateful thanks are also extended to Ing. Hana Šillerová, Ph.D. for her advice and assistance in proceeding the ICP-OES analysis of the samples.

I would also like to extend my thanks to the technicians of the laboratory of the department of Environmental Geochemistry at the Czech University of Life Sciences, as well as of the laboratories of the Czech Geological Survey for providing the opportunity to use their equipment and facilities for running my experimental work.

I would like to thank the members of the study department of my faculty, especially Ing. Lukáš Pospíšil, Kumble Petr, Ph.D., Ing. Molnárová Kristina, Ph.D. and Ing. Helena Michálková for their invaluable help in organizational questions during my studies at CULS and their patience.

I would like to aknowledge the support given by the Internal Grant Agency of the Czech University of Life Sciences as a part of the grant project (KGEV 42400/1312/3177). Also, during the course of the work I was partly supported by the founding of European Commission Project (FP7 SoilTrEC 244118). I am grateful for the opportunity to participate in this project, get to knowledge while doing my practical work and for the chance to make my input into its' developement

Finally, I wish to thank my parents, my friends and my groupmates for their great support and encouragement throughout my study.

Abstract

This study was intended as a contribution towards better understanding of a coupled chemical, biological, physical, and geological processes within the Crtical Zone, operating together to support life at the Earth's surface (Brantley et al., 2007). The primary goal was to better quantify the mobility and biogeochemical pathways of three major base cations (Ca, Mg, K) and selected toxic metals (Ni, Cr) during weathering, soil formation processes and biological uptake in a forested serpentinite catchment of Pluhův Bor, Slavkov Forest, Czech Republic (Krám et al., 2009). Specfically we analyzed by ICP-OES elemental compositions from complete weathering profle, reaching the depth of 26.14 meters below the surface, which was recovered by scientific drilling under the European 'SoilTrEC' project (http://www.soiltrec.eu/).

A simple normalization approach (i.e., tau-parameterization) was used to quantify the dynamics of elemental release/accumulation during weathering processes and biological uptake, with titanium used as an immobile element, to generate 'normalized concentration profiles' as a function of the depth (Brantley et al., 2007). It was expected that elemental regolith profiles of Ca and Mg and K, which are major nutrients, would exhibit typical biogenic or depletion-enrichment, whereas Ni and Cr, as typical toxic metals were expected to show depletion profiles.

The results of our elemental analysis confrmed, in agreement with the prevous visual examination of the drill-core, that there are major lithological changes with the depth: ranging from serpentinite, through tremolite schist to amphibolite and actinolite schist. Hence, the Tau - normalization approach needed to be used only to the monolithological (serpentinitic) upper part of the drill core, which however covered only the upper 5.6 meters. Results from this part of the core showed *depletion-enrichment* profiles for Ca and K, as expected, however for Mg shows, surprisingly depletion profile. This points to significant decoupling of biogeochemical cycling of Ca and Mg in our settings. As to the Ni and Cr profiles, these shows indications of enrichment trend in the

deeper part up to three meters below the surface, but closer to the surface, both of the toxic metals show strong depletion trends, indicating their high mobility. Also strong coupling of Ni and Cr was observed along the entire weathering profile in agreement with previous studies(Suzuki, et al., 1971).

The approach, described here, allowed to quintify the losses and gains of the above elements at the study site and implications are discussed for the cycling of these nutrients and the toxic metals for the forest ecosystem studies and weathering processes.

Key words: weathering, soil, profile, regolith, ultramafic rocks, mafic rocks, transport

Abstrakt

Tato studie přispívá k pochopení interakcí mezi chemickými, biologickými, fyzikálními a geologickými procesy, které probíhají v rámci "kritické zóny" na zemském povrchu (Brantley et al. 2007). Primárním cílem byla kvantifikace mobility biogeochemických cyklů hlavních bazických kationů (Ca, Mg, K) a vybraných toxických kovů (Ni, Cr) v průběhu zvětrávání, tvorby půdního profilu a biologických procesů v rámci lesního ekosystému na serpentinickém (hadcovém) podloží na lokalitě Pluhův Bor, Slavkovský Les v České Republice (Kram et al. 2009). Tato studie analyzovala s pomocí ICP-OES koncentrace vybraných prvků z kompletního zvětrávacího profilu, který dosahuje hloubky 26.14 metrů pod povrch, a který byl vzorkovaný díky vědeckému vrtu v rámci evropského projektu SoilTrEC (http://www.soiltrec.eu/).

Kvantifikace dynamiky akumulace a odnosu (t.j. vyluhovaní) vybraných prvků v průběhu zvětrávání a biologických procesů byla realizována pomocí jednoduchého "normalizačního principu", takzvané "tau-normalizace", kde byl použit nemobilní prvek Titan (Ti) jako reference (Brantley et al. 2007). Očekávalo se, že zvětrávací (regolit) profily prvků Ca, Mg a K budou mít typicky "biologický profil", a naopak toxické prvky jako Ni a Cr budou vykazovat typicky "ochuzený profil".

Koncentrační profily vybraných prvků (Ca, Mg, K, Ni, Cr) nám potvrdili, že v rámci vrtu (0 až 26.14 metrů) dochází k hlavním litologickým změnám s hloubkou; a horniny které jsou zastoupené v našem zvětrávacím profilu jsou: *serpentinity (hadec), amfibolity, tremolitové a aktinolitové břidlice.* Z důvodu změny litologie s hloubkou jsme mohli použít pro náš "tau-normalizovaný" přístup jen nejvyšší část vrtu (t.j. 0 až 5.6 metrů), která je dominovaná serpentinitem. Výsledky z této mono-litologické části zvětrávacího profilu (vrtu) ukázali, že biologicky aktivní prvky jako Ca a K vykazují typické "biologické" nebo "ochuzené-obohacené" profily, avšak trend Mg překvapivě ukázal "ochuzený" profil. Tyto výsledky dokazují, že v našem zvětrávacím/lesním systému dochází k výraznému rozdělení biogeochemických cyklů hlavních bazických kationtů Ca a Mg. Co se týká Ni a Cr, tyto prvky vykazují znaky obohacení v hlubších částech zvětrávacího profilu (cca 3 metry pod povrchem), ale blíže k povrchu oba prvky vykazují výrazně "ochuzené"

trendy, které potvrzují vysoku mobilitu Ni a Cr v průběhu zvětrávání. Rovněž jsme pozorovali silnou korelaci mezi koncentracemi Ni a Cr napříč celým zvětrávacím profilem, v souladu s předešlými studiemi (Suzuki et al., 1971).

Závěrem, postup prezentovaný v této studii nám umožnil kvantifikovat ztráty a zisky vybraných prvků (Ca, Mg, K, Ni, Cr) v rámci zvětrávacího profilu na naší lokalitě. Tyto informace jsou důležité pro biogeochemický cyklus výše uvedených bazických a toxických prvků ve studovaném lesním ekosystému.

Klíčová slova: zvětrávání, půda, profil, regolit, ultramafické horniny, transport

Content

Introduction

It is well-known (Anderson & Humphrey, 1989, Anderson et al., 2002, Brantley et al, 2007), that the existence and cycling of all elements and substances within and in between the geological layers is highly *interconnected*, forming so-called "Critical zone", which serves as an "engine" that determines the life conditions for the flora and, consequently, the fauna of the corresponding site. In addition

Special attention should be turned on elements, which are major nutrients (and are usually abundant) or elements which are toxic and may play crucial role even though are present in very small amounts (such as trace metals).

Naturally base-poor forests are particularly sensitive to environmental perturbations including phenomena such as anthropogenic input of acid compounds, contamination of forest soils by toxic metals, and/or excessive timber harvesting. Human-induced processes accelerate the export of base cations from the ecosystem, causing acidification and degradation of soils, which in turn have negative influence on the overall health and productivity of the affected forest. Temperate coniferous forests developed on naturally highly acid-resistant soil and (Krám et al., 2009), located in the industrialized parts of the Czech Republic, can also reflect the above phenomena and their negative effects. Hence, a better understating of elemental fluxes and biogeochemical cycling of nutrients, as well as the toxic metals, in these forests is of primary importance for sustainable forest management strategies

The current study is a part of a larger project for investigation of mobility and biogeochemical cycling of major base cations and selected toxic metals during weathering processes in two geologically distinctive forest ecosystems of Slavkov Forest, Czech Republic and was co-financed by the Internal Grant Agency (IGA) grant from the Czech University of Life Sciences (KGEV 42400/1312/3177) and the European Commission Project (FP7 SoilTrEC 244118, Menon et al., 2014). It was targeted to systematically examine the mobility and biogeochemical pathways of major base cations (Ca, Mg and K) and selected toxic metals (Ni and Cr), during weathering processes in the geological forest ecosystems located near the town

Marienbad (Mariánské Lázně) in western Bohemia, about 120 km west of Prague. The study site, serpentinite-dominated catchment 'Pluhův Bor', is located in Slavkov Forest, which is a region of a Protected Landscape Area (CHKO Slavkovský les) (Krám et al., 2012). The local bedrock (i.e., serpentinite) is mainly composed of serpentine group minerals ($Mg3Si_2O5(OH)_4$) with occassional occurences of amphibolite, and tremolite/actinolite schists (i.e., silicate minerals and rocks enriched in Ca, Mg, and Fe) (Krám et al., 2009). This complicated geological composition creates specific habitat with an unusual and challenging environment for plant growth which is even more worth to study.

1. Purpose and aims of the study

The scientific project, described in this paper had the target to improve the existing knowledge of the mobility and biogeochemical pathways of major nutrient base cations (Ca, Mg, K) and selected toxic metals (Ni, Cr) with the regard to their involvement into the weathering and bio-processes, namely using the materials from forest ecosystem of the geological environment of a complex mixture of the rock-types of Pluhuv Bor located in the Slavkov Forest, in the Czech Republic.

The main purpose of the experiment was to:

- *generate continuous weathering profiles for the elements*, based on the analysis of elemental concentrations in the samples of rocks/soils that were recently recovered by drill core in *serpentinite-dominated Pluhův Bor*. The scientific drilling at the site was accomplished only recently, in summer 2012, and was funded via the European 'SoilTrEC' project (http://www.soiltrec.eu/, Menon et al., 2014). Drill core reached a depth of up to 28 meters below the surface, and thus the recovered sample materials cover a significant portion of the local 'weathering profile', with potentially well-defined concentration gradients Ni and Cr, controlled by the weathering intensity and biological activity at our sites.

- using the profiles of elemental concentrations, as a function of depth, which, to *quantify the rate of release (or accumulation)* of the specific elements along the weathering profile.

- Use this results *to identify the zone(s) of maximum leaching and/or accumulation* of the element of interest during the weathering and/or biological uptake by forest biomass, which has *implications for possible sources and bio-availability of these elements for the growth of local forest.*

Moreover, the current project was developed in parrallel with a study of a more geologically simple granitic site of the Lysina catchment situated in the

vicinity, and so characterized by similar conditions with the exeption of the different bedrock, which allows to distinguish between the main factors which might determine the particular behavioral characteristics of the elements.

2. Review of literature

3.1. The concept of Critical Zone

3.1.1. The term of Critical zone

To understand the meaning of Critical Zone (CZ) one should refer to the idea that any geological component may play crucial role in formation of a geoecosystem and all the cycles and processes that occur within it. So, scientists have introduced the term of Critical Zone (CZ) to describe the fragile skin of the planet defined from the outer extent of vegetation down to the lower limits of ground water, that supports all life on Earth. Generally speaking, CZ can be broadly defined as a system of coupled chemical, biological, physical, and geological processes, that supply nutrients and energy for the growth and sustenance of the aboveground forest biomass (Brantley et al, 2007). The name comes from the idea that CZ is essential in natural and managed ecosystems, and as the interactions between various processes are widely recognized as critical in understanding the effects of changes in climate, tectonic uplift rates, erosion, (Raymo et al, 1988), landscape evolution (Anderson & Humphrey, 1989), and geochemical cycling.

The strong interplay among these processes makes it difficult to disentangle their interactions in the weathered profile. (Anderson et al., 2002).

The potential feedbacks between erosion and chemical weathering were brought to prominence by the erosion-driven climate change hypothesis. (Raymo et al., 1988, Raymo & Ruddiman, 1992)

Physical weathering processes expose fresh rock and mineral surfaces to chemical weathering, whereas chemical weathering reduces the strength of rock, making it more susceptible to physical breakdown. It also controls landscape evolution due to the balance between removal of debris by transport processes and the breakdown of rock into movable material by weathering, that can run on different rates, which makes it possible to differentiate between weathering-limited (landscapes dominated by bare bedrock) and transport-lomited (landscapes with deep regolith mantles) landscapes. More than that, it has been proved, that the same concepts could be used to explain the evolution of chemical loads of large rivers.

(Stallard, 1985). In addition, it has been observed, that according to recent empirical data, regolith-production rates really declines under increasing soil cover (Heimsath et al., 1999), while, by an alternative model, regolith production reaches a maximum under a particular soil depth and is reduced under both shallower and deeper soil cover (Rosenbloom & Anderson, 1994, Stallard, 1985; Anderson & Humphrey, 1989;).

Chemical reactions proceed both abiotically and through catalysis by organisms, providing nutrients and energy for the sustenance of terrestrial ecosystems. As rocks containing high-temperature mineral assemblages reequilibrate with fluids at the surface, environmental gradients develop. For better understanding the CZ as a sustainable system—a system "that lasts", geologists conceptualize the CZ as a weathering engine or reactor, in which rocks at depth are fractured, ground, dissolved, and bioturbated into transportable materials.

So, as a result, the processes within the weathering engine occurring over variety of timescales combine to produce patterns a the grain (millimeter), clast (centimeter), pedon (meter), landscape (kilometer), and global (thousands of kilometers) scales (Brantley et al. 2007).

A good example to demonstrate this phenomena was described by Anderson et al. (2002) in the study of a headwater catchment in the Oregon Coast Range (US), which shown that solid-phase mass losses due to chemical weathering were equivalent in the bedrock and the soil, even though the long-term rate of mass loss per unit volume of parent rock was greater in the soil than in the rock. The authors explained this by effects of biotic processes in the soil and to hydrologic conditions that maximize contact time and water flux through the mineral matrix in the soil, supporting their idea, firstly, by an earlier work that proved that rock and soil contribute equally to the solute flux, and by new arguments that the basin is in dynamic equilibrium with respect to erosion and uplift.

The finding that the silica flux from the basin was several times larger than from older soils elsewhere, but comparable to the sites with similar physical erosion rates argues that physical denudation or uplift rates are important for setting the chemical denudation rate and can act in different ways in this direction:

-   Limiting chemical evolution by removing material,

thus setting the residence time within the weathered rock and the soil;

- Mixing rock fragments into the more reactive soil by bioturbation to maintain high soil porosity, allowing free circulation of water.

Thus, the authors suggest that that the chemical denudation rate will diminish where uplift rates (and physical denudation rates) are great enough to lead to a bedrock-dominated landscape, and chemical denudation rates will increase with physical-denudation rates, as far as the landscape remains mantled by soil (Anderson et al., 2002).

If we would talk more closely about zones with temperate climate, which is generally true for most part of Czech Republic, here the most important process which is driven by abiotic factors in well drained soils is leaching, which moves elements, after they have been released from parent material by weathering. Leaching acts on the soluble and exchangeable pools of elements, as, in the first stages of soil formation, they are the most available and poorly retained by soil components, due to the low cation exchange capacity. At the beginning of soil development, element mobility mainly depends on element characteristics, such as ionic charge and radius, but not the sorption sites along the soil profile, as genesis of secondary soil minerals has not yet proceeded (Bonifacio et al, 2012).

Another factor, which also plays important role in developing of profiles, is plants, as their presence on the soil provoke the biotic factor to deeply influence element distribution through nutrient uptake and inputs of elements back to soil with litter. The process of biocycling, contrasts leaching (Schaetzl & Anderson, 2005), and induces an increase in available element concentration towards the top of the soil profile. Several factors control biocycling, such as element mobility and persistence in the soil solution. The intensity of element biocycling is also affected by plant species.

However, biocycling does not occur for all elements that are present in the soil solution, as shown by Jobbágy and Jackson (2004). The budget between leaching and biocycling will thus determine the vertical distribution of the elements. In temperate climate, the organic horizons are of utmost importance in replenishing nutrient pools and up to 90 % of annual nutrient uptake derives from soil litter (Bonifacio et al., 2012).

An interesting observation was made by Rad et al. (2011), as a result of her investigation in the Area of Carribean Islands. By her suggestion, in contrast to what is often assumed by the majority of the society, as well as by many scientists, human

(agricultural) activity does not disturb necessarily critical zone processes. Indeed, in her study of chemical weathering and erosion rates in tropical volcanic islands of that region, it was shown that among the combined impacts of all parameters (climate, runoff, slope, vegetation, etc.), the basin's age seemed to be the control parameter for chemical weathering and land use: the younger was the basin, the higher the weathering rates were. Here, a combined effect between the higher erodibility and a higher climate erosivity of the younger reliefs was observed (Rad et al., 2011).

In general, Earth's weathering engine provides nutrients to nourish ecosystems and human society, controls water runoff and infiltration, mediates the release and transport of toxins to biosphere, and creates conduits for the water that erodes bedrock. The weathering engine also affects the sequestration and release of greenhouse gases that impact climate change, and generates aerosols and dust that provide nutrients to the land and ocean (Brantley et al., 2007).

Thus, it could be concluded that dynamic interactions of solid, liquid and gaseous materials in the Critical Zone (CZ), as recorded in the 'geochemical gradients', being developed along weathering profile, are of great interest to our society as the biogeochemical processes operating within the CZ have a direct and indirect influences on water quality, soil productivity and the ecosystem health.

2.1.2. Chemical Gradients in Regolith

Chemical profiles in the regolith—the record of the CZ, written at the pedon scale in the language of geochemistry, are similar to the concentration–depth profiles of marine sediments in that biological, chemical, and physical factors are all important (Goldhaber, 2004).

For the latter this complexity has been categorized successfully by applying simple models, so such simple approaches for regolith profiles, would be useful in understanding the long-term evolution of the CZ (White & Brantley, 1995). Thus, considering profiles of concentrations normalized to the parent rock as a function of depth, one can identify five end-member categories of elemental regolith profiles: **immobile profiles** (parent concentrations at all depths); **depletion profiles** (depletion at the top, grading to parent concentration at depth); **depletion–enrichment profiles** (depletion at the top, enrichment at depth resulting from

precipitation or translocation, and a return to parent concentration at greater depth; **addition profiles** (enrichment from external input at the top grading to parent concentration at depth); and **biogenic profiles** (enrichment at the top and a depleted zone that grades downward to parent concentration at depth (Brimhall & Dietrich, 1987; White & Brantley, 1995).

The elemental concentrations of regolith should first be normalized to the concentration of an immobile element (Brimhall & Dietrich, 1987; White & Brantley, 1995) to correct for contraction or expansion of soil and for apparent dilution or enrichment effects that occur when multiple elements in a system react.

The parameter τ is used to describe elemental concentration normalized to account for volume changes and relative loss or gain of elements (Brimhall & Dietrich, 1987).

$$\tau_{i,j} = (C_{j,w}\, C_{i,p})/(C_{j,p}\, C_{i,w}) - 1$$

Where C represents concentration of immobile (i) or mobile (j) elements in weathered (w) or parent (p) material. When t = 0, concentration is identical to that of the parent; when t < 0 or > 0, there is elemental loss or gain, respectively; where t = -1 stands for 100% loss of the element.

Concentration–depth profiles experience evolution through time. In regolith not experiencing significant erosion, a reaction front moves downward with time at a rate we term the *weathering advance rate*.

Once the normalized elemental or mineralogical concentrations at the top of the profile no longer change with time, the profile becomes quasi-stationary (Lichtner, 1988), where the shape of the reaction front remains constant while the entire profile moves downward. Otherwise, true steady-state profile can develop, where the concentration–depth curve remains constant with time and the rate of erosion equals the rate of weathering advance, so parent material through the weathering engine is ongoing and support ecosystems with constant nutrient delivery. In a steady-state system, the erosion rate, *W*, must equal weathering advance rate *w*. At steady state, the thickness of any layer in the weathering system, as well as the rate of transformation of each layer into material of the overlying layer, must be constant in time. The erosion rate is easier to measure than the weathering advance rate, though estimates of the first, do not necessarily agree, when made using different techniques.

At the same time, the understanding of regolith formation processes and rates, i.e. the value of w, is limited. Estimates of weathering advance, that for now can be done from approaches based on mass balance, cosmogenic isotopes ([10]Be), slope curvature, and dissolved-solute loss from catchments, rates have been shown to vary over 7 orders of magnitude when compared across laboratory to watershed spatial scales (Navarre-Sitchler & Brantley, 2007). Quantification of the rates of processes occurring within the CZ range extremely in scales of space and time. A useful approach to these scaling issues is to study processes from both ends of the time and distance spectra. While silicate dissolution kinetics have been observed to vary by up to five orders of magnitude across temporal scales, up to seven orders of magnitude variation has been seen in these rates across spatial scales (Navarre-Sitchler & Brantley, 2007).

Thus, patterns in chemical signals documented at the pedon scale, as in the examples illustrated in Figure 1 must be renormalized for comparison to patterns developed at larger spatial scales as in Figure 2. Soil geochemical surveys have been conducted globally to delineate geochemical and textural patterns at scales of approximately 1:10,000,000 (national scale), 1:1,000,000 (state or regional scale), and 1:1000 (local scale) (Jobbagy & Jackson, 2001; Reimann , 2005).
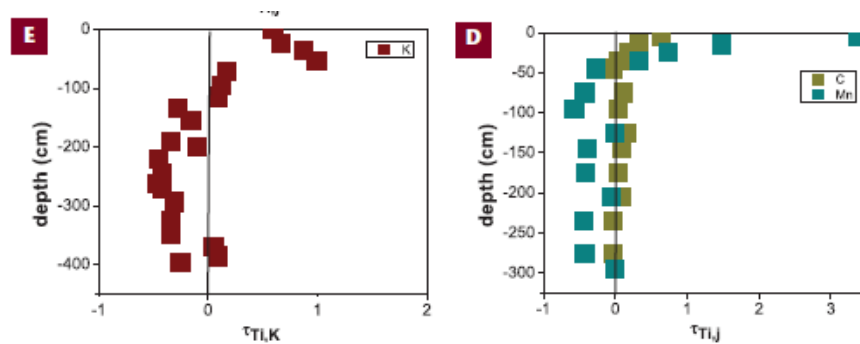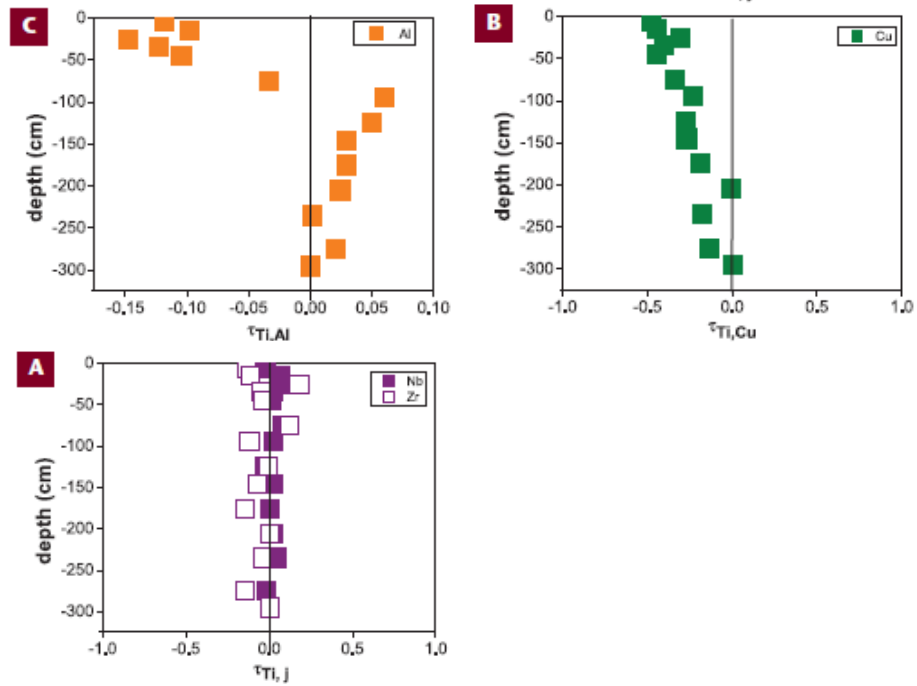
Figure 1. Plots of normalized concentration, t, versus depth: an example from soils developed in the Shale Hills watershed on the Rose Hill Shale (A–D) and on the Gettysburg Diabase (E), both in central Pennsylvania, USA.

(A) tau (τ) for Nb and t for Zr: **immobile profiles**

(B) tau (τ) for Cu: **depletion profile**

(C) tau (τ) for Al: **addition–depletion profile**

(D) tau (τ) for Mn and t for C: **addition profiles**

(E) tau (τ) calculated for K: **biogenic profile**
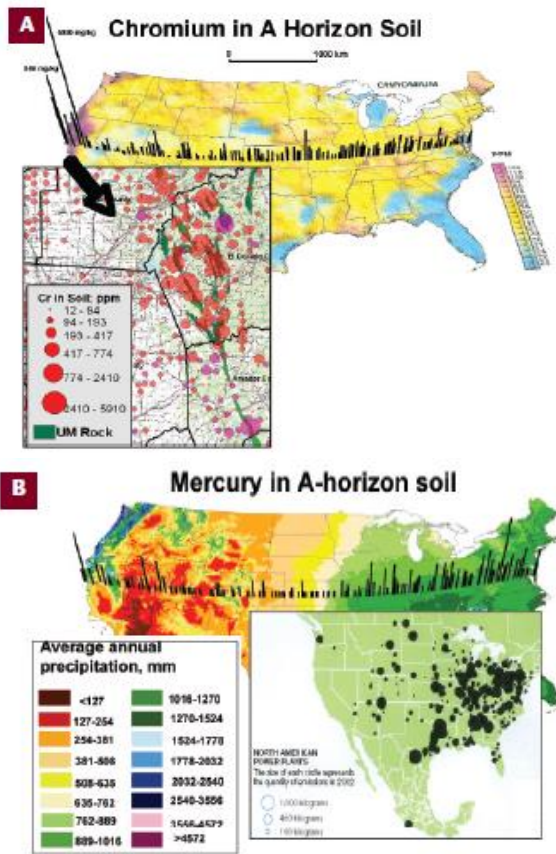
Figure 2 (**A**) Chromium in A-horizon soils across the United States; (**B**) Mercury in A-horizon soils across the United States.

Given the importance of the CZ in terms of "pollutants" and with respect to nourishing ecosystems and humans, new scientific and societal paradigms should be developed to understand the full range of CZ processes, from microcosms, through individual landscape features, family farms, and watersheds, to the global scale. This requires interdisciplinary teams of scientists who can cross scales of time and space to unravel the important chemical, physical, biological, and geological factors.

Despite its importance for life, the knowledge of the CZ's central component soil (i.e., the complex biomaterial) that promotes the growth of terrestrial organisms, is remarkably limited. Thus, for scientific approaches and funding paradigms have not promoted and emphasized integrated research agendas to investigate the above mentioned coupling processes in the Critical Zone. The investigations are to be evaluated by a CZ Exploration Network with short-term deployments of instrumentation at field sites along environmental gradients as well a long-term sites that should be instrumented hierarchically and intensively (Brantley et al., 2005)

It is expected, that different elements behave differently in the soil-rock profiles depending on their nature.

As for the serpentinite rocks and the corresponding soils at our studying site, we have analyzed the concentrations and their changes as a function of depth for a range of metals, both base and trace. Among them, particularly K, Ca, Mg, Ni and Cr have shown the most characteristic and interesting biogeochemical behavior during serpentinite weathering. So, it is important to give a more explicit description of properties and cycling of these elements in general to further examine and understand their behavior in serpentinite environment.

2.2. Description of the elements investigated by this study

3.2.1. Selection of the elements

From the chemical point of view, serpentinite has a complicated composition. We have chosen several elements such as chromium, nickel, magnesium, potassium and calcium, for a more detailed analysis due to their particular role in the biogeochemical cycling and weathering and the specificity of their element cycling.

To discuss more closelythe cycling of these elements within Critical Zone, it would be appropriate to divide these elements into two major groups. Namely those that are represented as *base cations* (alkaline (K) and alkaline earth metals (Ca and Mg)) and *trace metals* (Cr and Ni), thus we will keep this structure in the following discussion.

3.2.2. Nutrient base cations (Ca, Mg, K): elemental characteristics, role, distribution, and biogeochemical cycling.

3.2.2.1. General characteristics of the elements

Calcium and Magnesium are both alkaline earth elements and belong to group 2 of the periodic table.

Calcium is the fifth most abundant element on Earth, constituting approximately 3% by weight (equivalent to 4.2% CaO) of the upper continental crust, and about 5.29% (7.41% CaO) for the bulk continental crust (McLennan and Taylor 1999). It is a widespread refractory lithophile element forming several common minerals including calcite, gypsum, dolomite, anhydrite and fluorite and is a part of such igneous rocks as anorthosite, which is composed predominantly of calcium-rich plagioclase feldspar, common in mafic rocks. (De Vos& Tarvainen , 2006).

Magnesium is the seventh most abundant element in the Earth's crust with a quoted average of 2.76% by mass. It is a lithophile metallic element and a major constituent of many mineral groups (silicates, carbonates, sulphates, phosphates and borates), and is a major component of many mafic rock-forming minerals, such as olivine, e.g., forsterite, pyroxene, amphibole, spinel, biotite mica, chlorite, serpentine, talc, and clay minerals. (De Vos & Tarvainen , 2006; Wedepohl , 1978).

In magmatic systems, Mg is concentrated in high temperature minerals like olivine and pyroxene, which precipitate relatively early, but for high water and oxygen fugacity, the precipitating phases are more likely to be amphibole or mica. MgO concentrations range from >40% in some ultramafic rock types, e.g., dunite, through to <0.5% in calc-alkali rocks, such as calc-alkali rhyolite (Wedepohl , 1978). High Mg values indicate mafic or ultramafic rocks (in association with Cr, Ni, V, etc.) or calcareous rocks (with Ba, Ca and Sr). (De Vos& Tarvainen, 2006)

Potassium is an alkali metal of group 1 of the periodic table and it is the eighth most abundant element in the Earth's crust. It is a lithophile and biophile metallic element, and is a major constituent of many rock-forming minerals, including important silicate minerals such as alkali feldspar, leucite, biotite, muscovite, phlogopite and some amphiboles, as well as phosphate, halide and sulphate minerals. As a major constituent in many igneous rocks, it is often the base for their petrographic classification. It is progressively concentrated during magmatic fractionation, and is thus enriched in felsic relative to mafic igneous rocks (De Vos & Tarvainen, 2006).

3.2.2.2. Role of the major base cations in ecosystem.

The role of the base cations (Ca, Mg, K, Na) is important to the biogeochemistry of forest ecosystems; in particular, Ca, Mg, and K are essential nutrients for plant growth, and low supply rates may affect forest productivity (Krám et al., 2009).

Calcium is an essential nutrient element for plants and animals for the development of bone, nervous system and cells, and generally non-toxic. Moreover, in some areas with low stream water pH, added Ca has been shown to reduce the toxic effects of high concentrations of Al (De Vos & Tarvainen, 2006)

Magnesium is essential for all organisms and is also non-toxic under normal circumstances.

Deficiencies of magnesium are much more common than problems concerned with its toxicity. Magnesium is a key plant nutrient and is essential for photosynthesis in plants, where it forms the active site in the chlorophyll enzyme molecule (De Vos& Tarvainen, 2006).

Potassium is an essential element for all organisms. Together with N and P, potassium is essential for the survival of plants. Its presence is of great importance for soil health, plant growth and animal nutrition. Its primary function in plants is in the maintenance of osmotic pressure and cell size, thereby influencing photosynthesis and energy production. Very high levels of K^+ in soil water can, however, cause damage to germinating seedlings, inhibit the uptake of other minerals and reduce the quality of crops (De Vos& Tarvainen, 2006).

3.2.2.3. Sources and cycling of base cations.

Atmospheric deposition and mineral weathering are the principal sources of soluble base cations in forest ecosystems, and these inputs are critical in regulating the acid-base status of forest soils and soil solutions (van Breemen et al., 1984 Hruška & Krám, 2003).

The main anthropogenic activity that would lead to an increase of **calcium** in the drainage system is the long-established agricultural practice of liming land to correct for soil acidity. Other anthropogenic sources of calcium include cement

factories, fertilisers and dust, although geogenic sources are much more important than anthropogenic ones in the environment (Reimann & de Caritat, 1998, De Vos& Tarvainen, 2006).

Calcium generally has a high mobility and, except under strongly alkaline conditions, occurs in solution as dissociated Ca^{2+} ions.

Soluble major ions, such as Ca, influence the quantities of soluble trace elements. Solutions of most soil types contain an excess of Ca, which constitutes more than 90% of the total cation concentration; Ca is therefore, the most important cation in governing the solubility of trace elements in soil (Kabata-Pendias, 2001). As soil acidity increases, Al replaces Ca as the dominant exchangeable cation. De Vos& Tarvainen, 2006)

Anthropogenic sources of **magnesium** include fertilisers and liming (Reimann & de Caritat, 1998). Many magnesium compounds are also very soluble, Mg is highly mobile after its release by weathering, under all environmental conditions and is almost exclusively present as Mg^{2+} ions (De Vos& Tarvainen, 2006)

As for **potassium**, fertilisers are the main anthropogenic source of this element. Many K salts have important chemical and medicinal applications, including the hydroxide, nitrate, carbonate, chloride, chlorate, bromide, iodide, cyanide, sulphate, chromate and dichromate. However, natural sources are considered to be far more important in the environment than anthropogenic ones (Reimann & de Caritat, 1998).

Although K is an abundant element, its mobility is limited by three processes: (a) it is readily incorporated into clay-mineral lattices because of its large size; (b) it is adsorbed more strongly than Na^+ on the surfaces of clay minerals and organic matter; and (c) it is an important element in the biosphere and is readily taken up by growing plants De Vos& Tarvainen, 2006).

So, all these elements are quite soluble, and, according to the Goldschmidt's sequence (Goldschmidt, 1937), leaching of these base cations such as Ca, Mg and K is expected to be high in comparison to many other cations.

As all metal elements still derive mainly from the lithosphere as their natural source, they need to be released into the soil from the weathering of the parent mineral/rock material before they become plant-available (Bonifacio et al., 2012).

The concentration of exchangeable *potassium* forms often shows high concentration both in the top soil horizons because of biocycling, and low in the bottom ones, due to leaching. Biocycling was also demonstrated for Ca (Blum et al. 2008). Though, these processes are affected by plant species (Jobbágy et Jackson, 2004).

Calcium is expected to show an important release upon litter mineralization, due to passive transpiration flux via the xylem, though without being retranslocated into the branches and stem before litter fall, however for K this process is even faster as it can be released from stem and branch residues (Bonifacio et al., 2012).

As many *magnesium* compounds are very soluble as well, Mg is highly mobile after its release by weathering, under most environmental conditions and is likely to be present almost exclusively as Mg^{2+} ions (De Vos& Tarvainen, 2006).

3.2.2.4. Distribution of base cations in the soils of Europe

According to the survey held towards the preparation of the Geochemical Atlas of Europe (De Vos& Tarvainen, 2006), The median CaO content in subsoil is 1.13% and in topsoil 0.92%, with a range varying from 0.02 to 51.6% in subsoils and 0.03 to 47.7% in topsoils. The average ratio topsoil/subsoil is 0.702.

To talk more closely about the abundance of Ca and its geographical distribution, low CaO values in subsoil (<0.38%) developed on base-poor bedrock occur in the eastern Iberian peninsula, the Armorican Massif and the Central Massif in France (all Variscan areas), over most of England, Wales and Ireland, and in the glacial drift area of Denmark, northern Germany and Poland. The topsoil pattern is very similar.

 Ca is more abundant in the sedimentary rocks of calcareous ($CaCO_3$) regions with higher content of CaO values (>2.97%) included limestone regions of eastern Spain, southern Italy, Greece, the Dalmatian coast, southern France and the western Alps, the eastern part of the Paris Basin, western Ireland, and the Baltic states (Estonia, Latvia, Lithuania). On the other hand, high CaO content was shown also for some regions with igneous bedrock, such as Fennoscandia and Albania, characterized by greenstone belts and other mafic and ultramafic crystalline rocks with Ca-rich

plagioglase. The topsoil CaO distribution map generally shows the same pattern as the subsoil map, with only minor differences (De Vos& Tarvainen, 2006).

The median MgO content in subsoil is 0.98% and in topsoil 0.77%. The average ratio topsoil/subsoil is 0.796. High MgO values are observed on the subsoil map over northern Fennoscandia (greenstone belts), central Norway, Latvia and western Estonia (Devonian dolomitic clay and dolomite), a zone from western Slovakia over the Austrian Alps up to Graubünden in Switzerland, some isolated anomalies in the Vosges and Black Forest, central and northern Greece and Albania, the north-western Appenines, Corsica, the eastern Pyrenees, and the mountains of southern Spain (Jurassic dolomite in Sierra de Segura, amphibolite and amphibole gneiss in Nevado-Filábride unit of Baetic Cordillera).

The distribution of MgO is geologically controlled, with greenstone belts, ophiolitic belts, and crystalline mafic rocks causing most of the anomalies, but there are also high values over some dolomitic areas (e.g., Greece), and also magnesite mineralisation (Austria, Greece). The MgO topsoil map is very similar to the subsoil map, but with no anomaly in Latvia and Estonia (leaching of dolomite), which is due to the tendency of MgO to be leached during pedogenesis (De Vos& Tarvainen, 2006).

The median K_2O content is 2.02% in subsoil and 1.92% in topsoil, ratio topsoil/subsoil of 0.940. Low K_2O values in subsoil occur in central Norway, in Ireland, in the glacial drift area from the Netherlands to Poland, central Hungary, northern France, the Garonne basin in south-west France, in calcareous southern Spain, Sicily, eastern Greece and Crete. High K_2O values present in the granitic Fennoscandian shield, with concentrations increasing from Archaean rocks in the north-east towards Proterozoic rocks in the south-west; also found in Estonia and Latvia (Devonian clay and basal Quaternary till rich in mica), northern Scotland, south-west England, central Germany, the French Massif Central (two-mica granite is known to be enriched in K, Rb and Cs) and to a lesser extent Brittany, the Alps near the Austrian-Italian border, the western Iberian Peninsula (Central System of the Iberian Massif with granitic and metamorphic lithologies). Furthermore, the crystalline areas of northern Portugal, the eastern Pyrenees granitic intrusives, Corsica, and a few points in the west-Italian alkaline province. A high K value near Santander in northern Spain is caused by the Polanco salt diapir within Triassic shale

and sandstone. The topsoil K_2O map is very similar to that of subsoil (De Vos& Tarvainen, 2006).

The correlation between K and Rb is very strong, in both subsoil and topsoil. pointing to their association in feldspar and phyllosilicate minerals in shale and igneous rocks. Also, Ba and K_2O show a strong correlation due to the ionic substitution of Ba^{2+} for K^+ in K-containing silicates (De Vos& Tarvainen, 2006).

3.2.3: Trace toxic metals (Ni, Cr): elemental characteristics, role, distribution, cycling.

3.2.3.1. General characteristics of Ni and Cr

Chromium (Cr) is an element with the atomic number of 24 and atomic mass of 51.996, situated in the secondary subgroup of the sixth group and the fourth period of the periodic table of chemical elements of Mendeleev and is a member of the first row transition series of elements It is hard metal of bluish-white color and with a high chemical resistance. Chromium compounds are usually of bright coloring, which is, in fact the reason for its name. There are four stable natural isotopes of Cr: ^{50}Cr (4,31%), ^{52}Cr (87,76%), ^{53}Cr (9,55%) and ^{54}Cr (2,38%) (I-Think: Chromium, 2013).

In Earth crust chromium is a lithophile metallic element and forms minerals such as chromite $FeCr_2O_4$ and the crocoite $PbCrO_4$. It is also contained as an accessory element in several others, such as spinel, amphibole, mica, pyroxene and garnet. The trivalent ion Cr^{3+} with an intermediate-size ionic radius of 62 pm, readily substitutes for Fe and Mg, and is partitioned into spinel and pyroxene during the earliest stages of crystal fractionation. Thus, this metal is enriched in ultramafic rocks (1000–3000 mg kg^-1). The principal ore mineral of Cr is chromite, and is generally mined from ultramafic rocks and basaltic magmas, along with Cr-enriched magnetite and ilmenite (Wedepohl 1978) Olivine is generally poor in Cr, but pyroxene, amphibole and mica may be enriched (Ure & Berrow 1982).

Elevated Cr values are indicative of mafic or ultramafic rocks, even in strongly-weathered environments, such as laterite. In sedimentary rocks, Cr may be

present in primary detrital phases such as chromite, magnetite and ilmenite (Kabata-Pendias & Pendias, 2001).

Nickel (Latin Niccolum, denoted by Ni) is a siderophile chemical element with atomic number 28 and atomic weight 58.69, is an element of secondary subgroup of the eighth group of the periodic system of Mendeleev and one of the three elements from the family of iron. Metallic nickel is a plastic and malleable transitional metal of silvery-white color with a yellowish tinge, is very hard, can be polished, and is attracted by the magnet. In the nature, nickel is represented by five stable isotopes: ^{58}Ni (67,88% by weight), ^{60}Ni (26,23%), ^{61}Ni (1,19%), ^{62}Ni (3,66%) and ^{64}Ni (1,04%) (I-Think: Ni, 2013).

As siderophile metallic element with chalcophilic and lithophilic affinities Nickel forms several minerals, including pentlandite $(Fe,Ni)_9S_8$, nickeline NiAs and ullmannite NiSbS. With the size of Ni^{2+} ion (69 pm) being intermediate between Mg^{2+} and Fe^{2+}, it substitutes for those during fractionation, and it is partitioned into ferromagnesian minerals such as olivine (up to 3000 mg kg^{-1} Ni), orthopyroxene and spinel. It is, thus, strongly enriched in ultramafic and mafic lithologies relative to felsic igneous rocks. Nickel, like Co, is a siderophile element, but in the Earth's crust it also exhibits chalcophile and lithophile characteristics. The abundance of Ni in igneous rocks, therefore, generally correlates with those of Mg, Cr and Co. It is also presented in appreciable amounts in common sulphide minerals, such as pyrite and chalcopyrite, and often correlates well with Cu in sulphide-rich rocks (Wedepohl, 1978). In sedimentary rocks, Ni is mostly held in detrital ferromagnesian silicate minerals, detrital primary Fe oxides, hydrous Fe and Mn oxides, and clay minerals. It is concentrated in shale (up to 90 mg kg^{-1}) relative to greywacke (ca. 40 mg kg^{-1}), quartzitic sandstone (ca. 20 mg kg^{-1}) and limestone (<5 mg kg^{-1}). Organic matter and coal can contain Ni concentrations in excess of 50 mg kg^{-1} (De Vos& Tarvainen, 2006).

3.2.3.2. Role of the trace metal elements

Increased abundance of common trace metals (e.g. Cr, Ni) in the environment is a characteristic property of only a few terrestrial ecosystems. The role of these trace metals in ecosystems depends on the degree and type of dispersion as gaseous

compound or aerosols in the atmosphere and on their solubility and mobility in wet depositions. Trace metals have gained in importance due to human activities that have fundamentally changed their biogeochemical cycling. They are emitted into the environment by numerous industrial processes and are dispersed by the application of sewage sludge, biogenic waste, pesticides and fertilizers.

Most trace metals play an ambivalent role in the environment: Depending on the concentration they are both essential micronutrients and toxic components for plants and soil organisms (Larcher, 2003; Alloway & Reimer, 1999). Therefore the emission and deposition of trace metals and their cycling in the environment are important issues in environmental research (Smidt et al., 2012).

As both Ni and Cr represent also valuable natural resources and are attractive from the economical point of view a couple words about their role in industry should be said.

3.2.3.2.1. Role of Ni and Cr in industry

It is metallurgy that is the major consumer of metallic **nickel** (up to 80% out of all the smelted nickel), as this metal serves as a precious alloying element. Here additive of nickel into steel helps to increase chemical resistance of composition, so nickel is used as an essential component of all the stainless steels. In addition, nickel alloys are characterized by a range of other precious properties, such as high mechanical, anticorrosive, magnetic or electric and thermoelectric qualities.

Out of several thousands of alloys iron-nickel and copper-nickel, as created by nature, still remain the basic ones for the most of the nickel alloys. (I-Think, 2013: Ni)

Chromium is widely used in doping of steels and alloys, providing them with corrosion and heat resistance. More than 40% of the pure metal, which is obtained, is consumed for the manufacture of "superalloys".

The best known are resistance alloys, represented by nichromes with 15-20% contain of Cr, superalloys (13-60% Cr), stainless steel (18% Cr) and ball bearing steel (1% Cr). Addition of chromium to the conventional steels improves their physical properties and makes the metal more susceptible to thermal processing (I-Think, 2013: Ni).

3.2.3.2.2. Role of Ni and Cr metals in ecosystems

Nickel is one of the fifteen essential (vital) elements and is known to be involved into a number of enzymatic reactions in the bodies of animals and in plants (hydrolysis of peptide bonds, carboxylation, etc.)

It is accumulated in keratinous tissues of animal organism, particularly in birds feathers. (MACs (maximum allowable concentration) for metallic nickel in water is 0.1 mgl^{-1} and in soil 3.0 mg kg^{-1}) (I-Think, 2013: Ni).

On the other side, regarding the ecological aspects, this elements are believed to be representatives of the most hazardous ecotoxicants and are undesirable components in natural ecosystems, in the case if their amount exceeds some certain critical level. Due to the toxicity of Cr and Ni they can cause negative effects on many types of living organisms of different levels, and several investigations have been investigating impact of these toxic metals on organisms (Burton &. Morgan, 1983, Gribovsky, 2000, Kram et al., 2009, Somerfield et al., 1994)

Nickel has been shown to be essential for microorganisms and also in human metabolism (McGrath & Smith, 1995). The World Health Organisation recommends a daily intake of 10 µg day^{-1} for humans (WHO, 2006). Nickel deficiency retards growth and impairs iron uptake. Most Ni compounds are relatively non-toxic, but some compounds are highly toxic, and extreme excesses of Ni are both toxic, causing serious threats to both plants and animals (WHO, 2006; De Vos& Tarvainen, 2006).

In one of the studies, held in South Wales, the upper critical concentrations of Ni was determined for Sitka spruce (*Picea sitchensis*). The values obtained were 8.5 mg kg^{-1} (of dry matter). It has been shown that nickel might be present at sufficiently enhanced levels in the foliar tissues of trees in certain forest areas of South Wales to affect normal functioning and growth.

Forestry plantations in South Wales are now characterized by poor growth in certain areas, and the study proves that the toxic effects of heavy metals should be a possible factor influencing growth of Sitka spruce. The authors conclude that non-essential elements, such as Ni, have an upper critical level above which yields are reduced because of toxic effects of this element (Burton &. Morgan, 1983).

It has been officially acknowledged for more than 40 years by now, that the pastures of the geochemical region of the upper reaches of the Ural River, which are characterized by Ni-enriched soils, are inhabited by abnormal plants, and the livestock in this area is prone to cataract, keratitis, high mortality due to anemia and poisoning. According to Gribovsky (2000), high nickel content in soils and vegetation of this area is dangerous not only for livestock, but for human health as well.

Also, it has been shown that, out of the whole group of ecotoxicants, Ni represents a microelement with a remarkably large range of the possible negative effects on the human in comparison to the other chemical elements and organic compounds.

One of the hazardous characteristics of nickel is its mutagenic properties, which has been confirmed by numerous investigations as well as paleodata (Solovyov, 2003.)

As for **chromium**, once thought to be non-essential, is now known to have at least one important biological function (Frausto da Silva & Williams 1991). It is needed in small amounts for metabolism of proteins and carbohydrates. Chromium has a varying toxicity depending on its valency and speciation in the environment. Soluble Cr^{3+} is considered relatively harmless at levels normally encountered, but Cr^{6+} is highly toxic, causing liver and kidney damage and acting as a carcinogen (De Vos & Tarvainen, 2006). In soil pH, Cr(III), mainly present as $CrOH^{2+}$, and is rather benign and being easily adsorbed there, whereas the Cr(VI), present as $HCrO^{4-}$, is highly toxic and soluble (Fendorf, 1995).

Different studies have shown the high toxicity of Cr(VI) to plants. Turner and Rust (1971) showed that 0.5 mg l^{-1} Cr(VI) in nutrient medium of soybean decreases the yield and the element concentrations of plants for different macro- and micro-nutrients.

Maleci et al. (1999) also showed a marked reduction of root and leaf lengths of two species of Calendula with 1 mg l^{-1} Cr(VI). Sharma et al. (1995) showed that the grain yield and different metabolic activities were severely affected on wheat by the supply of 0.05 mM of Cr(VI) (Becquer et al., 2003).

It has been claimed, that, since Cr is a non-essential element for plants, there is no uptake mechanism; Cr is taken up passively with other essential elements such as sulfate through sulfate transporters. Cr accumulation in plants causes high toxicity

in terms of reduction in growth and biomass accumulation, and Cr induces structural alterations. Cr interferes with photosynthetic and respiration processes, and water and minerals uptake mechanism. Various enzymatic activities related to starch and nitrogen metabolism are decreased by Cr toxicity either by direct interference with the enzymes or through the production of reactive oxygen species. Cr causes oxidative damage by destruction of membrane lipids and DNA damage. Cr may even cause the death of plant species. Few plant species are able to accumulate high amount of Cr without being damaged. Such Cr-tolerant, hyperaccumulator plants are exploited for their bioremediation property. (Singh et al., 2013)

As it is stated by Suzuki et al. (1971) states, abnormally high nickel content in the serpentine soils, seriously affects the crops as a result of metal toxicity. However, when it contains a high quantity of chromium comparable to that of nickel, no affect of the metal toxicity is seen in the crops. With special regards to this, it has been proved that the harmlessness of chromium was closely related to its low solubility. It was shown that the difference of impacts to plants by nickel and chromium on plant growth is not only affected strongly or weakly by the metal itself, but also by the different oxidation state of the metal in soils, which is also an important cause for the metal toxicity (Suzuki et al., 1971).

3.2.3.3. Sources of toxic metals (Ni and Cr) and their cycling within the geo-ecosystem

Generally the sources of trace metals, such as Ni and Cr in the environment could be devided into two big groups: natural (geogenic) and not natural (anthropogenic).

3.2.3.3.1. Anthropogenic sources of Ni and Cr in the environment

The input of these elements by anthropogenic sources is caused by human activities that have fundamentally changed the biogeochemical cycling of these elements. They are emitted into the environment by numerous industrial processes and are dispersed by the application of sewage sludge, biogenic waste, pesticides and fertilizers.

The vegetation as well as the soil is able to accumulate and transfer trace elements within the ecosystems. The "rough surfaces" of forests are effective filters for atmospheric contaminations, dissolved substances and particles. The deposition, litterfall and stemflow affect soils by the transfer of trace elements in the surface soil layer and accumulate there. Wash-off and leaching due to precipitation, litterfall, percolation in the soil and uptake by plants determine the internal cycle of trace elements. The input into the biogenic cycle takes place by wet, dry and occult deposition, output by harvesting, runoff into the groundwater and to a minor part by volatilisation (e.g. carbonyles and/or alkyles of Hg, Ni, Pb). Plants are able to take up trace metals actively via the roots and passively via the leaves.

A set of legal and effect-related limit values was established defining the trace metal

concentrations that have adverse effects in terrestrial ecosystems. The trace metal input into ecosystems can be determined by chemical analyses of aerosols, rain water, topsoils, or by means of bioindication which is a low cost option for plants, fungi and animals accumulating trace metals as natural archives. (Markert et al., 2003). The anthropogenic impact on the soil can be detected by comparison of concentration levels of lower and upper soil horizons. If anthropogenic impacts of trace metals exist, higher concentrations in the "O-layers" and upper mineral soil layers (0-5 or 0-10 cm) than in deeper soil layers (deeper 30 or 50 cm) are observed. The relation between the concentrations in the upper and deeper layers is the enrichment factor (EF). An EF > 1 indicates accumulation of a specific trace element, an EF < 1 means a depletion. In general the EF should be at least > 1.5 for an indication of anthropogenic inputs (Smidt, et al., 2012)

3.2.3.3.2. Geogenic sources of Ni and Cr in the environment

The major natural source of heavy metals in agri-ecosystems is represented by rocks (such as sedimentary, igneous, metamorphic rocks), that give the rise to the formation the soil layer due to the weathering processes (Ilyin, 1991). Herein the upper mantle, basalts and granites act as primary repositories of Cr and Ni metals, while the secondary ones are represented by sedimentary rocks, ocean waters, and living matter of the planet.

Other natural sources of Cr and Ni metals include hydrothermal waters and brines, star and meteorite dust, volcanic gases.

Chromium sources and cycling

Chromium is the 21st most abundant element in the Earth's crust. Nearly all naturally occurring chromium is in the trivalent state (Cr^{3+}), usually in combination with iron or other metal oxides. Under typical environmental and biological conditions of pH and oxidation–reduction potential, the most stable form of chromium is the trivalent oxide. This form has very low solubility and low reactivity resulting in low mobility in the environment and low toxicity in living organisms (Barnhart, 1997).

During weathering, the behaviour of Cr^{3+} resembles that of Fe^{3+} and $Al^{3+,}$ leading to widespread accumulation in secondary oxides and clays. Its adsorption by clay is also highly dependent on pH, specifically Cr^{6+} adsorption decreases with increasing pH, and Cr^{3+} adsorption increases with increasing pH. The dominant effect of organic matter is the stimulation of the reduction of Cr^{6+} to $Cr^{3+,}$ the rate of which increases with soil acidity (Kabata-Pendias & Pendias, 2001)

Cationic Cr^{3+}, $CrOH^{2+}$ and $Cr(OH)^{2+}$ are the main forms of chromium in reducing environments between pH 5 and pH 9. In alkaline oxidising environments, Cr may be present as the chromate ion, CrO_4^{2-}, although this species is reduced naturally in stream sediment over time (De Vos& Tarvainen, 2006)

The chemistry of Cr in soils and in natural waters, particularly the conversions between its two oxidation states, has also been described by Fendorf (1995), who explain that Cr(III) can only be oxidized to Cr(VI) by manganese oxides, while Cr(VI) is reduced to Cr(III) by organic matter, Fe(II) and sulfites. Some studies indicated that Cr is mobile within ultramafic soils. Soane and Saunder (1959) found appreciable quantities of Cr on cation exchange resins inserted in serpentine soils from Rhodesia. Gasser et al. (1994) found concentrations from 0.1 to 3.2 μM l^{-1} in serpentinitic soils from the Swiss Alps. However, (Anderson et al. (1973), who extracted soil solution by centrifugation on a range of ultramafic soils, reported low Cr concentrations ranging between 0.2 and 0.4 μM l^{-1}. (Becquera et al., 2003).

Sources and cycling of nickel in geo-ecosystems

Nickel in the Earth's crust occurs naturally in combination with other elements in various minerals There are over 100 minerals which contain nickel and the ones that are most commonly mined are pentlandite and garnierite.

Although nickel is common, it is widely distributed. On average, the Earth's crust contains about 5 parts per million (ppm) nickel, which is 0.0075% of nickel.

Taking the entire Earth into consideration (including the mantle and core along with the crust), nickel is the fifth most common element (Nickel Institute, 2013).

A large proportion of the Ni in stream sediment is held in detrital silicate and oxide minerals that are resistant to weathering. Limited dissolution of Ni^{2+} may occur at low pH, but its mobility is generally restricted by its tendency to be sorbed by clay minerals or hydrous oxides of Fe and Mn (Ure & Berrow 1982). In soil, Ni is strongly related to Mn and Fe oxides but, especially in surface soil horizons, which occurs mainly in organically bound forms Kabata-Pendias & Pendias, 2001). The range of Ni values in soil vary from 0.2 to 450 mg kg^{-1} according to rock type. Nickel is highly mobile under acidic, oxidizing conditions. In natural water, Ni may exist in one of three oxidation states (+2, +3 and +4), although the free ion Ni predominates. Chloride, NO and SO compounds of Ni are very soluble in water, but NiCO and, in particular, Ni(OH) and Ni (PO) are insoluble). (McBride, 1994) Average Ni concentrations in surface water vary from less than 1 to about 10 µg l^{-1} (Hem, 1992). Anthropogenic sources of nickel include fertilisers, steel works, metal plating and coinage, fuel combustion and detergents (Reimann & de Caritat, 1998)

As it is reported by Kabata-Pendis (2001), Ni recently has become a serious pollutant that is released in the emissions from metal processing operations and from the increasing combustion of coal and oil. The application of sludges and certain phosphate fertilizers also may be important sources of Ni. Anthropogenic sources of Ni, from industrial activity in particular, have resulted in a significant increase in the Ni content of soils (Table 1).

Site and pollution source	Mean or range in content	Country
Soil over serpentine rocks	770 1700-5000	Australia New Zealand

	3563-7375	Zimbabwe
Mine wastes	2-1150	Great Britain
Metal-processing Industries	206-26,000	Canada
	500-600[a]	Great Britain
	304-9288	Russia
	26-36[b]	Sweden
Sludged farmland	23-846	Great Britain
	31-101	Netherlands
	50-84	Germany

Table 1 Nickel Enrichment and Contamination in Surface Soils (ppm DW). Site and Pollution Source Mean or Range in Content Country Ref .(Here indexe a -Soluble in HCl.b -Needle litter and humus layer, respectively (Kabata-Pendias & H. Pendias, 2001)

In particular, Ni in sewage sludge that is present mainly in organic chelated forms is readily available to plants and therefore may be highly phytotoxic. (Kabata-Pendias & Pendias, 2001).) Soil treatments, such as additions of lime, phosphate, or organic matter, are known to decrease Ni availability to plants.

In the presence of some organic complexing agents, Ni is capable of forming neutral or negatively charged complexes, making the metal highly mobile in relation to other trace elements. Consequently, Ni concentrations may be high in stream water contaminated by sewage and leachate from waste tips (De Vos & Tarvainen, 2006).

Relationship between Ni and Cr during weathering and soil formation

A recent study to assess the relative mobility of Cr and Ni in volcanic andosols of the Auvergne (France) has shown that their respective mobility was lower than 40 and 25% respectively and that the natural uptake of Ni by plants was very low, i.e., 2 mg kg^{-1} for graminea and 0.4 mg kg^{-1} for corn (De Vos W., Tarvainen T., 2006).

In the study of serpentine soils in Horokanai (Hokkaido) by Suzuki et al. (1971), the content of both metals and their relative cycling and availability was analyzed. It was shown that chromium solubility was very low in comparison with nickel. Total chromium was concentrated at a high level in the nonmagnetic heavy minerals or ferromagnetic minerals, and the values were lowest in clay. Also, in the black hard mineral existing in the nonmagnetic heavy minerals, chromium occupied

70% of the heavy metals (chromium, manganese and iron). In the study it is further stated, thate nickel content was highest in clay in contrast with chromium, however, high concentrations such as seen in chromium was not. It was assumed that greater part of chromium in the soil was concentrated in chromite. Chromite is fairly stable in nature. It is not easily weathered, thus chromium is not released efficiently from the mineral. slightly soluble chromium may have originated in an other form of chromium, attached to clay and other secondary minerals. In contrast, most nickel exists in a soluble state, and the nickel content is the highest in clay, and is the lowest in nonmagnetic heavy minerals. In sand, nonmagnetic light mineral has a two fold concentration or over as compared with non· magnetic heavy minerals. So, nickel was concentrated in minerals which convert easily to clay (Suzuki et al., 1971).

3.2.3.4. Distribution of Ni and Cr in the European soils and connection to bedrock

Investigations towards assessment of the content and cycling of Cr and Ni in natural sites has been performed by scientists in several regions and on different levels.

As reported in the report for chromium, which was a part of a more general and fundamental survey of Geochemistry Expert Group towards preparation of the "Geochemical Atlas of Europe", the global average of Cr in surface soil has been estimated to be 54 mg kg^{-1}. Soil underlaid by serpentinite was reported to contain as much as 0.2 to 0.4% Cr, when sandy soil and Histosols contain on average 47 and 12 mg kg^{-1} Cr respectively.

The median total Cr content has been estimated by XRF analysis to be is 62 mg kg^{-1} in subsoil and 60 mg kg^{-1} in topsoil with the average ratio topsoil/subsoil of 1.096.

Low Cr values in subsoil occured in southern Fennoscandia, Estonia, parts of northern Germany and Poland, central Portugal and parts of central and eastern Spain. High values were shown over ophiolites in Liguria (Italy) and Corsica, over Slovenia and Croatia (high values in terra rossa over carbonate rocks), the Rheno-Hercynian, the Carpathians, northern Ireland (Antrim basalt), central Norway and a large area with greenstone belts in northern Fennoscandia. In central England,

elevated Cr levels are associated with Mesozoic sedimentary ironstone. Isolated high Cr values in Spain are related to the Peñas de Aya gabbro in the western Pyrenees, the Ordenes ophiolithic Complex in Galicia (north-west Spain) and other mafic facies in central and southern Spain.

The topsoil map for Cr is very similar to the subsoil map. Gran Canaria shows an anomaly due to basaltic volcanic rocks. In the whole, high Cr contents in European soil is mostly of the geogenic origin (De Vos & Tarvainen, 2006).

According to the data from the investigations by Geochemistry Expert Group in the run of EuroGeoSurvey, published in the "Geochemical Atlas of Europe", the median total Ni content, following ICP-MS analysis was 21.8 mg kg^{-1} in subsoil and 18.0 mg kg^{-1} is topsoil and the ratio topsoil/subsoil was 0.918. Low Ni values in subsoil (<10.5 mg kg^{-1}) occur in southern Fennoscandia, Estonia, in the glacial drift area from the Netherlands to Poland and Lithuania, in central Portugal and central Spain, and small areas in central Hungary and central France. The relatively low Ni values in Finland are surprising given the presence of greenstone belts and Ni-deposits. The subsoil Ni map shows a strong anomaly over most of Greece and Albania, caused by mineralised ophiolitic rocks, and sedimentary rocks derived from them.

There are high values of Ni over ophiolites in Liguria (Italy) and Corsica, over Slovenia and Croatia (residual soil over carbonate rocks), the Rheno-Hercynian, the Carpathians, northern Ireland (Antrim basalt), central Norway and a large area with greenstone belts in northern Scandinavia.

Some anomalies of both Cr and Ni appeared in Greece, and were associated with bauxite, Fe-Ni and polymetallic sulphide mineralisation. In southern Europe, some high Ni values were present and were explained by coprecipitation with Fe-Mn oxides of supergene origin, for example, in north-west Spain. The topsoil map for Ni was very similar. However, Southern Italy region was enriched in Ni in the topsoil only.

The overall correlation Cr-Ni was shown to be as strong as 0.89 in subsoil and 0.83 in topsoil. Besides, nickel in both subsoil and topsoil also showed a strong correlation with ? Co, and a good correlation with Fe, Sc, V, Cu and Te.

2.3.   Serpentines and Serpentinites

3.3.1. General description of the mineral

The rock type, which underlain the ecosystem, would also determine the chemical composition of soils and also weathering processes characteristic for this site. As mentioned above, in this work, we were concentrating on investigating the processes, taking place in the serpentinites, so it is crucial to give closer characterization of those Cr and Ni rich rock types.

Serpentinite can be defined as rocks made up mostly of serpentine minerals. At the same time, *serpentine* represents a family of silicate minerals rich in magnesium and water, derived from low-temperature alteration or metamorphism of the minerals in ultramafic rocks (intrusive igneous rocks very rich in iron and magnesium and with much less silicon and aluminum than most crustal rocks, most come from the Earth's mantle). Serpentine minerals are light to dark green, commonly varied in hue, and greasy looking; the mineral feels slippery (Stoffer & Messina, 2002).

To be more precise, and serpentine can be defined as mineral with the ideal approximated chemical formula of $Mg_3Si_2O_5(OH)_4$, or a group of minerals like antigorite, chrysotile, and lizardite (Krám al., 2009).

As highlighted by Kram et al (2009), in many disciplines, the term serpentine is broadly applied to all ultramafic rocks, plus, in pedology, botany, and ecology, the term serpentine rock or soil refers to rock or soil dominated by minerals with high Mg-silicate content (Alexander et al. 2007, Brooks, 1987, Coleman, 1971).

Serpentine minerals are formed from olivine minerals (and pyroxenes), usually in peridotite, that are exposed to water, where peridotite is represented as a coarse-grained rock composed chiefly of olivine with or without other mafic minerals such as pyroxene and amphibole, or by its' more specific forms such as are dunite and harzburgite (Alexander et al. 2007, Coleman, 1971). As typical ultramafic rocks serpentinite and peridotite contain more than 90% of magnesium-ferrous, dark-colored minerals and with the content of SiO_2 below 48%. (Kram et al., 2009)

3.3.2. The origin of serpentinite

The origin of serpentinite is inferred to be a metamorphic alteration product of mantle rock or oceanic crustal rock, and most of the serpentine in the world is derived from ultramafic mantle rocks through the process of serpentinization. In this process, water invades fractured mantle rock and alters it to serpentinite. Complete serpentinization of an ultramafic rock requires a dramatic influx of water that produces a large expansion of volume up to 33%, with a corresponding decrease in density from 3.3 to 2.5 Mg m^{-3}, as the newly formed serpentine minerals require much more volume than the primary minerals they replace. In this slow and complicated process, the rock changes from a brittle, strong, dense peridotite to a plastic, weak, light serpentinite. The serpentinite is easily deformed and often rises in the form of buoyant rock as a diapir, when orogenic folding forces the light and weak serpentinite to migrate upward (Alexander et al., 2007, Hostetleret al. 1966.). Peridotite and serpentinite are chemically similar, but about 12–15% water is added to the crystalline structure in the conversion of peridotite to serpentinite. On the other hand, serpentinization is accomplished with no change in the relative amount of Si, Al, Mg, Cr, Mn, Fe, Co, and Ni. The only major component removed during serpentinization is Ca (Alexander et al. 2007), (Sleep et al, 2004.).

Serpentinites can be distinguished by their dominant serpentine mineral in the rock. The most common varieties are:

- antigorite-serpentinite
- chrysotile-serpentinite
- lizardite-serpentinite

Lizardite-serpentinite are characterized by pseudomorphic replacement of the original minerals olivine, pyroxene, amphibole and talc by the serpentine mineral lizardite (and sometimes magnetite or brucite). This serpentinite can be found in retrograde terrain. Also antigorite-serpentinites can be found in retrograde terrains similar to lizardite-serpentinite, but have been formed at higher temperature.
Chrysotile-serpentinites usually occur only in chrysotile asbestos deposits (Thesaurus of Cultural Heritage Computing at the University of Salzburg, 2014), Robertson, 1999, I-Think: Ni, 2013).

Minerals of the serpentine group are common examples of highly Ni-enriched phases during weathering processes and have been reported in worldwide mineral deposits (e.g. lateritic nickel deposits from Brazil, New Caledonia, Australia, etc.). The Ni analogues of lizardite and chrysotile (nepouite and pecoraite, respectively) can retain much more than a 30% of NiO, becoming frequently one of the main Ni-bearing phases in alteration zones of mineral deposits. Especially interesting are those nepouites in intimate mixture with kerolites (10 Å talc) or other hydrous silicates that may form the distinctive garnierite in the supergene domain (Suarez Bilbao et al, 2008).

3.3.3. Geographical distribution of serpentinites

Serpentinites can be found worldwide, particularly in greenstone belts, mountain chains and mid-ocean ridges, formed through the serpentinization of ultramafic rocks e.g. California, Penninic Units (Austria, Switzerland, Italy), Greece, Turkey (Thesaurus of Cultural Heritage Computing at the University of Salzburg, 2014, Robertson, S. 1999).

They are also found in deposits from Brazil, New Caledonia, Australia (Suarez Bilbao et al., 2008), when Suzuki et. al. (1971) presented a description of serpentinite sites in Hokkaido, Japan.

3.3.4. Serpentinite soils and ecosystems

Landscape with serpentinite bedrock tends to have thin or absent soil cover.

 Serpentinite soil tends to have low levels of all major plant nutrients (particularly calcium), and tend to be rich in magnesium, chromium and nickel. Many plants that grow on serpentinite will grow also on non-serpentinite soils, but they tend to be pushed out by other species, particularly non-native grasses. However, these do not grow well on serpentinite soil (Stoffer & Messina, 2002) (Bonifacio et al., 2012).

As mentioned by Bonifacio et al. (2012) this poor chemical fertility is directly linked to the elemental composition of the parent rock and is well known under the name of *serpentine-syndrome*: serpentinitic soils have low amounts of

phosphorus and potassium, an unfavourable Ca to Mg ratio and, in addition, high concentrations of potentially toxic heavy metals, such as Cr and Ni, inducing strong limitation in plant growth (e.g., Alexander, 1988)

It was stated, that, in general, ecosystems with serpentine soils are less productive than ecosystems with most other kinds of soils. Vegetation on serpentine soils is often sparser, smaller in stature, and atypical for its particular climatic zone, with an unusual plant species composition. Many endemic species are entirely or almost entirely restricted to serpentine areas (Alexander et al. 2007),

The formation of soil minerals was shown to be of little importance in the serpentinite soils, and the low development was demonstrated for C horizons from a wide range of environments, from Oregon (Burt et al. 2001), to the Vosges Mountains (Chardot et al., 2007), to western Italy (Bonifacio et al., 1977).

3.4. Behavior of selected elements in serpentinite profiles

Here, a more close review is given to describe the behaviour of some elements which are the among most characteristic for serpentinite soils.

3.4.1. Alkaline/alkaline earth elements in serpentinite soils

First, we will take a look at the distribution of alkaline and alkaline earth elements (Mg, Ca, Sr, K)

A wide variability in the concentration of Ca and Mg is typical for soils of serpentinite landscapes and depends on the type of parent material and on the presence of Ca-bearing accessory minerals (McGaham et al., 2009, Bonifacio et al., 2012).

Based on Bonifacio et al (2012), the abundance of serpentine minerals in the clay fraction of poorly developed soils is an index of varying fertility conditions and indeed, it affects the total concentration of Mg, Ca and K. In their survey, K deficiency was observed in the clay fraction of some serpentine-poor soils with low K_T contents. This also means, that among the factors inducing the serpentine-syndrome, K deficiencies seem the least specific. Ca and Mg which were also investigated in this study, were found to be released into the soil solution and then

leaching downwards, to take part in the formation of secondary minerals, or become sorbed on the soil exchange complex. The study also confirmed the previous ideas about Mg cycling, namely, that it dominated in serpentine-rich soils and was the sole element, which showed dependence from the parent material. Also, Mg high concentrations causes that the ratio between exchangeable Ca and Mg may be extremely low (e.g., Alexander, 1988). This also goes in hand with the conclusion, made by Jobbágy and Jackson (2001), who showed significantly higher proportions of K and Ca in the first twenty centimetres in a data set of over 8000 samples, while Mg in creased with depth since plant uptake from the soil limited its leaching to a lesser extent (Jobbágy and Jackson, 2001). In general, in the serpentine soils, the content of the metal was higher than in most soils in the same area. The study of Bonifacio et al. (2012) showed a more marked depth trend in serpentine-rich soils, especially for the availability of Ca indicating a sign of biocycling in the top and of leaching in the bottom horizons (i.e., depletion-enrichment profile). These and other authors also demonstrated that the higher element availability on serpentines was mostly related to inputs of elements through litter mineralization and element concentration in organic soil was more likely dependent on plants, than on presence of serpentine minerals (Oze et al., 2008, Bonifacio et al. 2012).

In the case of exchangeable Ca and K instead, the lack of dependence from the soil parent material suggested that biota, hence biocycling, may play an important role in affecting the distribution of the available Ca and K pools.

Though decomposition of litter seems to be little affected by soil nutrient availability, serpentinitic soils are expected to display a lower mineralization rate because of the effect of heavy metals on microbial communities (Kazakou et al. 2008).

Generally, the average availability of Ca and K was higher in the top horizons than in the deeper ones, while no depth trend was visible for Mg.

At the same time the one should note, that the role of biocycling of these alkaline/alkaline earth metals can vary depending on the dominating vegetation (esp. tree) species of the site (Pape, et al., 1989), plus contribution from the atmospheric deposition should also be considered (Reynolds et al., 2006).

3.4.2. Metal elements in serpentinite soils

Trace metals of serpentinites– especially Ni and Cr - are released by weathering processes and other natural sources of trace metals such as volcanic eruptions and the deposition of marine aerosols. In the soil some trace metals are strongly adsorbed to the mineral matrix or fixed in stable complexes with soil organic matter, other ones are quite mobile. Here these elements show high affinity to humic acids, iron oxides, clay minerals and carbonates in the soil (Smidt, et al., 2012). Chemical and textural studies of the nickeliferous serpentine in Aguablanca, Spain, highlight the presence of two different mechanisms for the Ni retention during the exogenic cycle (i.e. cycles, operating at the Earth's surface): for (i) Ni metal structurally bounded and for (ii) Ni metal as pure native particles. The authors also report about heterogeneous distribution of the Ni along the hydrous silicate layers, which should be related to the different local growth conditions of the minerals with possible influence of disequilibrium conditions, and as well as to the different weathering conditions at low temperatures, which play an important role in the processes of Ni supergene enrichment (Suarez Bilbao et al., 2008.)

The study of Murmansk region by Pavlov et al. (1998), revealed that average contents of Cr in the B and C horizons for loose sediments were generally comparable within the area, though certain increase of the Cr content in horizon B was observed, due to that in horizon B stable minerals of chromium were exposed to the intensive influence of organic acids, which contributed to its extraction by acid extracts.

The same survey has shown that Ni distribution was governed by the same patterns as distribution of Cr.

A study towards investigation of serpentine soils was held by to Suzuki et al. (1971) and also allowed to describe special characteristics of these soils. As it was mentioned, the significant effect on the crops due to metal toxicity, which is caused by high nickel content in these soils, is not observed in the case of high quantity of chromium comparable to that of nickel. This fact led to the assumption that the harmlessness of chromium was closely related to its low solubility. In the study, nickel and chromium extraction by different solvents has shown that chromium was about 2 times of the total nickel content when comparing soluble nickel and

chromium. As for the total element of the soil fraction, the chromium content was high in the ferromagnetic minerals and nonmagnetic heavy minerals, while nickel content was low in both minerals. In particular, it was the lowest in the ferromagnetic heavy minerals. Although the nickel content was the highest in clay, magnetite or illumenite; great quantities of chromium, manganese and iron were detected in mineral grains.

The results of the study proved that heavy metal toxicity on plants in serpentine soil of Horokanai in Hokkaido, were due to exchangeable nickel in the soil and could not be caused solely by the high total chromium content, because of its low solubility. The growth injury of crops was due to the high level of both total and soluble concentration of nickel. Total chromium was high in nonmagnetic heavy minerals or ferromagnetic minerals, black hard mineral in the nonmagnetic heavy minerals, and the lowest in clay. The nickel content was highest in clay in contrast with chromium, however, high concentrations such as seen in chromium were not found (Suzuki et al., 1971).

3.5. Approaches of geological investigations

3.5.1. General notes

According to the exact aim, different chemical and physical methods can be used for investigation of the structure and chemical composition, as well the changes of those in space and time are being used. Among them, the most popular are represented by such techniques as X-ray analysis, spectroscopic and spectrometric methods, which usually require the corresponding preparatory steps.

In general, geochemical projects demand general requirements for chemical analysis such as:
- the analytical methods used must be sufficiently sensitive to allow detection of a wide range of determinands in all of the sample media at background levels;
- the analytical precision must be good, preferably significantly better than natural geochemical variation;

-   data and other records pertaining to the analysis and testing must be fully documented and traceable.

The last point is particularly important if data are planned to be used extensively for environmental purposes, such as in the assessment of background concentrations of elements in different materials for setting up or updating national or European maximum contaminant levels (MCLs).

Total element concentrations are most relevant for geochemical interpretation of data. For solid materials, this means that the silicate matrix either needs to be fully decomposed by mixed acid digestion before instrumental analysis, or a solid sampling technique such as X-ray fluorescence needs to be used. Information on leachable concentrations of the elements is also considered to be important (Salminen, 2005).

As a preliminary step for the scientific surveys of this kind, registration and record of unusual features of the neighborhoods of assay, such as traces of forest fires, violations of ground vegetation and soil, effects of logging areas or other economic activities can also be performed.

Special description of the types and composition of samples is also noted down.

It is useful to have the samples inspected visually, for each layer, starting from the A-layer and moving downwards. For the top layers, the large roots and stones should be removed first. Further the samples are usually dried at the corresponding temperatures and homogenized with special technical means to bring them to the state and size of the particles that would be appropriate for the further analysis (Niskavaara 1995).

As an example of the X-ray analysis application, the use of high-resolution techniques of electron microscopy was described in a study of almost monomineralic areas of Ni-serpentine in the Aguablanca deposit with the evaluation of the different sorption mechanisms of Ni related to the present weathering conditions at low temperature. It gave nice results, showing that serpentine occured as an accessory mineral in the middle-low parts of weathering profiles but represented the main Ni-bearing silicate in the supergene domain of the Aguablanca deposit (Suarez Bilbao et al., 2008).

If determination of bulk content of elements in the organic horizons is completed by analytical methods such as ICP-MS and ICP-OES, additional step of

extraction of elements with chemical digestion procedures is usually needed, where acids or their mixtures are used (with the latter being especially useful for the mineral samples), together with relevant standards. (Niskavaara, 1995).

To demonstrate this method, one could refer to a study of Pavlov (1998) in the area of Monchegorsk, Murmansk region, which outlines the main features of behavior of the elements in the soil horizons B and C with ICP-OES, and was quite successful, when extraction step was done by a mixture of nitric and hydrochloric acids.

Bulk content of rare and trace elements in the upper soil can be also performed by neutron activation analysis (INAA), however, as shown by Niskavaara (1995), for the mineral soil horizons, this method does not provide the required sensitivity, and, thus, good reproducibility for a wide range of elements. At the same time, extraction of elements mixture of concentrated nitric and hydrochloric acids (aqua regia) and the subsequent analysis methods ICP-AES or ICP-MS could be characterized by sufficient sensitivity and good reproducibility of the elements.

As the major analytical technique that was used in the run of the current study, ICP-OES method is be described in more detail below.

3.5.2. The choice of analytical techniques

When choosing the analytical equipment to use for the specific study, one need to think about which technique would better correspond to the aims and criteria for the particular applications. For this purpose, the immediate analytical task should be described precisely and estimation of the amount of work should be done. The points to be considered are:
- The number of elements to be determined and their concentration range in the sample
- The type of elements
- The type of the matrix and the possibility of interference
- The amount of sample available
- The required precision of the analysis and speed, number of determinations and their costs

From comparison of such technics as, for example, Flame Graphite furnice AAS, ICP-OES or ICP-MS, ICP technologies have advantage if the number of

elements is five or more. To reduce the possible interference, ICP technics would usually be a better choice, then AAS, and have a better detecting power. The possibility of interference by matrix in ICP-AES might appear due to sample transport, rather than to chemical interference.

To talk about the speed, though AAS is generally a faster technique, ICP-OES would be preferable, as it allows to proceed determination of several elements simultaneously at one step. In addition, ICP –OES have large working ranges, so the time is saved by not having to dilute the samples.

Regarding all these recommendations, ICP-OES was the most suitable method for our data analysis, as, firstly the study implied determination of several elements, which could all be determined simultaneously by this instrument (in accordance with the recommendations of Nolte (2003), and the concentrations of the elements could differ significantly, from one element to another, within a certain range, which is still within the detection under determination limits of ICP-OES (Nolte, 2003).

3. Methodology

4.1. Description of the study site

The study site is represented by an area with naturally enhanced concentrations of Ni and Cr, located in the petrologically diverse Slavkov Forest (Slavkovsky les), which is a Protected Landscape Area with an area of 610 km^2 (Majer et al., 2005) in western Bohemia, Czech Republic, about 120 km west of Prague. (Figure 3, 4). The highest elevations are in the southwest; Lesný at 983 m and Lysina at 982 m have the highest summits.
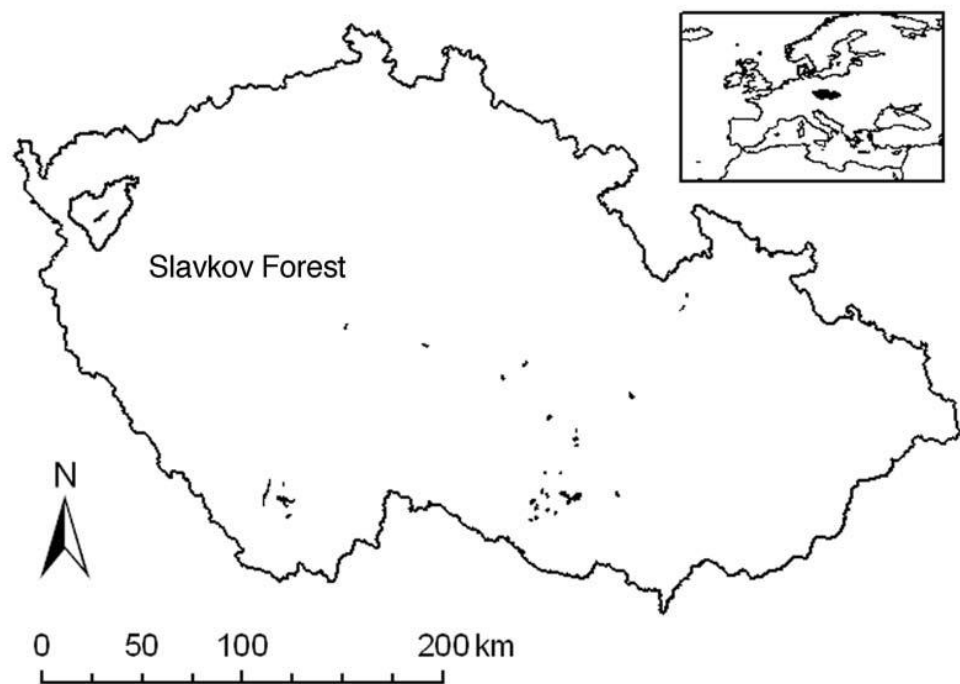
Figure 3. Schematic map of Czech Republic with the location of the Slavkov Forest in the west and occurrences of ultramafic rocks (e.g. serpentinites) in the Czech Republic (Krám et al., 2009)
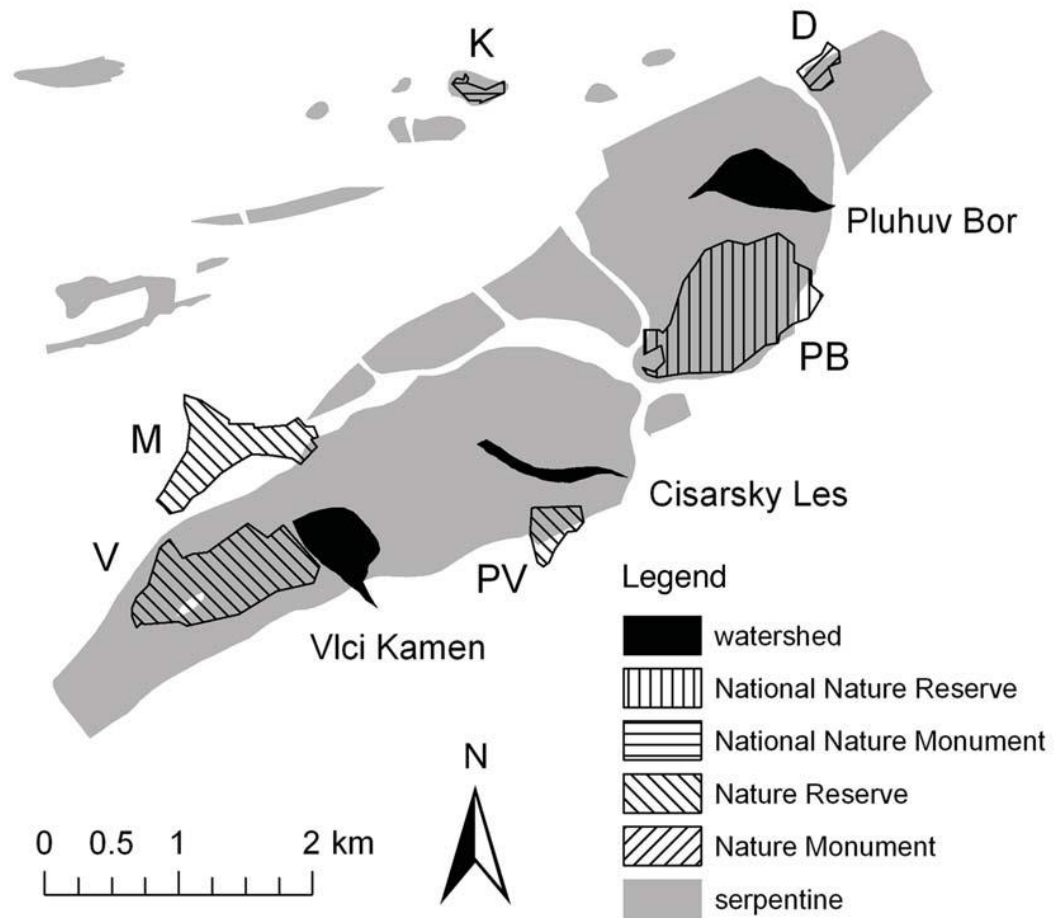
Figure 4. Map of the central part of the Slavkov Forest, showing occurrences of the Ni and Cr rich ultramafic rocks (mainly serpentinites), and also our study watershed Pluhuv Bor (Krám et al., 2009).

The region was not glaciated and is overlain by residual soil. The 21.6-ha Pluhuv Bor watershed is almost entirely forested by a nearly 110-year old plantation of *Picea abies* (Norway spruce) mixed with native *Pinus sylvestris* (Scots pine) in the highest elevations.

It is mainly underlain by serpentinite, with occassional tremolite and actinolite schists and amphibolite outcrops. Tremolite schists and especially serpentinites are characterized by extremely high concentrations of Mg, Ni, and Cr and by negligible concentrations of K, Ca, and Na creating an unusual and challenging environment for plants. The spruce growth rate is very slow, apparently as a result of K deficiency, Mg oversupply, and Ni toxicity (Kram et al., 1997, Kram et al. 2009).

The geoecology of this serpentinite-dominated site in the Czech Republic has already been investigated by rock, soil, water, and plant analyses. As it has been shown Slavkov Forest possess the most extensive accumulation (230 km^2) of metamorphic mafic and ultramafic rocks in the Bohemian Massif, the large craton of Central Europe. This accumulation has a triangular shape and is called the Mariánské Lázne Complex (MLC). It forms an independent unit (allochthonous body) of an ophiolite nature with foliations dipping mostly to the southeast. The MLC is associated with a first-order tectonic zone, interpreted as a subduction related boundary between the Saxothuringian Zone (SZ) and the Teplá Crystalline Unit (TCU). The ultramafic complex of the MLC spans approximately 9 km^2. The main strip of the ultramafic ridge (Vlčí Hřbet), 8.1 km long and up to 1.6 km wide. In addition, about ten smaller, elongated bodies of basal serpentinites occur as isolated pods or outliers of the MLC rocks. In the study, of Krám et al. (2009), 47 outcrops were described in the Pluhuv Bor watershed and its immediate vicinity. Twenty-four (51%) outcrops were formed by serpentinite, seven (15%) by tremolite schist or tremolitite, six (13%) by actinolitic schist or actinolitite, and another six (13%) by amphibolite and other geochemically similar rocks. The four major rock types differ markedly in chemical composition. Tremolite schists and serpentinites are characterized by extremely high concentrations of Mg, Ni, and Cr, and only negligible concentrations of K, Na, and Al. (Kram et al., 2009) . More details about abundance of selected toxic metals and cations in the rocks of our site are given in the Table 2a,b.

Content, %	Serpentinite	Tremolite schist	Actinolite schist	Amphibolite
CaO	0,34	7,27	9,78	8,8
MgO	36	24,9	12,6	8
K$_2$O	0,018	0,024	0,15	0,23
Na$_2$O	0,022	0,087	2,8	4,5
Al$_2$O$_3$	1,21	2,6	14,5	16,4
Fe$_2$O$_3$	6,37	4,06	2,03	2,4
Ni	0,197	0,131	0,023	0.007

Cr	0,241	0,255	0,055	0,010

Table 2a Elemental composition (mass percentage) of major rocks in the Pluhuv Bor watershed (Kram et al., 2009).

Content, ppm	Serpentinite	Tremolite schist	Actinolite schist	Amphibolite
Ca	2429,953	51958,11	69896,88	62892,9
Mg	21709	150156	75982,54	48242,88
K	149,427	199,236	1245,222	1909,34
Na	163,209	645,416	20772	33383,57
Al	6403,925	13760,5	76741,25	86797
Fe	44553,44	28396,7	14198,35	16786,22
Ni	1970	1310	230	70
Cr	2410	2550	550	100

Table 2b. Elemental composition (ppm) of major rocks in the Pluhuv Bor watershed (Kram et al., 2009).

Spruce tissue concentrations were also estimated and extremely high concentrations of Ni were observed, and Ni was especially concentrated in the bole bark. Concentrations of Ni in *Picea abies* at Pluhuv Bor were about twice the upper critical concentration, representing the point at which yield starts to decline (Table 3a, b) (Krám et al., 2009).

Spruce tissue	Concentration in g kg^{-1}				Ni mg kg^{-1}
	Ca	Mg	K	Na	
Foliage	6.53	2.71	3.27	0.027	11.4
Branches and twigs	3.67	1.00	1.80	0.017	10.0
Bole bark	8.37	1.57	2.03	0.010	20.0
Bole wood	0.53	0.16	0.14	0.010	0.70
Cones	0.16	0.47	1.10	0.022	10.9

Table 3a Mean total element concentrations and pools of *Picea abies* tissues in the Pluhuv Bor watershed (Krám, 1997)

Spruce tissue	Dry weight pool in kg m^{-2}	Pool in g m^{-2}				Ni mg m^{-1}
		Ca	Mg	K	Na	
Foliage	1.0	6.6	2.7	3.3	0.027	11.4
Branches and twigs	2.4	8.7	2.4	4.2	00.039	23.7
Bole bark	1.9	15.5	2.9	3.8	0.019	37.0
Bole wood	15.3	8.1	2.5	2.1	0.154	10.7
Cones	20.5	38.8	10.5	13.4	0.240	82.9

Table 3b Mean total element concentrations and pools of *Picea abies* tissues in the Pluhuv Bor watershed (Krám et al., 2009).

Streamwater at Pluhuv Bor has been under environmental observation since 1991. A typical feature of serpentine waters is an elevated concentration of Ni and the long-term mean streamwater concentration of potentially toxic Ni was 88 μg L^{-1} at Pluhuv Bor (standard deviation= 45 μg L^{-1}, range = 23–253 μg L^{-1}) (Kram et al., 2009). These values were always above 20 μgL-1, the European Union annual mean limit for inland surface waters (Anonymous, 2008). The main characteristics of the catchment are listed in the Table 4.

Location	50^{0}04'N, 12^{0}46'E
Altitude (m)	690-804
Drainage area (km^2)	0.216
Mean slope (%)	13.0
Aspect	South-Eaast
Forest stands structure	Forest>20 years (93%) Young forest and grass (7%)
Tree species	Norway spruce (Picea abies) (92%) Scots pine (Pinus Silvestris (8%)
Average age of spruce trees (yr)	120
Prevailiing soils	Euthropic brown forest earth
Bedrock	0.529 Serpentinite
Precipitation (open areas) 1992-2013 (mm)	800
Throughfall (bellow spruce canopy) 1992-2013 (mm)	564
Runoff 1992-2013 (mm)	307

Table 4 Characteristics of the Pluhuv Bor catchment (Hruska & Krám, 2003, Krám et al., 2014)

4.2. General structure of geochemical survey

Usually the studies of intrusive rocks should include several steps of different spatial scale and precision as follows:

1) Study in the field: to identify the geometry, size, and position of the rock of interest;

2) Study at the mesoscopic scale: to define the structure of the rock, i.e. the set of its' most obvious features externally;

3) Petrographic (microscopic) study: to define the compositional and textural characteristics, i.e. the arrangement of the various constituent minerals in the rock and their semiquantitative chemical composition;

4) Chemical study: to define the chemical composition using analytical techniques: X-ray fluorescence analysis (XRF) of the whole rock, the electron microprobe analysis of individual mineral phases, mass spectrometry of rocks and individual minerals.

The information provided by just one sole study method may not be sufficient.

So, geological studies are carried out by coupled petrographic, macroscopic and chemical analyses (Garofalo, 2014).

The study, described in the current work represents an input made into such a complex project, developed by the scientists of the Czech Geological Survey, and below the detailed description of the activities is provided.

4.2.1. Setting of the experiment and sampling

Spatial variations of the bedrock and soil by depth in the weathered profile underlined by serpentinite and another ultramafic rocks (mainly tremolite and actinolite schists) and mafic amphibolite in the area of Pluhův Bor, catchment in the Slavkov Forest in the western part of the Czech Republic, were investigated by coring and digging soil pits. First, a 26.14 m – long core was obtained from at the top of the PB catchment, with a truck-mounted drill rig. The drilling process itself took

place in the location at 50°03.778´N and 12°46.619´E at the height of 801 m above the sea level, on 29-30th August, 2012. The diameter of the core was 175 mm preborehole (for the uppermost part), 89 mm conductor casing (for the uppermost part) rest, 76 mm borehole (for the main part). More detailes can be found in the Appendix 1.

The drilling was done by Stavební geologie IGHG Tachlovice using the machinery ADBS, Mercedes Benz Atego. The scientific drilling at the site funded via the European 'SoilTrEC' project (http://www.soiltrec.eu/, Menon et al., 2014) as the current study represents a part of this bigger project.

Core recovery, estimated as the relation between the sum of length of core pieces and total length of the core was found close to 99% , i.e. can be classified as "excellent" . The best location for the planned borehole, situated between several serpentinite outcrops and very close to the SoilTrEC soil pits was unfortunately not accessible to the drilling truck. Therefore the location for the actual drill core has been chosen as the the closest accessible to the first location by the truck. The sole drill core was done, but exposures of soil and bedrock interface in outcrops were also used for visual estimation of the spatial differences in weathered-profile development.

In the whole, 74 samples were taken for the analysis, among which sixty samples were taken from the rock-part 26.14 m core to characterize the unweathered parent material and the weathered rock, while the other 14 samples represented the upper (soil) layer. The large pieces of the core were then sectioned into the shorter parts by sawing those by lengths to obtain smaller cylindrical samples of cca 3-5 cm thickness, which represented the soil profile at different depths and were used for the further studies and chemical analysis (Photo 1 a, b)
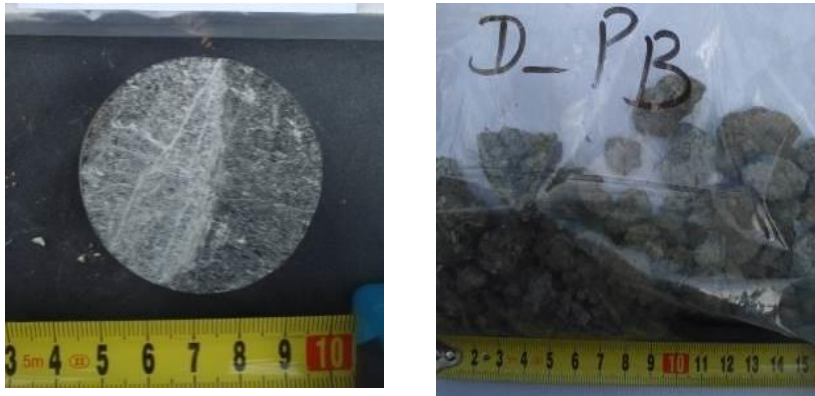
Photo 1. Examples of bulk rock/soil samples prepared for the homogenization and further chemical analysis (Left): unweathered rock parent material from the drill core and (Right): a soil sample underlained by the corresponding bedrock

Specifically, separate samples were taken at the intervals of approximately each 20-40 cm of the length of the core. Here the certain parts were chosen by the subjective opinion of the researches, based on the objective characteristics, such as structural integrity and the visible geological homogeneity and representiveness of each particular piece, which would serve for more convenient and reliable analysis at the further step, and according to mineralogical variations by depth. All the samples were weighed using analytical electronic scales, and so the weight of separate samples before the anaysis was shown to be within the range of 59 g as the minimum and 422 g as the maximum with the avearage of 138 g. The exact depths and and weight of each sample, taken for the analysis are documented in the Table 19 (see results section). The Appendix 1 also contains the summary of the field description as well as petrological and mineralogical characteristic and their variations along the total length of the core which were first done by visual examination by the experienced petrologists of the Czech Geological Survey (Veronika Štědrá, Tomáš Jarchovský) before the chemical analysis was evaluated. Further the microscopic analysis of the thin-sections was completed to confirm the mineralogical composition. Veronika Štědrá performed the microscopic/mineralogical analysis, these results are represented in the Appendix 2 of the current work. This information was important, as it could provide the general overview on the profile and was useful for setting up the further, more accurate experimental steps for the chemical analysis. The thin sections were made at the magnification of 2X0,1 in both in plane-polarized

light (PL) and cross-polarized light (XL). Here the samples, that represent different litholocal types are represented. According to this analysis, the sample from the depth of *4,5* of the drill core can is almost pure serpentinite with some magnetite veinlets, brittle cracks filled by secondary minerals. The sample of *7,5* m represents mostly magnetite-rich amphibole with coarse-grain chlorite. For the sample of 17,1 m depth it was possible to observe some law propotion of plagioglas in the partly-altered amphibole matrix with enclosures of magnetite and chlorite. The sample of 22,4 demonstrates vained structure, with larger amphibolitic crystals in the extremely finely grained amphibole matrix, which includes opatite, as accessori mineral, with rutile, epidote group minerals.

4.2.2. Physical and mechanical elaboration of the samples.

Soil samples were let to get dried. Rock and soil samples were prepared for chemical analysis by producing powder with a grind mill (electric agate mortar), giving homogenized product with a microscopic grain. The homogenization procedure was evaluated using the facilities of the laboratory of Czech Geological Survey

As the next step, aprroximately 0.1 g was weighed from each sample for the further digestion procedure using analytical balances (the exact amounts of each sample can are documented in Table 19. The weighed samples were then transferred into the Teflon vessels.

4.2.3. Digestion procedure

The first part of the digestion procedure was done in the Clean Laboratory of the Czech Geological Survey.

- As a preparatory step, chloric acid of 6 M concentration was prepared by dissolution of concentrated HCl acid.

- 1 ml of concentrated nitric acid (HNO_3) was added to each vial together with 3 ml of concentrated fluoric acid (HF). The vials were then closed tightly and put at on the hotplate and left there to react at 130^0 C for the period of 2 days.

Here HF was used to digest of the silicates and break-up calcium fluoride (CaF_2) contained in the samples, while HNO_3 served for breaking the organic compounds, as well as some weaker minerals, such as phosphates.

- Next, after the first digestion step has been accomplished to give clear solutions, the vials were opened and put on the hotplate, set at 130^0 C, again to let the solutions evaporate until dryness.

- After the vessels with the dry mass were put away from the hotplate and cooled down the first portion of concentrated HNO_3 in the amount of 1 ml was added to each sample.

- The vessels were kept open again at the hotplate at the temperature of 130^0 C for cca 1 day to evaporate till dryness. This step was done to ensure the dissolution of fluorides.

- For the samples with high content of organic matter, namely the samples from the top-soils, hydrogen peroxide (H_2O_2) in the amount of 1 ml was also added to guarantee the release of the organic compounds.

The vessels with the samples were then transported to the laboratory of the department of Environmental Geochemistry at the faculty of Environmental Sciences of the Czech University of Life Sciences in Prague, and the rest of the procedures, described below, were conducted using the facilities of this laboratory.

- The previous procedure (step 4) was repeated two times more (i.e. dissolution by nitric acid with the consequent evaporisation was completed three times in total to ensure that the fluorides were dissolved totally).

- 8 ml - portions of concentrated chloric acid HCl were added to the vessels. The vessels with these solutions were closed tightly and kept again on the hotplate for cca 12 hours at the temperature of $70-80^0$C. As a result of this clean-sample solutions were obtained. This step also helps to get rid of fluoride.

- The vessels with the clear solutions were put again onto the hotplate opened and kept to evaporate until dryness.

- After having been purified according to the steps, described above, the samples were made into the clear solutions to be ready for the analysis, using the ICP-OES. This has been achieved by dissolving the dry masses with 3 ml of concentrated HNO3 with the consequent heating at the hotplate at the temperature of 130^0 C, where they were kept overnight. After the clean solutions were obtained, they were transferred to 100 ml plastic bottles and made to the volume by pure MilliQ

water, so that 100 ml of the solutions of each sample were prepared in 3%-HNO3, which was suitable for ICP-OES analysis.

Precautionary measures for the digestion procedure were:

1. The solutions after digestion at each step should be clear and not have any dark spots of sample or any floating material otherwise the process should be repeated.

2. The solutions and the acids must be at ambient temperature before commencing the dissolution process

3. Excessive heating of the solution should be avoided also.

4. Due to the small amounts of the samples used and small concentrations of the elements under study (trace elements), special attention should have been paid to keep the working place clean to avoid or, at least, minimize the possible contamination of the samples.

5. For the same reason, it was also important to try to minimize the direct/inderect contact of the samples with metal (including using metallic appleances for preparatory and analytical procedures).

6. As using glass appliances may also contribute to the content of some elements in solution, as those can be released from the glass material at the amount, which is significant for such sensitive experiments as provided here, the laboratory equipement made of some more inert Teflon materials should be used.

7. Concentrated hazarduous acids were used in digestion procedures, so these steps were done in the ventilation chamber. Here, due to that small small amounts of the samples were used and to the fact, that on some steps they presented in the form of powder, it was important that the ventilation was switched to the level, that would be enough for ventilation of harmful fumes for safer working conditions, but not too high, so that the powedered samples would not be blown away.

4.2.4. Spectrometric Analysis

The last step of physico–chemical part of the work involved spectral analysis of the samples in 3%-HNO$_3$ solutions, using the last-generation technical facilities of the laboratory of the Department of Environmental Geochemistry at the Faculty of Environmental Sciences of the Czech University of Life Sciences in

Prague, namely Inductively Coupled Plasma-Optical Emission Spectrometry (ICP-OES).

Below the general information about the techniques of ICP-OES is provided.

4.2.4.1. Basic information about ICP-OES, as the main technical tool of elemental analysis.

General definition

Inductively Coupled Plasma-Optical Emission Spectrometry (ICP-OES or ICP-AES) is one of the most important techniques of instrumental elemental analysis and can be used for the determination of approximately 70 elements in a variety of matrices. (Nolte, 2003).

Here, a more broad term of *spectrometry* implies a technique for quantification that uses the emission or absorption of light from a sample, used for determination of concentrations.

Particulary, ICP-OES can be used for the analysis of rocks, which is usually of interest to geologists, mining companies and relevant government bodies. This may be for academic or commercial reasons. As a preparatory step, rock sample must usually be dissolved before it can be analyzed by an appropriate technique (Liberatore, 1994)

Advantages of ICP-OES:

1) The first advantage of the method is that all elements can be determined *simultaneously or very rapidly* one after another, so the analytical results for a sample can be obtained after a short analysis time.

2) For determination of an element, *no specific equipment* is needed, but only a calibration solution of the elements is analyzed.

3)In environmental analysis, the *working ranges* for many elements correspond to the concentrations usually found in the samples, so the technique is widely used in environmental applications, and there are a number of standards and regulations that apply.

Principle scheme of an ICP-OES machine:

In ICP-OES sample introduced into the ICP as liquid form, and this is the most common technique for sample introduction. For solid samples, sample is converted to liquid by dissolve it into proper solvent. Liquid sample goes through different steps when injected to the ICP. In nebulization process the sample is converted by pressure to a mist of finely divided droplet called aerosol, which is followed by separation of aerosol in the spray chamber, so that only fine droplet carried to the plasma, as illustrated in the Figure 5 (CHEMIASOFT, 2014).
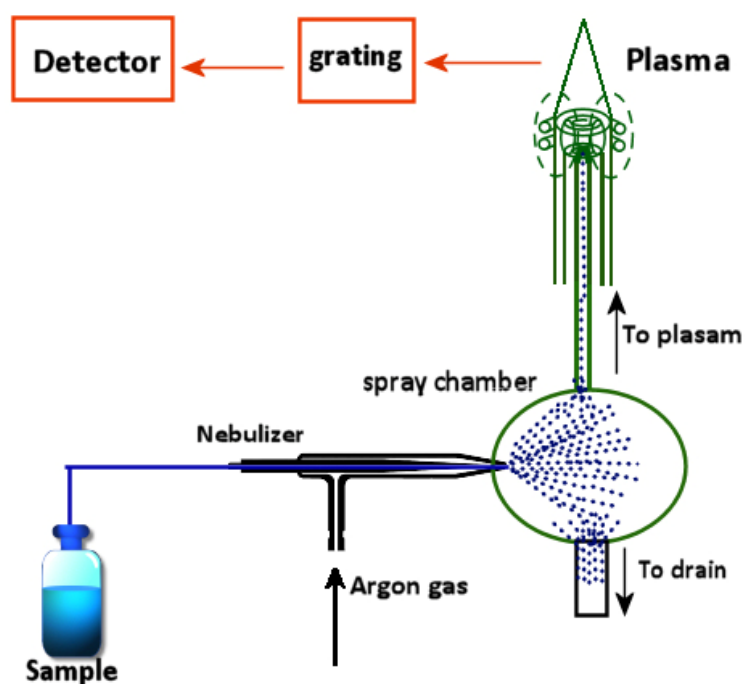
Figure 5 Diagram of sample introduction to ICP-OES (CHEMIASOFT, 2014)

The heart of an ICP emission spectrometer is plasma (extremely hot gas with a temperature over several thousand Kelvin). It is so hot that atoms and ions are formed from the sample to be analyzed (Nolte, 2003).The emitted radiation from the plasma is then used for analysis. The emitted light is *spectrally resolved* with the aid of diffractive optics, and the emitted quantity of light (its intensity) is *measured with a detector* (CHEMIASOFT, 2014).

Principle of analysis by ICP from the point of view of physics:

The very high temperature in the plasma ionizes the sample completely, so that the analytical result is not usually influenced by the nature of the chemical bond of the element to be determined, which means absence of chemical interference.

In the plasma, atoms and ions are excited to emit electromagnetic radiation (light). The energy in the plasma is transferred by collision of argon, with the energy of 15.76 eV, ion with another atom. The ionization energy of many metals is typically approximately 7-8 eV. Namely, for the elements under our study it equals 7.64 eV for Ni, 6.77 eV for Cr, 4.34 eV for K, 6.11 eV for Ca and 7,65 for Mg (Nolte, 2003). So there is plenty of energy still available for further excitation of an ion to enable many transitions originating from ions. The degrees of ionization of the two elements are 91% for Ni, 98% for Cr and for Mg, 99% for Ca and 99.9% for K. The number of certain species of atom or ion (e.g. charged singly, doubly, etc) depends on the temperature, and each of them would have a characteristic peak of its' concentration at some certain temperature.

Outcomes of ICP-OES analyses:

In ICP-OES, the wavelengths are used for the *identification* of the elements, while the intensities serve for the determination of their *concentrations*.

There is a linear relationship between intensity and concentration over more than 4 to 6 decades. This intensity concentration function depends on a number of parameters, some of which are unknown, so there is a need for empirical proportionality factors, which should be determined before the analysis by calibration.

After having been excited, the electron stays on briefly in this state, and the energy difference between the two energy levels is emitted as electromagnetic radiation predominantly in the ultraviolet and partly in visible wavelength regions. So OES results in spectra which is more line rich than e.g. in AAS.

In an energy level diagram, the possible energy levels of the orbitals are visualized where the ordinate indicates the energy difference to the ground state of the atom or ion.

Method development:

The method development, using the ICP-OES includes the following steps:

1. Setting up the spectrometer
2. Selecting the wavelengths for the elements
3. Generating spectra (for calibration solution, for representative samples, for quality control samples)
4. Show spectra in graphic display mode and evaluation.
5. Adjust scale, set background correction points.
6. Measure again at other wavelength(s), choose the wavelength.
7. Check and correction of undisturbed analytical line and non-spectral interference.
8. Optimize excitation conditions
9. Validate method.

The **goal of the method development** is to choose parameters which produce clear and undisturbed signal for analytical measurement. To be processed unambiguously, signal should stand out of clearly from the *background*, which requires a large signal/background ratio. All measured intensities are accompanied by random fluctuations, also described as noise, that can be caused by various reasons. The *reproducibility* may be used as a performance criterion for an adequately intense signal.

In ICP-OES, similarly to other analytical techniques, systematic or random deviations of the measurements from the true value are observed which are a result of interference, caused by components of the sample (matrix). In the course of method development, the measurement parameters which are used in the analytical measurement program of the spectrometer, are specified. The most important are

− Analytical lines (Table 9, 10)
− Excitation conditions
− Measurement times and repeats
− Selection of the processing techniques (particularly the background correction)

– Checking for and correcting fro non-spectral interference

The results may be *influenced* by the characteristics of the spectrometer, particularly resolution and the utilizable wavelength range. Excitation conditions of the plasma have a substantial influence on the intensity of the emission line due to the spectral interference. Thus, the optimization of the excitation conditions may be an important step during the method development. It is usually recommended to measure repeatedly in order to get meaningful information (Davies & Fearn, 1996).

To reduce carryover, the delay time may be increased.

Besides of spectral interference, non-spectral interference may occur, which should also be determined and corrected or compensated for.

Before samples are measured by ICP-OES, a number of operating procedures should be performed. All of them will influence the result. The most important operating steps are:

– Sampling of representative sample. Here inhomogeneity should be taken into account

– Sample storage and stabilization of the analytes

– Transport to the laboratory

– Taking of laboratory sample from the original sample

– Specific sample pretreatment in order to convert it or the analytes into a form, that can be used by the analytical instrument.

– Measurement of the physical information value

– Conversion of the signal into a concentration (processing)

– Data transmission, preferably electronically

– Interpretation of the data

For a method development for particular application, it is important to check the suitability of recommended wavelengths while working with a certain spectrometer, due to possible differences in such parameters as resolution, utilizable wavelength range, generator and sample introduction system). Nolte (2003) recommends the specific wavelengths for determination of Ni and Cr in geological and soil samples. Also, it should be noted that the choice of analytical line must be made for each type of rock individually (Table 9) (Nolte, 2003).

Element	Wavelength [nm]	Alternative wavelength [nm]	Further wavelength [nm]
Ni (soil)	231.604	221.648	
Ni (rocks)	231.604	221.647	
Cr (soil)	267.716	205.552	283.552
Cr (rocks)	267.716	205.552	283.563
Ca (rocks) (CaO)	315.887	317.933	422.673
Ca(soils)	315.887	317.933	422.673
Li (rocks)	670.781	610.362	
Li(soil)	n.i.	n.i.	
Sr(rocks)	407.771		
Sr(soils)	407.771	421.552	
Ti(rocks) (TiO$_2$)	334.940	336.121	
Ti(soil)	334.941	336.121	
Mg(rocks) (MgO)	285.213	279.553	279.079
Mg (soil)	285.213	279.079	279.553

Table 9 Analytical lines for environmental samples (Nolte, 2003)

Element	Wavelength [nm]	Alternative wavelength [nm]	Further wavelength [nm]
Ca	315.887	317.933	393.366
Cr	283.563		
Li	670.783		
Ni	231.604		
Sr	421.552		
Ti	334.941	336.122	
Mg	285.21	280.270	279.553

Table 10 Analytical lines used for the samples from Slavkov Forest drill core

The measures for quality assurance to be taken at the preliminary and analytical steps.

For the first, general *recommendations* include:

- to avoid using of glass, particularly when working in the trace range, due to the effects that are likely to be caused by absorption and desorption processes.

- taking fewer steps in the analytical procedure to reduce the risk of contamination and absorption, which overweighs the potential volumetric error and can reach up to several orders of magnitude and is of particular importance in the case of trace elements.

- using a medium, that insures stability for all solutions. As a rule, they are acidic, and the concentration of the acid frequently decides the stability of the analytes in the solution.

It is generally true to say that the higher the concentration, the larger is the analyte signal. Though, the possible interference by easily ionizable elements should be taken into account, especially in the presence of alkali metals. So the optimal concentration of the salt should be determined experimentally by checking the sensitivity as a function of the dilution factor.

- the lower the concentration to be measure, the more care should be taken at every step and the reagents and the water for dilution must be extremely pure.

Principles of quality assurance have been developed for the analytical step (analytical quality control, or QC). Those originate from the quality supervision of mechanical series production, which include checking of *diameter of screws*, the *quality control samples*, prepared independently from the calibration solutions (ideally, standard reference materials) with known concentrations.

The standardized quality judgment is based on Shewhart quality control charts with the main parameters to be registered being mean value, blank reading, recovery and span width. The limits to describe the quality of analysis include Warning limits (+/- 2s) and Control limits (+/- 3s), where s is standard deviation of the mean values, determined during the pre-period.

The control of the a complex system of ICP-OES is insured by efficient, well-designed and intuitively usable software, which allows to make an *evaluation of*

the data possible after the analysis, to *represent the spectra* during the analysis for visual control of the accuracy of the results, and to *archive* data.

Notes and challenges of application of ICP-OES techniques in geological analysis:

The prime goal of environmental analysis with ICP-OES is the supervision or determination of concentration of elements in a variety of "natural" matrices of extremely diverse composition. (Nolte, 2003). This variability of matrices, which is, in particular, typical for geological materials, means that special attention should be paid to some details of the procedure, specific for this type of samples. Firstly, interference, which is not usually important in one sample, may suddenly dominate in another. In order to safeguard the results in such cases, it is recommended to determine an element, using several lines.

Digestion methods of geological samples, that are used to bring the "raw" samples to the state, in which they can be used for analysis, are also as different as the materials and are mainly fusion or acid digestions. . This is caused mainly by the variability of matrices and applications (Liberatore, 1993). The same is true for soil samples, e.g. they may have Si-matrix, Al-matrix, Ca-matrix, so that no uniform recommendation can be given for line selection. (Warda et al., 1980, Nolte, 2003).

To demonstrate the application of the method for rock samples. Liberatore (1993) described the analysis of geological samples by ICP-OES for 30 elements using 3 dissolution methods as follows:

- *US Geological (USGS) method:* using concentrated HNO_3, a mixture of concentrated HF and HNO_3, dilution by $HClO_4$ and distilled/deionized water.

- *double acid method* involving addition of concentrated HNO_3 to the samples to smaller amounts of the powdered samples in comparison to the US method were used adding HF with the following heating to get rid of Si as SiF_6, and distilled/deionized water.

- *Fusion method*, using a borate flux mixed added to the samples in platinum crucible and fused in furnace at 1000º C, addition of nitric acid, and distilled/deionized water to get made samples to the volume.

The values found in this study correspond well to the certified values.

From his results, Liberatore (1993) concluded, that for best detection limits the acid dissolution was better. The digests also were characterised by a lower probability to be contaminated compared with the fusion method. From the other hand, he also highlights that for rock samples, different dissolution methods need to be employed, depending also on the target elements. For example, for Al and Si and traces to be determined, performing the one fusion would satisfy both major and trace determination for most elements, while for if lithium or boron is determined the fusion method is appropriate, due to the large lithium concentration from the lithium metaborate flux.

The major problem for the case of trace elements is the contamination from chemicals and during sample preparation, which is why the use of pure reagents is paramount and the use of clean rooms is advised. All rock samples could have Ni successfully determined on the acid digests but not on the fusion sample (Liberatore, 1994).

The determination of majors in geological samples by ICP-ES has been described by the same autor, but using mainly the fusion method. The values found compare very well with the certified values indicating that this methodology is totally suitable for these geological samples (Liberatore, 1994).

4.2.4.2. Application of ICP-OES for the investigation of Pluhuv Bor studying site

The model of the machine

Agilent 720 Series ICP-OES- machine of axially viewed plasma type was used for the analysis. The machine had previously been reported to be approved for determination of toxic elements in waters, soils and sediments, metals and trace elements in waters and wastes, heavy metals in soils. It was optimized to give maximum sensitivity for trace-level applications, including the determination of trace and toxic elements in soils and waters.

The Agilent 720/730 axial meets all US EPA Contract Required Detection Limits (CRDL) for waters and waste waters and is capable of routinely handling up to 5% dissolved salts.

The machine is equipped by a user-friendly software with all instrument controls, sample results and signal graphics accessible from one window, which allows monitor results at two or more wavelengths for each element — giving confidence in the accuracy of the results and confirming they are interference free (Agilent Technologies, 2010)

The Agilent 720 ICP-OES features a custom designed CCD detector which provides true multaneous measurement, full wavelength coverage from 167 to 785 nm and fast read-out enabling short sample analysis times. The CCD detector has pixels arranged in continuous angled arrays that are matched exactly to the two-dimensional image from the Echelle polychromator. The optical system is housed within a thermally stabilized environment at 35 °C and contains no moving parts, ensuring excellent long-term stability. The polychromator can be purged with either argon or nitrogen gas for improved performance when measuring at low UV wavelengths. A conventional one-piece axial torch was used. The sample introduction system consisted of a concentric glass nebulizer and a glass cyclonic chamber. Agilent ICP Expert II software was used for instrument operation. Due to control system, the sample does not contact the peristaltic pump tubing at any time, reducing carry-over (Hoobin & Vanclay, 2011).

Limits of determination are represented in Table 11 which shows that mainly they were lower the expected values for the elements under study in our samples, and so made it reasonable to assume that the machine was suitable for determination of those. The only element, that was problematic to be determined was Ba.

Element	Al	Ba	Ca	Fe	K	Li	Mg	Ni	Sr	Ti	Cr	Na
Determination limit, mg/L	0,005	0,01	0,001	0,0005	0,005	0,001	0,0002	0,0004	0,0002	0,001	0,001	0,01

Table 11 Determination limits of ICP-OES procedure for selected elements for

The reference element technique (internal standardization) were usedmthroughout the analysis. Internal standardization allows correction for physical differences that may exist between sample types. A solution containing 0.1 mg/L yttrium (reference element) was prepared in a 3% nitric acid matrix (matched to the sample) was added on-line to the sample stream, using the third channel of the peristaltic pump. With on-line addition of the internal standard, sample preparation is kept to a minimum. (Hoobin & Vanclay, 2011).

Preparation of calibration solutions

Calibration solutions were prepared using standards of ANALYTIKA spol., CZ9090 MIX 010 which contains determination of 26 elements with concentrations of 100 mg/L. The standard was diluted in 5%-HNO3 and five points of the calibration were created with the concentrations of elements of 5, 10, 20, 50 and100 mg/L.

The procedure was repeated twice, where the two methods differed by the working power of the spectrometer (1.20 kW for method 1 and 1.30 kW for method 2).

The details of the working parameter of the spectrometer for the both methods are represented in Table 12, 13.

Parameter	Method 1	Method 2
Power (kW)	1.20	1.30
Plasma flow (L/min)	15.0	15.0
Auxiliary flow (L/min)	1.50	1.50
Nebulizer flow (L/min)	0.80	0.80
Replicate read time (s)	5.00	5.00
Instr. Stabilization delay(s)	35	35

Table 12 Working parameters of spectrometer

Sample introduction settings (methods 1 and 2)	Value
Sample uptake delay (s)	25
Pump rate (rpm)	11

Rinse time (s)	200
Fast pump (Sample delay/rinse)	On
Replicates	3

Table 13 Sample introduction settings

As an "etalon", to verify accuracy of the measurements of our experiment, we used the certified standard reference material, namely certificate UB-N (serpentinite powder), provided by *Centre de Recherches Petrographiques et Geochimiques, CNRS*, France. The referential concentration values, according to the certificate, for all the elements that were measured in the study are represented in the Table 14 (de la Roche & Govindaraju, 1967).

Element	Analytical data (concentration in sample)
Ni	1740 - 2130.3 µg/g 24 values (compiled: 1942 - 2000 µg/g, 3 values)
Cr	2090 - 2516 µg/g 17 values (compiled: 2300 - 2421 µg/g, 3 values)
Al	15600 µg/g
Ba	23.99 - 31.1 µg/g 31 values (compiled: 26.81 - 27 µg/g, 3 values) (uncertain : <23 µg/g)
Fe	52700 - 58300 µg/g 4 values g/g
K	< 200 - < 5000 µg/g 2 values, uncertain
Li	23.4 - 32 µg/g 12 values (compiled: 27 µg/g)
Mg	199000 µg/g
Na	950 - 1084 µg/g 3 values
Sr	6.7 - 11.8 µg/g 30 values (compiled: 7.7 - 9 µg/g, 3 values) (uncertain: <50 µg/g)
Ca	8080 - 9000 ľg/g 2 values
Y	2.17 - 5.5 µg/g 32 values (compiled: 2.5 µg/g)

Table 14 Overview of analytical data for the referential serpentinite powder of UB-N-cerificate (de la Roche & Govindaraju, 1967).

Table 15 shows the selected elemental concentration range covered by the calibration solutions for each element, that has been aquired by two different methods. As mentioned above, the difference between the two methods was mainly due the different power of spectrometer, chosen for setting up the spectrometer (Table 12). The wavelengths for each element were selected in the way that the resulting concentration values of measurement would agree better with the corresponding values the certificate. Sensitivity, linear dynamic range and freedom

from spectral interferences were taken into consideration during wavelength selection. For elements, such as Ca, Ti and Mg, more than one wavelength have been tested.

As it can be seen from Table 15, the results of the analysis using method 2 appeared to be more appropriate in comparison to method 1, as it matched better the concentration ranges of the reference values. So this method was used for the futher determination of the elements in the samples.

Element	Reference value (µg/g)	Method 1 (µg/g)	Method 2 (µg/g)	Wavelengths (nm)
Ca		7,9280	8,31039	317.933
Ca	8.08 -9.00	8,3496	8,64881	393.366
Ca		7,8991	8,20243	315.887
Cr	2.09-2.516	2,29251	2,28493	283.563
Li	0.0234-0.032	0,02553	0,03397	670.783
Ni	1.740-2.1303	1,84894	1,88580	231.604
Sr	0.0067-0.0118	0,00720	0,00724	421.552
Ti	0.529-0.677	0,56963	0,55886	334.941
Ti		0,56784	0,55955	336.122
Mg		58,66090	55,40703	279.553
Mg	199	94,12696	93,87988	280.270
Mg		149,61424	141,1896	285.21

Table 15 Comparison of the results of concentration measurements for selected elements from two methods of ICP-OES at CULS compared and certified referencial values

As the next step, 3%-HNO_3 solutions of the samples, that were prepared earlier by the methodology, described in the *Digestion procedure* part, were introduced into the machine.

The results of the analysis described represented concentrations of the elements in the solutions, and after were recalculated to values of the concentrations of the corresponding elements on each sample per one gram of the soil or rock sample, using the Equation 1:

$$C_{gram} = \frac{(C_{sol} \cdot 100)}{m_{samp}}$$

Equation 1: Calculation of concentration of an element per one gram of sample, using the results of its' concentration from ICP-OES analysis.

In this equation C_{gram} stands for the concentration of the element in one gram of the sample,

C_{sol} is concentration of the corresponding element in the 3%-HNO$_3$ - solution, used for analysis in ICP-OES, and m_{samp} represents mass of the sample, that was weighed and used for the preparation of the 3%-HNO$_3$ - solution for ICP-OES-analysis.

These calculations were visualised as graphs to create an view about the changes of concentrations of each element by depth, which should correspond to the changes of the rock type, and so would allow to confirm the previous visual estimations by preliminary visual field and petrological and mineralogical description. According to these results, the certain sector out of the whole length of the drill core, which represented serpentinite rock, was chosen for the further analysis.

From these concentrations, elemental losses and gains due to weathering processes in the soil and rock were quantified. For this purpose, a chemical mass balance model, which had been described by Brimhall et al was used (Brimhall et al., 1987, 1991) was used. This model was developed based on identification and characterization of the parent rock. It has been successfully implemented for several scientific investigations aimed on estimation of the processess in Critical Zone, such as that by Anderson et al. (2002). The model is elaborate, but simple and clear, which makes it more reliable at the same time. The logic comes from the idea, that physical deformation, or strain, accompanying weathering can be calculated by conserving the mass of an element that is unaffected by chemical weathering, so it enables to quantify both the chemical transformations and physical deformation in the weathering profiles.

The general assumption here is that the mass of a chemical element, m_j, in a volume of weathered material, V_w, is equal to the mass of the element in the volume of fresh parent rock, V_p, that weathered to produce V_w and the mass of the element added or lost in the weathering process, mj flux . It is shown in the balance Equation 2

$$\frac{1}{100}\left(V_w \rho_w C_{j,w}\right) = \frac{1}{100}\left(V_p \rho_p C_{j,p}\right) + m_{j,flux}$$

Equation 2 Mass balance for an element, presented in the weathered material and parent rock.

Here V_w - volume of weathered material, V_p - volume of the corresponding fresh parent rock, $m_{j,flux}$ - mass of the element added or lost in the weathering process, ρ - the bulk density, C_j - the concentration in weight percent of element j, subscripts w and p - weathered material and parent rock, respectively.

So, the volume changes, that appear in the weathering processes should be found in order to estimate the mass gains or losses within the same processes. Here the concept of immobile element, which does not have an external source, can be used to simplify the equation, as its' $m_{j,flux}$ term in the equation 2 is zero. Due to this volumetric strain, $\varepsilon_{i,w}$, of the weathered material relative to the parent rock can be found by the Equation 3:

$$\varepsilon_{j,w} = \frac{V_w}{V_p} - 1 = \frac{\rho_p}{\rho_w} \frac{C_{i,p}}{C_{i,w}} - 1$$

Equation 3: Volumetric strain, $\varepsilon_{i,w}$, of the weathered material relative to the parent rock, $\varepsilon_{i,w}$ - volumetric strain, i indicates immobile element.

Now mass gains or losses due to weathering can be calculated expressed as absolute mass changes per unit volume of parent rock, $\delta_{j,w}$, with units of mass per unit volume (Equation 4):

$$\delta_{j,w} \equiv \frac{m_{j,flux}}{V_p} = \frac{1}{100} * \left(C_{j,w} \rho_p \frac{C_{i,p}}{C_{i,w}} - \rho_p C_{j,p}\right)$$

Equation 4 absolute mass changes per unit volume of parent rock

The same can be represented as mass-change in percentage related to the mass of the element in parent rock giving the dimensionless element-mass-transfer coefficient, $\tau_{j,w}$ (Equation 5):

$$\tau_{j,w} \equiv \frac{m_{j,flux}}{V_p \rho_p C_{j,p}} 100 = \frac{C_{j,w}}{C_{j,p}} \frac{C_{i,p}}{C_{i,w}} - 1$$

Equation 5 Mass gains or losses due to weathering expressed as element-mass-transfer coefficient, $\tau_{j,w}$.

The resulting τ-values were used as the function of depth to create the graphs, depicting the elements losses and gains.

4. Results

1) The samples were examined visually for petrologial and mineralogical characterics.

Here, the lithological changes were defined in general and then confirmed by means of microscopy, showing that serpentinite ultramafic rocks are only dominant at the shallower depths of the first ca. 6 meters below the surface, and then they are often changed by dike rocks, partially melted amphibolic rocks and shear zones rich in Mg minerals. Serpentinite zone ends up at the depth of cca 6 meters below the surface. Massive amphibolite, with rutile as an indicator of a higher metamorphic overprint occurs only in the lower parts of the borehole The sample at 1960 cm can still be regarded geochemically as ultramafic rocks, but it already has a different character and mineralogical composition than pure serpentinized peridotite due to the higher content of Al and Ca, which corresponds rather transformed pyroxenic peridotites.

2) Approximately 1 g of each depth sample was weighed for the analysis using the analytical balance. The exact values are available in Table 16, and they were used for the further calculations.

3) After the digestion procedure, the samples were introduced into the ICP-OES machine in the form of 3%-HNO_3-solutions for the elemental concentration analysis.

The primary line was chosen for elements to eliminate possible interferences (Figures 12, 18), and the corresponding concentrations of each element in the samples solutions were measured (Table 16,).

Depth, cm	Weight, g	Concentration of the element in the solution, mg/L													
		Ca 315.887	Cr 205.560	Li 670.783	Ni 231.604	Sr 421.552	Ti 334.941	Ti 336.122	Mg 285.213	K 766.491	Fe 239.563	Al 396.152	Ba 455.403	Na 588.995	Y (internal standard correction factor)
-15	0,1048	24,646	3,273	0,020	1,288	0,086	2,587	2,639	124,158	6,195	82,688	44,544	0,159	8,330	1,00
-35	0,1	3,108	3,390	0,013	1,725	0,014	1,054	1,079	178,242	3,081	68,628	25,480	0,050	1,858	1,00
-70	0,1022	1,792	5,439	0,010	1,932	0,010	0,898	0,919	187,911	2,586	77,884	28,115	0,037	1,376	0,98
-95	0,1052	1,401	4,410	0,010	2,023	0,005	0,393	0,402	211,397	1,209	70,597	13,032	0,014	0,625	0,98
-120	0,1033	0,893	4,432	0,011	2,068	0,004	0,387	0,396	209,190	1,057	71,012	12,057	0,011	0,658	0,96
-160	0,0978	0,640	4,748	0,007	1,967	0,001	0,256	0,262	204,630	0,284	69,582	10,946	0,001	0,265	0,83
-195	0,0989	0,117	4,439	0,007	1,593	0,001	0,763	0,783	207,381	0,180	66,383	27,292	-0,001	0,210	0,98
-215	0,1025	0,116	5,293	0,002	2,099	0,001	0,326	0,335	210,795	0,133	76,723	18,604	-0,001	0,091	0,95
-255	0,1037	0,326	3,717	0,004	1,906	0,001	0,222	0,229	217,479	0,068	68,137	12,668	-0,002	0,099	0,98
-295	0,1023	0,410	3,823	0,003	2,198	0,001	0,198	0,205	218,988	0,069	63,052	5,442	-0,001	0,095	0,96
-315	0,1172	2,285	8,436	0,002	2,909	0,002	0,196	0,200	239,457	0,057	89,776	3,132	-0,002	0,085	0,94
-355	0,1081	0,539	5,474	0,001	2,629	0,001	0,103	0,104	232,552	0,114	85,951	2,428	-0,001	0,099	0,94
-395	0,1174	0,790	5,171	0,002	2,936	0,001	0,093	0,094	245,520	0,092	80,133	2,131	-0,001	0,085	0,94
-415	0,11023	0,143	5,006	0,001	2,328	0,001	0,084	0,085	215,686	0,105	66,523	2,261	-0,002	0,086	0,95
-455	0,1008	0,285	2,797	0,005	1,845	0,001	0,089	0,092	214,465	0,221	50,643	2,925	-0,001	0,276	0,95
-495	0,1006	0,164	2,864	0,002	2,067	0,001	0,061	0,062	217,776	0,063	54,438	2,711	-0,002	0,091	0,94
-537	0,1084	0,321	2,404	0,004	1,940	0,001	0,106	0,108	231,690	0,133	59,606	4,272	-0,002	0,218	0,98
-560	0,1004	0,604	2,098	0,011	1,904	0,001	0,084	0,086	211,211	0,067	55,414	11,359	0,000	0,147	0,94
-597	0,106	0,795	0,901	0,001	0,420	0,001	4,541	4,647	185,770	0,143	74,707	94,785	-0,002	0,204	0,99
-616	0,1	7,183	1,897	0,002	0,872	0,003	3,739	3,820	172,552	0,142	104,507	87,154	-0,002	0,355	0,94
-671	0,104	19,507	4,952	0,003	2,080	0,004	0,286	0,291	182,924	0,106	65,166	18,798	-0,001	0,574	0,95
-720	0,1122	92,819	1,069	0,029	0,494	0,076	3,668	3,745	94,390	4,474	70,492	91,164	0,356	17,618	0,95

Depth, cm	Weight, g	Concentration of the element in the solution, mg/L													
		Ca 315.887	Cr 205.560	Li 670.783	Ni 231.604	Sr 421.552	Ti 334.941	Ti 336.122	Mg 285.213	K 766.491	Fe 239.563	Al 396.152	Ba 455.403	Na 588.995	Y (internal standard correction factor)
-785	0,108	55,306	0,851	0,052	0,496	0,042	2,295	2,342	125,449	1,965	71,319	76,308	0,044	13,088	0,94
-850	0,1082	76,764	1,220	0,047	0,430	0,203	2,894	2,962	94,987	3,881	70,951	82,583	0,093	20,194	0,95
-894	0,102	82,397	0,823	0,034	0,277	0,035	2,512	2,565	104,738	2,557	67,863	73,270	0,023	15,954	0,93
-951	0,1044	58,205	0,342	0,028	0,161	0,341	3,773	3,851	58,905	3,967	48,496	84,035	0,103	26,098	0,98
-1005	0,1006	53,684	0,253	0,025	0,173	0,372	4,235	4,325	65,321	3,409	56,066	85,723	0,090	24,503	0,94
-1055	0,113	75,143	0,244	0,039	0,107	0,358	4,310	4,410	67,744	3,736	61,729	91,502	0,077	24,643	0,97
-1090	0,1083	76,931	1,182	0,043	0,434	0,091	2,675	2,729	93,192	3,267	70,586	78,209	0,036	17,586	0,94
-1135	0,1032	77,753	0,973	0,026	0,403	0,082	2,572	2,632	94,202	2,189	76,784	74,557	0,028	15,437	0,96
-1175	0,1037	61,027	0,164	0,032	0,090	0,381	3,773	3,856	50,262	5,297	48,353	90,479	0,122	26,404	0,96
-1237	0,1022	50,889	0,203	0,032	0,091	0,345	3,729	3,818	54,838	6,299	61,531	90,075	0,111	25,227	0,96
-1290	0,1129	64,326	0,892	0,038	0,273	0,303	3,070	3,140	78,361	4,464	68,754	83,501	0,084	23,849	0,97
-1345	0,1071	60,464	0,425	0,025	0,448	0,207	3,036	3,105	85,595	2,755	74,733	73,704	0,063	19,398	0,97
-1395	0,1025	47,416	0,013	0,034	0,110	0,394	3,960	4,048	69,346	3,597	63,249	88,730	0,089	25,264	0,96
-1429	0,1037	52,153	0,352	0,033	0,161	0,511	2,761	2,827	58,123	3,965	87,797	100,569	0,101	26,593	0,98
-1489	0,1187	88,249	0,892	0,033	0,513	0,095	3,909	3,993	106,377	2,283	82,011	88,182	0,054	18,655	0,94
-1529	0,1134	87,085	0,011	0,026	0,175	0,088	7,076	7,241	96,970	1,789	99,639	84,221	0,035	18,765	0,99
-1576	0,1066	85,614	0,823	0,030	0,421	0,063	4,551	4,653	99,599	1,646	75,163	73,655	0,020	16,141	0,97
-1623	0,1061	95,126	1,309	0,007	1,286	0,022	0,286	0,289	137,799	0,299	47,614	19,640	-0,001	6,867	0,97
-1652	0,104	61,789	0,019	0,017	0,085	0,546	4,848	4,950	56,975	2,577	51,470	91,682	0,096	28,511	0,97
-1697	0,117	109,189	0,013	0,062	0,052	0,695	4,680	4,777	47,608	10,955	75,933	128,380	0,120	14,145	0,97
-1723	0,0995	47,779	0,010	0,018	0,036	0,506	3,806	3,892	43,085	2,909	54,850	90,331	0,106	29,778	0,98
-1782	0,1045	59,808	0,142	0,027	0,245	0,269	2,745	2,797	74,676	2,860	78,356	83,764	0,087	20,545	1,01

Depth, cm	Weight, g	Concentration of the element in the solution, mg/L													
		Ca 315.887	Cr 205.560	Li 670.783	Ni 231.604	Sr 421.552	Ti 334.941	Ti 336.122	Mg 285.213	K 766.491	Fe 239.563	Al 396.152	Ba 455.403	Na 588.995	Y (internal standard correction factor)
-1848	0,103	62,179	0,339	0,015	0,117	0,332	3,651	3,735	54,073	3,065	56,140	85,628	0,146	25,773	0,98
-1897	0,1018	60,165	0,281	0,049	0,230	0,058	3,749	3,819	98,587	1,413	66,078	68,099	0,020	15,934	1,00
-1932	0,1052	62,047	0,213	0,019	0,089	0,491	3,754	3,833	48,457	6,018	44,651	90,882	0,145	27,202	0,95
-1997	0,1028	64,555	0,300	0,016	0,123	0,438	4,650	4,744	62,604	3,502	54,232	88,221	0,088	25,331	0,99
-2046	0,1038	55,631	0,157	0,025	0,099	0,539	3,221	3,290	48,805	3,973	47,658	99,117	0,111	30,441	0,97
-2095	0,1047	56,734	0,008	0,017	0,034	0,327	2,510	2,556	35,049	4,676	39,942	100,051	0,095	33,266	0,96
-2130	0,1123	58,328	0,008	0,017	0,038	0,268	3,633	3,709	44,668	4,783	45,683	97,768	0,100	34,558	0,98
-2174	0,1147	55,613	0,007	0,019	0,037	0,244	3,490	3,561	44,177	3,823	50,648	95,483	0,089	34,764	0,97
-2245	0,1067	118,533	0,001	0,041	0,258	0,572	4,652	4,748	76,062	4,988	38,439	117,859	0,091	15,367	0,97
-2276	0,1032	85,951	1,452	0,077	0,856	0,101	2,770	2,822	102,475	3,591	53,011	92,337	0,120	18,104	0,97
-2317	0,1014	78,324	1,203	0,002	1,256	0,018	0,272	0,277	156,374	0,182	34,725	17,328	0,000	1,886	0,97
-2555	0,109	44,985	0,012	0,029	0,038	0,616	4,496	4,581	40,557	6,046	42,849	107,543	0,379	35,893	0,99
-2607	0,0997	30,536	0,118	0,024	0,055	0,259	3,118	3,182	41,011	3,348	51,426	84,819	0,257	34,694	0,95
-2670	0,1107	31,484	0,007	0,032	0,043	0,349	3,896	3,975	44,169	5,280	49,964	99,876	0,474	36,435	0,99
-2719	0,1017	35,059	0,009	0,035	0,046	0,421	3,175	3,246	43,205	4,497	45,224	84,579	0,201	32,456	0,96
-2768	0,1042	46,983	0,091	0,018	0,065	0,415	5,080	5,173	43,716	4,151	50,192	92,823	0,198	34,229	0,96
-450	0,1061	0,160	1,497	0,001	1,122	0,000	0,027	0,027	123,409	0,000	33,698	0,995	-0,003	0,026	0,95
-785	0,1012	47,800	0,654	0,100	0,360	0,027	1,481	1,508	120,536	5,533	64,080	73,050	0,034	12,215	0,98
-1020	0,0998	119,977	1,322	0,007	1,013	0,039	0,166	0,168	137,665	0,134	34,508	14,073	-0,002	3,581	0,98
-1165	0,1071	76,643	0,188	0,042	0,095	0,443	3,612	3,681	49,132	5,693	53,590	102,255	0,125	22,846	0,97
-1530	0,1015	81,472	0,757	0,019	0,845	0,056	3,476	3,547	96,052	1,203	78,367	64,041	0,018	14,781	0,96
-1705	0,1128	69,578	0,012	0,063	0,064	0,269	6,806	6,931	83,519	5,845	102,508	99,546	0,155	20,556	0,98

71

Depth, cm	Weight, g	Concentration of the element in the solution, mg/L													
		Ca 315.887	Cr 205.560	Li 670.783	Ni 231.604	Sr 421.552	Ti 334.941	Ti 336.122	Mg 285.213	K 766.491	Fe 239.563	Al 396.152	Ba 455.403	Na 588.995	Y (internal standard correction factor)
-1750	0,109	34,437	0,062	0,014	0,048	0,416	2,612	2,663	33,639	2,176	48,839	71,393	0,103	24,970	0,99
-1955	0,1	39,590	0,623	0,051	0,366	0,017	5,151	5,239	143,299	2,046	73,108	79,164	0,007	8,226	0,95
-2030	0,103	50,365	0,197	0,033	0,097	0,413	3,595	3,662	49,578	4,325	45,096	85,800	0,088	26,635	0,99
-2135	0,1034	56,802	0,006	0,016	0,030	0,267	2,855	2,903	37,917	4,669	40,378	93,141	0,089	31,514	0,96
-2245	0,102	91,351	0,829	0,018	0,426	0,049	2,937	2,980	99,925	1,692	55,639	84,695	0,042	18,519	0,98
-2310	0,1034	66,991	1,797	0,001	1,299	0,012	0,243	0,247	152,766	0,055	39,919	19,873	-0,002	1,266	0,99
-2515	0,1014	38,609	1,602	0,009	1,173	0,010	0,106	0,106	115,061	0,095	29,300	7,558	-0,002	2,124	0,97
-2775	0,1011	31,057	0,016	0,014	0,050	0,342	4,532	4,600	33,707	2,814	33,328	74,385	0,156	30,573	0,97

Table 16 Concentrations of the elements in the solutions of samples, as determined by ICP-OES (Here: *Dept*h indicates the distance from the suface where the corresponding sample was taken., *Weight* is the mass of the corresponding solid sample, taken initially for the preparation of the solution, that was used for the further experimental step, the number under the name of the element stands for the wavelength, that was chosen for the determination, nm)

From these values, the concentrations of each element in rock and soil samples were calculated, using Equation 1 (see Methodology) giving the results, shown in the Table 17. Following the calculations, the plots were created to show the changes of concentrations of elements by depth, which, in turn, allowed to provide a more explicite differentiation between lithological changes along the depth of the drill core Figure 5. As seen from Figure 5, the plots can serve as a confirmation of the preliminary estimations of petrological and mineralogical analysis. As the current study was planned to investigate mostly serpentinites, which appeared to be represented in the upper layers of the profile, down to the depth of cca - 560 cm, the next steps of data elaboration elaboration for this relatively mono-lithologic serpentinite section were performed.
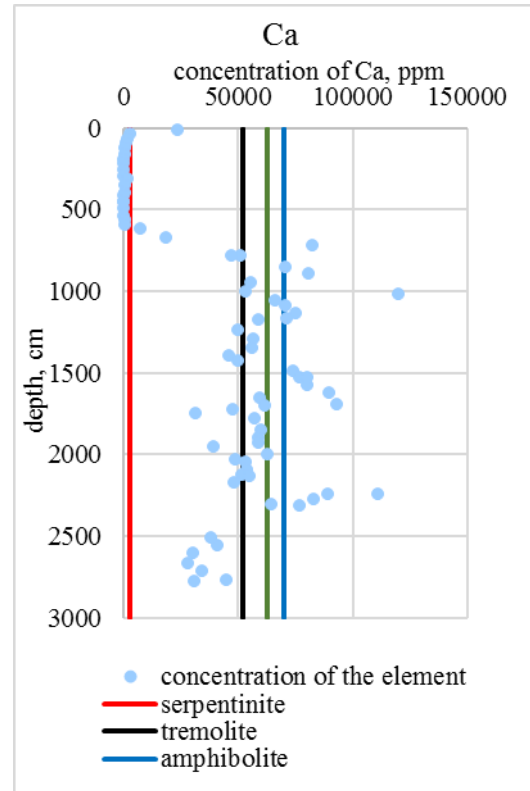
Depth, cm	Concentration of the element, recalculated per 1 g of sample, ppm													
	Ca	Li	Sr	Ti 334.94 nm	Ti 336.12 nm	Mg	K	Fe	Al	Ba	Na	Y (internal standard correction factor)	Cr	Ni
-15	23517,18	19,02547	82,46123	2468,681	2517,799	118471,6	5911,656	78900,32	42504,25	151,2526	7948,486	916,6497	3122,788	1228,583
-35	3107,51	13,29418	13,99778	1054,276	1078,554	178241,7	3080,933	68627,84	25479,73	50,25397	1858,39	952,8227	3390,107	1724,755
-70	1753,094	9,711284	10,19653	878,8081	899,0293	183865,6	2530,395	76207,3	27510,01	36,64229	1346,416	924,4258	5322,155	1889,989
-95	1332,023	9,480481	4,672887	373,3643	382,3499	200947,3	1149,055	67107,01	12388,25	12,84714	593,8705	897,4326	4192,285	1922,9
-120	864,8373	10,70428	3,972992	374,8853	383,327	202507,6	1022,818	68743,78	11671,73	10,41106	637,252	912,0968	4290,727	2002,058
-160	654,2878	7,511133	1,502534	262,0985	268,3394	209233,4	290,3712	71147,19	11192,14	1,249551	270,9009	960,6425	4854,332	2011,345
-195	118,3663	6,608333	0,812006	771,1075	791,4414	209687,9	181,9457	67121,48	27595,73	-1,42037	212,6997	952,7721	4488,689	1610,74
-215	113,273	2,025116	0,656903	318,4561	327,1222	205654	129,5293	74852,15	18150,42	-0,917591	88,64816	925,301	5163,854	2048,044
-255	314,1886	3,619934	0,564605	214,5171	220,4283	209719	65,73734	65705,77	12215,66	-1,79507	95,85354	911,6439	3583,951	1837,74
-295	400,6065	2,515169	0,678293	193,9951	200,0783	214064,1	67,08852	61634,77	5320,052	-1,412737	92,59938	921,8574	3736,608	2148,906
-315	1949,827	1,577781	1,683996	167,3096	170,3604	204315	48,75234	76600,79	2672,478	-1,40141	72,41013	802,0895	7197,735	2481,787
-355	499,0103	1,368395	0,808477	95,47854	96,65985	215127,1	105,4897	79510,45	2245,629	-1,25925	91,45561	873,6787	5063,704	2431,794
-395	672,7929	1,455474	0,741896	79,02916	80,1329	209130,8	78,43763	68256,44	1814,986	-1,179256	72,37994	803,4109	4405,003	2500,722
-415	129,9694	1,304296	0,521257	75,916	76,78691	195669,1	95,53785	60349,01	2051,028	-1,390895	78,16354	855,6303	4541,853	2112,374
-455	282,4605	4,486342	0,996889	88,43337	91,05136	212763,3	218,993	50241,55	2902,019	-0,781796	274,2093	937,926	2774,754	1830,155
-495	162,6325	1,784432	0,564891	60,20449	61,68548	216477,1	62,93081	54112,87	2694,594	-1,527893	90,86276	940,5144	2846,813	2055,013
-537	296,2805	4,123011	0,889683	97,52684	99,77796	213735,9	122,6384	54986,98	3941,32	-1,792978	201,2079	863,4923	2217,363	1789,477
-560	602,0211	11,38262	1,269828	83,51685	85,66208	210369,6	66,39062	55192,74	11313,65	0,420909	146,6114	945,4278	2090,053	1896,749
-597	750,3273	1,244024	1,108025	4283,957	4384,315	175254,9	134,6333	70478,48	89419,99	-2,010232	191,9835	880,251	849,8466	396,1679
-616	7182,518	2,209359	2,543448	3738,816	3819,84	172551,7	141,6065	104506,7	87154,14	-1,696737	354,5306	937,813	1897,262	871,6785
-671	18756,81	2,446338	3,419093	274,9097	280,115	175888,9	101,729	62659,89	18075,13	-1,001926	551,7191	903,8172	4761,285	1999,741
-720	82726,12	25,88348	67,57135	3269,506	3337,606	84126,65	3987,627	62827,16	81251,11	317,6689	15702,15	858,1758	952,4875	439,9534

Depth, cm	Concentration of the element, recalculated per 1 g of sample, ppm													
	Ca	Li	Sr	Ti 334.94 nm	Ti 336.12 nm	Mg	K	Fe	Al	Ba	Na	Y (internal standard correction factor)	Cr	Ni
-785	51208,97	48,07134	39,08895	2125,456	2168,509	116156,2	1819,464	66036,34	70655,76	40,78472	12118,73	869,549	788,0386	459,5854
-850	70946,2	43,14407	187,5337	2674,429	2737,099	87788,14	3586,909	65574,03	76324,29	86,07128	18663,13	885,9218	1127,176	396,9875
-894	80781,17	33,25007	34,73149	2463,196	2514,453	102683,9	2506,917	66532,07	71833,42	22,89724	15641,5	945,2168	807,1669	271,8788
-951	55752,14	26,4408	326,1809	3614,323	3688,407	56422,85	3799,616	46452,1	80493,77	98,81657	24997,89	924,0183	327,6309	154,0964
-1005	53363,95	25,11174	369,7461	4209,926	4299,648	64931,39	3388,23	55731,37	85211,58	89,80053	24357,15	961,0387	251,1735	172,0002
-1055	66497,92	34,65786	316,7528	3814,535	3902,64	59950,4	3305,786	54627,35	80975,56	68,57928	21808,01	859,6052	215,685	94,63505
-1090	71035,24	39,71052	83,89524	2469,557	2519,741	86049,61	3016,943	65176,28	72214,87	32,85638	16238,45	887,4724	1091,73	400,3142
-1135	75341,91	25,29913	79,21022	2492,603	2550,572	91281,45	2120,678	74403,52	72245,6	26,67986	14958,5	943,0921	943,2782	390,1137
-1175	58849,51	31,22429	367,1175	3637,915	3718,622	48468,27	5107,542	46628,18	87251,03	117,3281	25461,45	945,5604	157,7313	86,53821
-1237	49793,1	31,17255	337,7645	3649,186	3736,273	53657,42	6163,538	60206,17	88135,92	108,2144	24683,65	946,573	198,5668	89,02065
-1290	56975,73	33,22726	268,1178	2718,874	2781,036	69407,25	3954,193	60898,04	73959,88	74,13701	21124,06	860,7271	790,0402	242,0366
-1345	56455,68	23,79018	193,001	2834,512	2899,223	79920,24	2572,63	69778,41	68817,77	59,20247	18112,47	903,3408	396,7706	418,1439
-1395	46259,78	32,83509	384,2181	3863,161	3949,441	67654,47	3509,089	61706,33	86565,63	86,54493	24648,18	949,189	13,1	107,2895
-1429	50291,72	31,36948	492,4559	2662,772	2725,715	56049,15	3823,05	84664,82	96980,81	97,10511	25644,13	931,3459	339,6749	155,461
-1489	74346,3	27,49677	80,16723	3292,969	3363,878	89618,28	1923,703	69091,16	74289,5	45,21392	15716,14	825,7494	751,5506	431,9383
-1529	76794,58	22,84541	77,30573	6240,103	6385,548	85511,71	1577,83	87865,31	74269,09	30,9184	16547,84	886,7575	10,1089	154,0227
-1576	80313,13	27,97614	58,77202	4269,471	4364,5	93432,44	1543,759	70509,49	69094,65	18,7535	15142	918,1498	771,6897	394,8776
-1623	89656,62	6,928983	20,56045	269,4658	272,6756	129876,9	282,0187	44876,85	18510,68	-1,160852	6472,392	912,895	1233,449	1212,266
-1652	59412,2	16,2184	525,1151	4661,348	4759,705	54783,56	2477,991	49490,21	88156,03	92,7149	27414,21	936,5819	18,52138	81,66647
-1697	93323,85	52,78268	594,1236	4000,398	4083,045	40690,55	9363,399	64899,76	109726,7	102,4385	12089,89	834,8796	11,42662	44,11199
-1723	48019,58	17,61877	508,803	3825,042	3911,959	43301,49	2923,993	55125,82	90784,57	106,6227	29927,69	972,2424	10,50882	36,56549
-1782	57232,6	25,55813	257,0087	2626,522	2676,276	71460,11	2736,669	74981,81	80156,54	83,31286	19660,58	919,9436	135,9464	234,3486

Depth, cm	Concentration of the element, recalculated per 1 g of sample, ppm													
	Ca	Li	Sr	Ti 334.94 nm	Ti 336.12 nm	Mg	K	Fe	Al	Ba	Na	Y (internal standard correction factor)	Cr	Ni
-1848	60367,51	14,94718	322,149	3544,308	3626,311	52498,53	2975,487	54504,61	83133,98	142,1541	25022,21	946,6036	328,9789	113,5649
-1897	59100,76	47,71309	56,68097	3682,677	3751,227	96843,39	1388,493	64909,86	66894,46	19,57265	15652,62	950,1205	275,966	225,5401
-1932	58979,76	18,48578	466,9056	3568,127	3643,588	46061,62	5720,327	42444,13	86390,14	137,6701	25857,36	922,7938	202,5785	84,58561
-1997	62797,03	15,2976	426,4499	4523,458	4614,74	60898,68	3406,764	52755,14	85817,9	85,48851	24641,44	944,0446	291,6096	119,2768
-2046	53594,13	23,86054	519,0055	3103,067	3169,498	47018,11	3827,721	45913,52	95488,48	106,7419	29326,99	931,8008	151,0655	95,53328
-2095	54187,01	16,26854	312,6036	2396,995	2440,809	33475,2	4465,75	38148,81	95559,6	90,6857	31772,62	918,8296	7,854814	32,17016
-2130	51939,52	15,15411	238,584	3235,247	3302,522	39775,77	4259,467	40679,51	87059,42	88,6364	30772,49	856,996	7,10462	33,8175
-2174	48485,74	16,97226	212,5009	3043,101	3104,705	38515,64	3332,634	44157,05	83245,71	77,1637	30308,2	842,2654	6,189435	32,439
-2245	111090	38,62675	536,4027	4360,148	4450,03	71286,27	4674,571	36025,63	110458,5	84,86382	14401,77	1018,428	1,120133	242,0692
-2276	83286,05	74,40234	97,67926	2684,296	2734,264	99297,67	3479,547	51367,52	89473,36	116,1727	17543,1	996,0417	1407,369	829,3441
-2317	77242,96	1,713374	17,34271	268,6933	273,2842	154214,9	179,6759	34245,23	17088,47	0,431218	1860,266	937,9989	1186,456	1238,491
-2555	41270,63	26,69883	565,3591	4125,218	4202,759	37207,96	5546,705	39311,17	98663,58	347,9883	32929,18	897,3622	11,00065	34,71235
-2607	30627,95	23,69876	259,612	3127,687	3191,382	41134,73	3358,26	51580,99	85074,3	257,5495	34798,45	979,6126	118,1902	54,99797
-2670	28440,41	28,93871	315,5845	3519,255	3591,138	39899,87	4770,055	45134,68	90222,15	428,5871	32913,33	874,5758	6,755004	38,75009
-2719	34473,17	34,85765	413,5711	3122,158	3191,773	42483,08	4421,462	44467,88	83164,8	197,2673	31913	943,5909	8,510575	45,48401
-2768	45089,26	17,04204	398,0322	4875,642	4964,282	41953,53	3983,834	48168,51	89081,59	190,4641	32849,6	941,9049	87,49476	62,64472
-450	150,4799	0,614203	0,324511	25,78668	25,6055	116314	-0,39212	31760,86	938,2322	-2,724029	24,73792	907,2181	1410,617	1057,516
-785	47233,63	98,41994	26,4581	1463,293	1490,607	119107,2	5467,234	63319,97	72183,96	33,60695	12070,58	952,1411	646,1506	355,9265
-1020	120217,4	6,839625	39,26244	166,2959	167,8423	137940,8	134,4581	34577,49	14101,69	-1,767627	3588,675	949,4974	1324,742	1014,886
-1165	71561,64	39,50783	414,0899	3372,569	3437,401	45875,26	5315,859	50037,82	95476,28	116,3759	21331,45	909,8677	175,162	88,29627
-1530	80267,82	18,25236	54,95858	3424,287	3494,693	94632,54	1184,895	77209,21	63094,37	17,50927	14562,94	969,9433	745,8417	832,5759
-1705	61682,25	55,82768	238,0871	6033,883	6144,643	74041,89	5182,18	90876,24	88249,96	137,5236	18223,45	874,629	10,79657	56,8022

Depth, cm	Concentration of the element, recalculated per 1 g of sample, ppm													
	Ca	Li	Sr	Ti 334.94 nm	Ti 336.12 nm	Mg	K	Fe	Al	Ba	Na	Y (internal standard correction factor)	Cr	Ni
-1750	*31593,32*	*12,55539*	*381,9874*	*2395,906*	*2443,242*	*30861,12*	*1996,346*	*44806,53*	*65498,59*	*94,31*	*22908,57*	*887,6986*	*56,87497*	*44,20824*
-1955	*39589,68*	*51,24061*	*16,73547*	*5151,071*	*5239,126*	*143298,6*	*2045,738*	*73107,84*	*79163,82*	*6,995911*	*8225,999*	*968,5082*	*623,2424*	*365,8912*
-2030	*48898,09*	*31,84427*	*400,7271*	*3490,477*	*3555,143*	*48133,68*	*4199,412*	*43782,55*	*83300,89*	*85,08942*	*25859,37*	*942,8253*	*190,971*	*94,14967*
-2135	*54934,68*	*15,56158*	*258,3047*	*2761,515*	*2807,417*	*36669,91*	*4515,869*	*39050,39*	*90078,08*	*85,61943*	*30478,01*	*945,3108*	*5,372336*	*29,15992*
-2245	*89559,58*	*17,90427*	*47,77291*	*2879,458*	*2921,27*	*97966*	*1658,451*	*54548*	*83034,35*	*41,37737*	*18155,48*	*968,9392*	*813,2284*	*418,0056*
-2310	*64788,62*	*0,809424*	*11,20625*	*235,4605*	*238,7646*	*147743*	*53,40046*	*38606,36*	*19219,1*	*-2,406357*	*1224,219*	*922,4624*	*1737,726*	*1256,428*
-2515	*38076,28*	*8,524469*	*10,17099*	*104,2885*	*104,8386*	*113472,6*	*93,97928*	*28895,16*	*7453,654*	*-2,277792*	*2094,539*	*945,1445*	*1580,211*	*1157,102*
-2775	*30718,89*	*13,46718*	*337,9779*	*4483,054*	*4549,713*	*33339,79*	*2783,685*	*32965,68*	*73575,86*	*154,6451*	*30240,52*	*977,2207*	*16,30864*	*49,2871*

Table 17 Concentrations of elements calculated per 1 g of each depth sample for the drill core from Pluhuv Bor. Here the two columns for Ti correspond to two separate measurements that were done using two different wavelengths, which are indicated after the names of the element in the headings of the columns. The values typed in italic (below the double-line) represent data for a separate set of samples collected from the same core at earlier stage of the project.
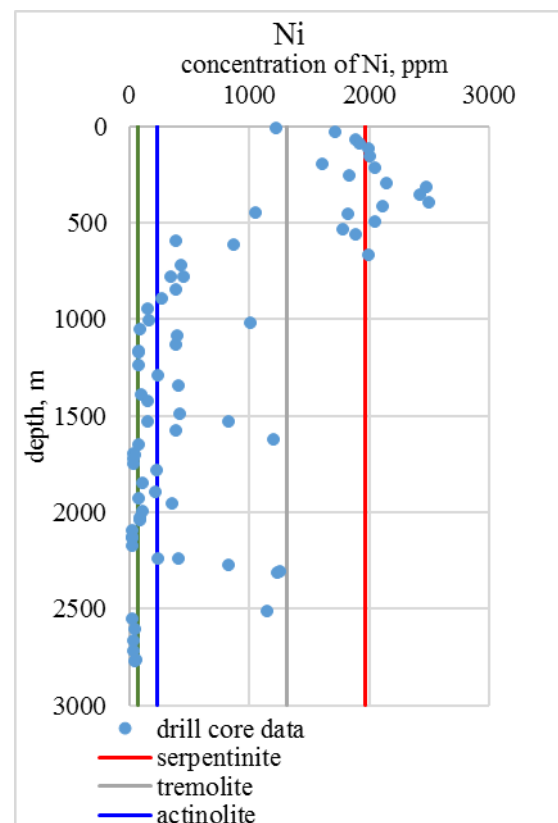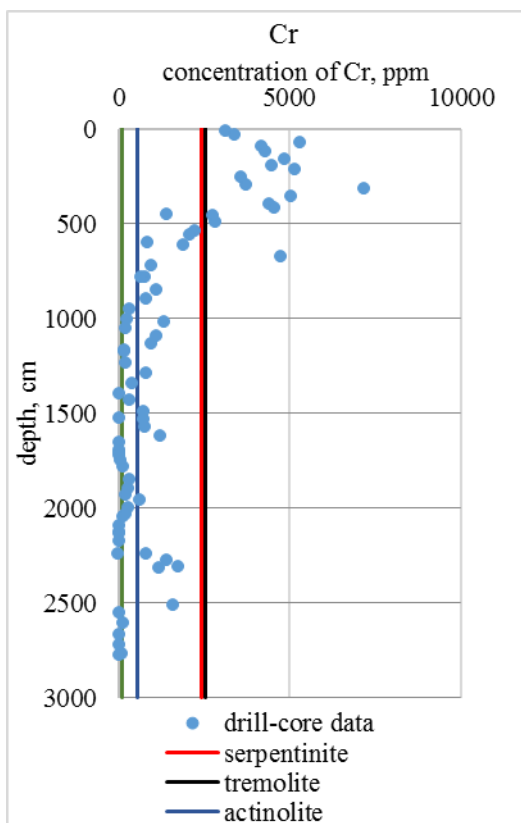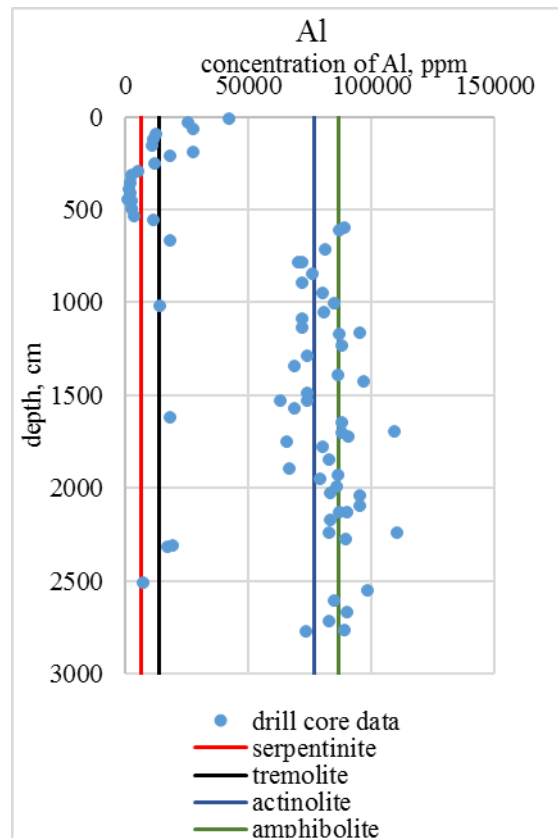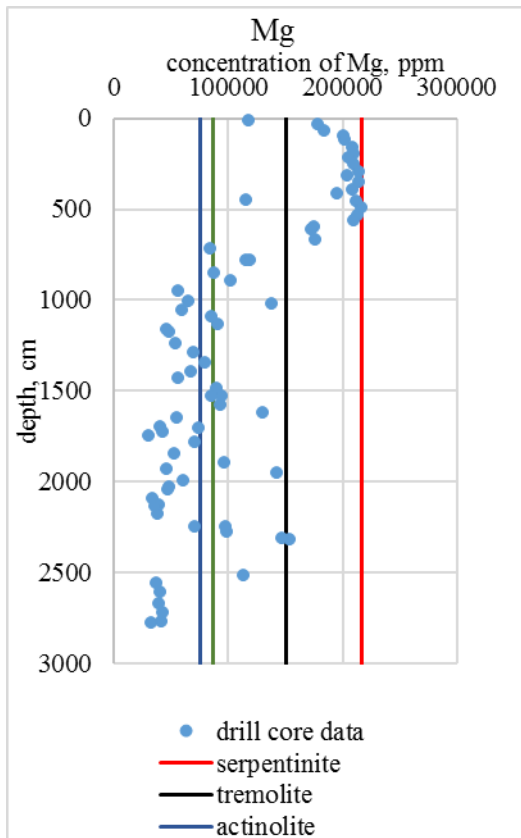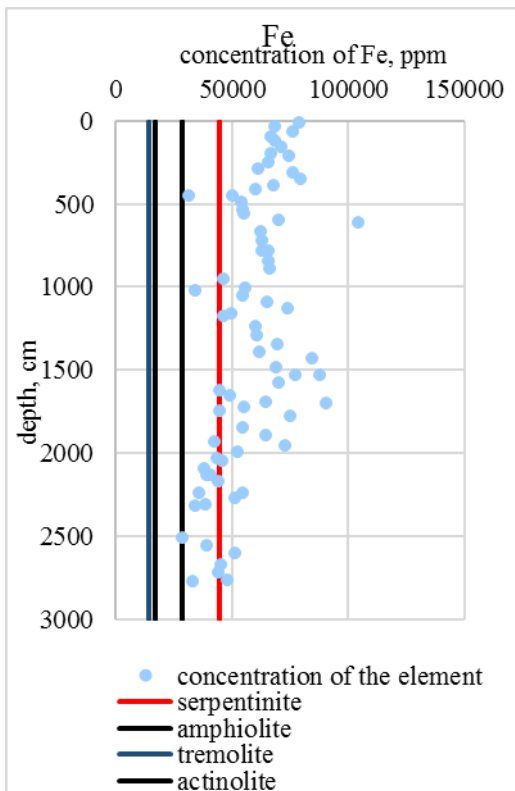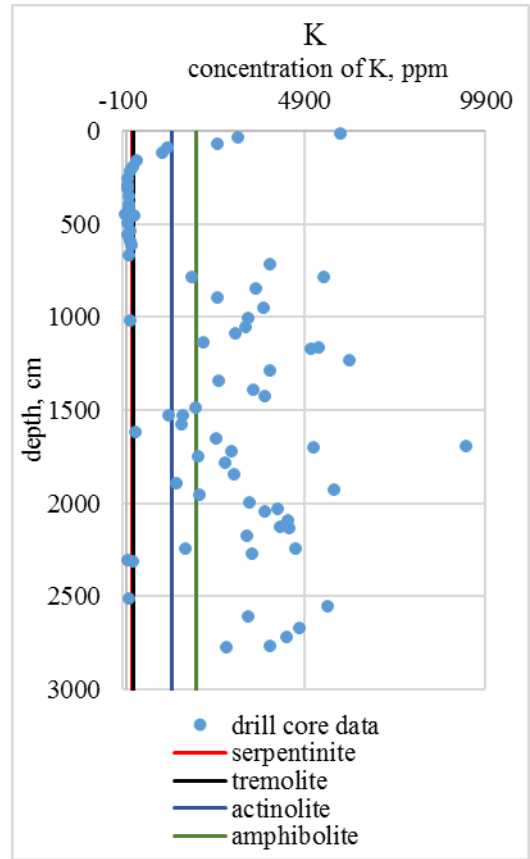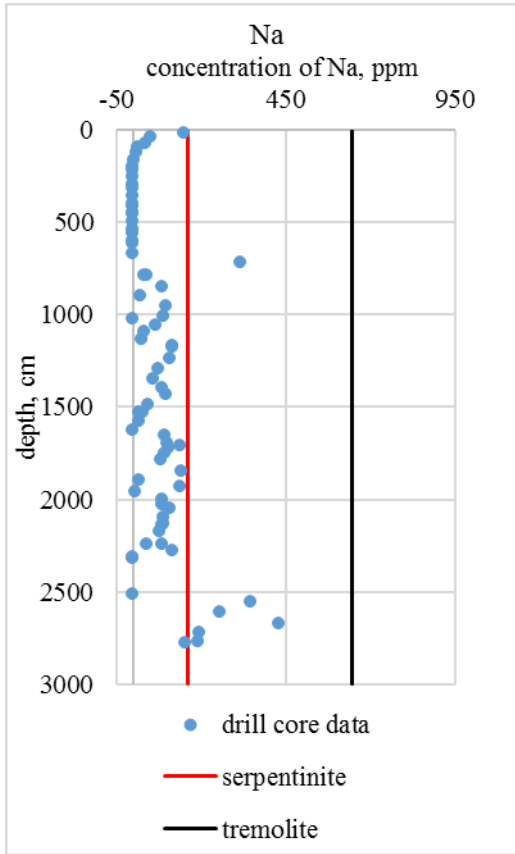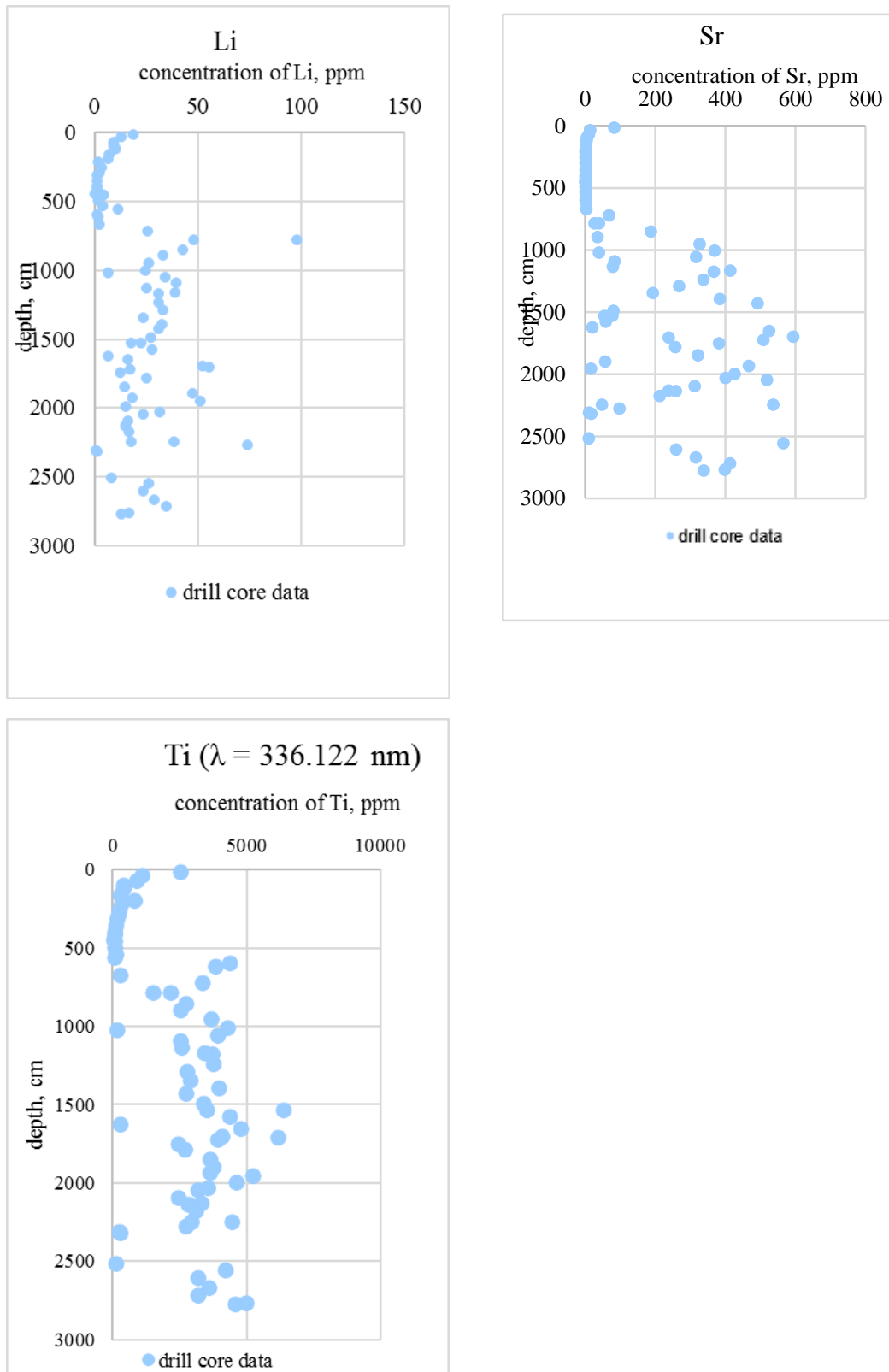
Figure 5 Concentrations of selected elements as a function of depth changing by depths, as calculated for the drill-core at Pluhuv Bor, Slavkov Forest, Czech Republic
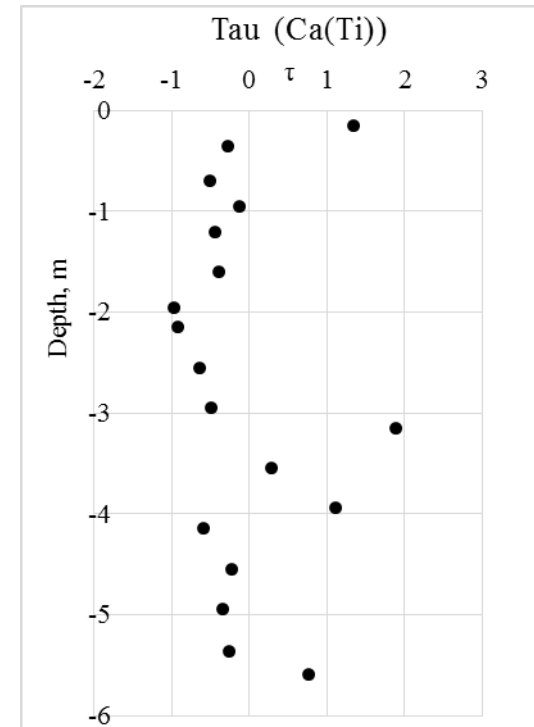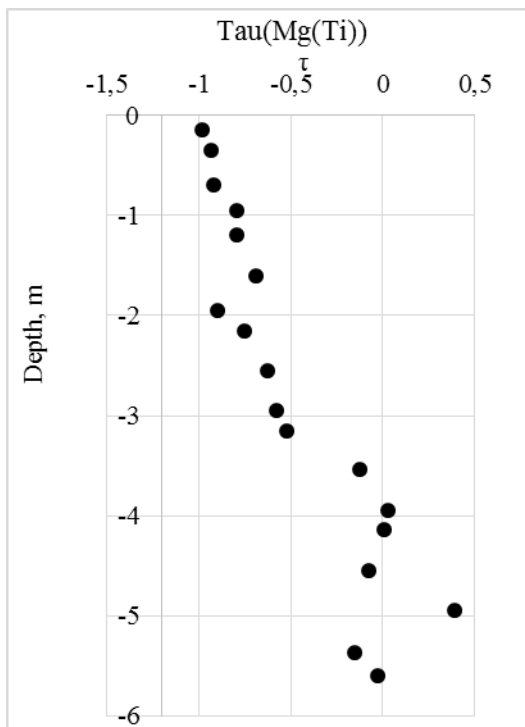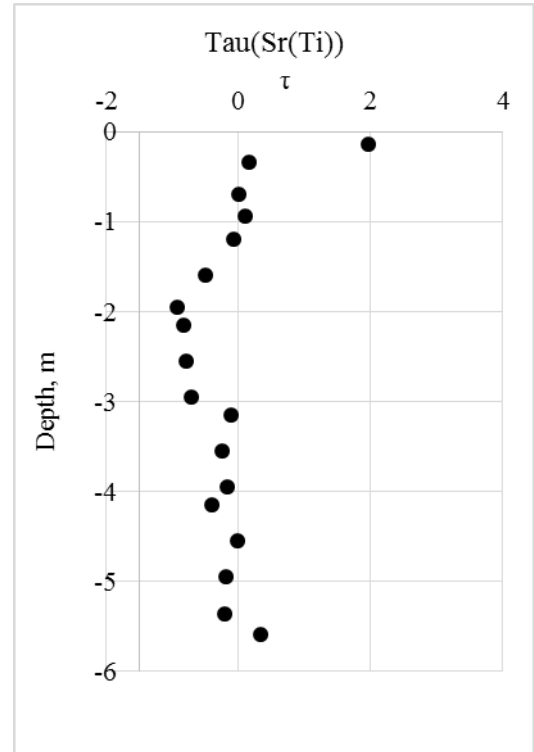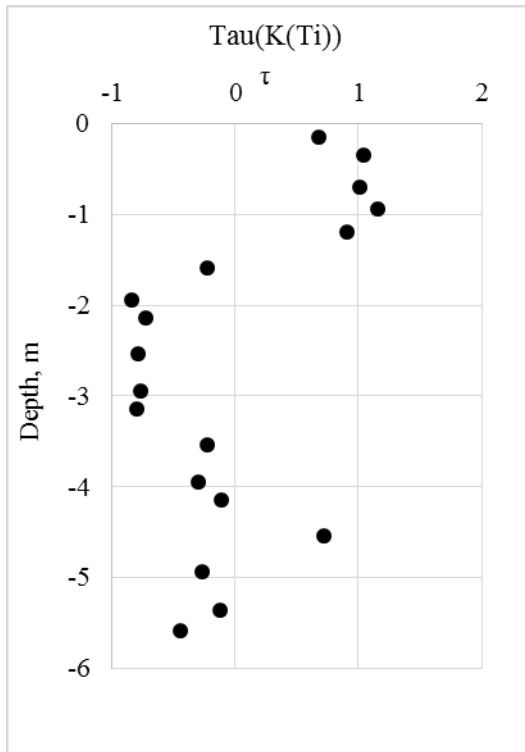
Mass gains or losses due to weathering were calculated for each element (Table 18) following the Equation 5 (see Methodology). Among the two series of results for Ti,

i.e. measured at the wavelength of 334.941 nm or 336.122 nm, the second was was used for the calculations. The change of Tau values with depth in the regolith profile was plotted for all elements in graphs (Figure 6). The Tau-graphs for two elements, Sr and Li were not plotted due to lack of information for these elements.

Depth, cm	Weight, g	Element-mass-transfer coefficients, $\tau_{j,w}$ calculated for an element at each depth using meanings of Ti-concentration as immobile element , measured at the wavelength of 336.122 nm										
		Ca	Li	Sr	Mg	K	Fe	Al	Ba	Na	Cr	Ni
-15	0,1048	1,35128	-0,88265	1,976319	-0,98135	0,685989	-0,9506	-0,72621	-6,51785	0,497559	-0,95776	-0,97821
-35	0,1	-0,27471	-0,80858	0,179418	-0,93451	1,051195	-0,8997	-0,61686	-5,27974	-0,18264	-0,89294	-0,92858
-70	0,1022	-0,50912	-0,83225	0,030692	-0,91895	1,021068	-0,86638	-0,50373	-4,74367	-0,28956	-0,79837	-0,9061
-95	0,1052	-0,12302	-0,61493	0,110644	-0,79172	1,157975	-0,72333	-0,47452	-4,08627	-0,2632	-0,62655	-0,77538
-120	0,1033	-0,43206	-0,56634	-0,05811	-0,79064	0,916	-0,71731	-0,50618	-3,49468	-0,21139	-0,61876	-0,76673
-160	0,0978	-0,3862	-0,5653	-0,49115	-0,691	-0,22297	-0,58205	-0,32355	-1,42772	-0,5211	-0,38385	-0,66522
-195	0,0989	-0,96235	-0,87033	-0,90676	-0,895	-0,83492	-0,86631	-0,43451	-0,83516	-0,87251	-0,80683	-0,9091
-215	0,1025	-0,91283	-0,90386	-0,81751	-0,75086	-0,71567	-0,6393	-0,10013	-0,74235	-0,87145	-0,46235	-0,72037
-255	0,1037	-0,64119	-0,74497	-0,76723	-0,62296	-0,78585	-0,53012	-0,10122	-0,252	-0,79372	-0,44622	-0,62763
-295	0,1023	-0,49597	-0,80478	-0,69192	-0,576	-0,75922	-0,51441	-0,56876	-0,35144	-0,78045	-0,36391	-0,52029
-315	0,1172	1,881162	-0,85617	-0,1017	-0,52472	-0,79451	-0,29122	-0,74558	-0,24441	-0,79837	0,439018	-0,34934
-355	0,1081	0,299582	-0,78015	-0,2399	-0,118	-0,21633	0,296659	-0,62321	0,196614	-0,55117	0,784273	0,123674
-395	0,1174	1,113541	-0,71793	-0,15864	0,034251	-0,29712	0,342704	-0,63266	0,351716	-0,57152	0,872295	0,393844
-415	0,11023	-0,57392	-0,73621	-0,3831	0,009843	-0,10658	0,238884	-0,5668	0,663779	-0,51712	1,014582	0,228693
-455	0,1008	-0,21907	-0,23481	-0,00503	-0,07396	0,727071	-0,13019	-0,48309	-0,21133	0,428619	0,037952	-0,10224
-495	0,1006	-0,33631	-0,55076	-0,16779	0,390746	-0,26743	0,382819	-0,29154	1,275089	-0,30125	0,571865	0,48796
-537	0,1084	-0,2525	-0,35828	-0,18969	-0,15109	-0,11741	-0,13129	-0,35936	0,65055	-0,0434	-0,2431	-0,19897
-560	0,1004	0,769145	1,063571	0,347122	-0,02678	-0,44348	0,015643	1,141998	-1,45132	-0,18811	-0,16899	-0,01103

Table 18 Mass gains or losses of specific element due to weathering, atmospheric deposition, and/or biological uptake expressed as an element-mass-transfer coefficient, tau-value ($\tau_{j,w}$
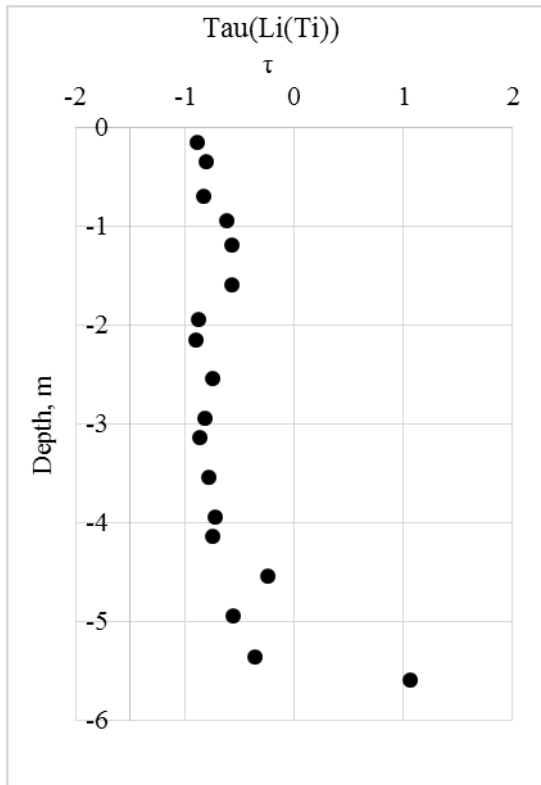
Tau(Cr(Ti))

Tau (Ni(Ti))

Tau (Na(Ti))

Tau (Al(Ti))
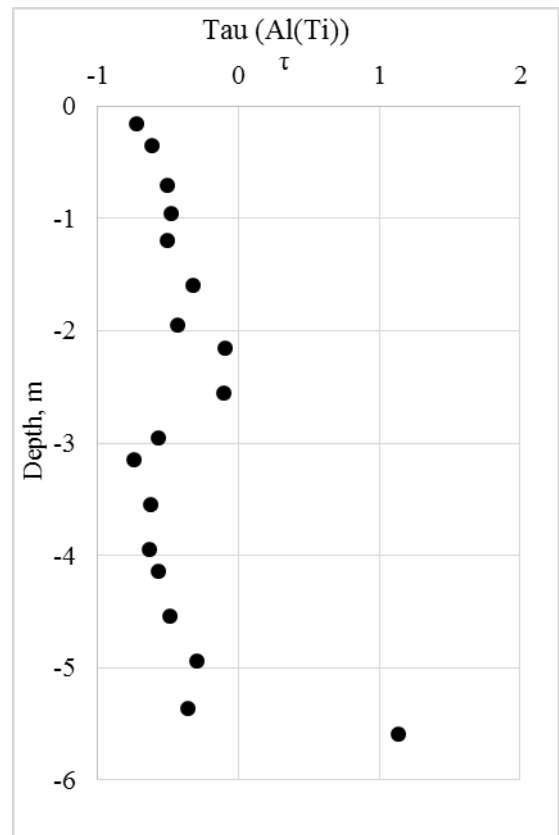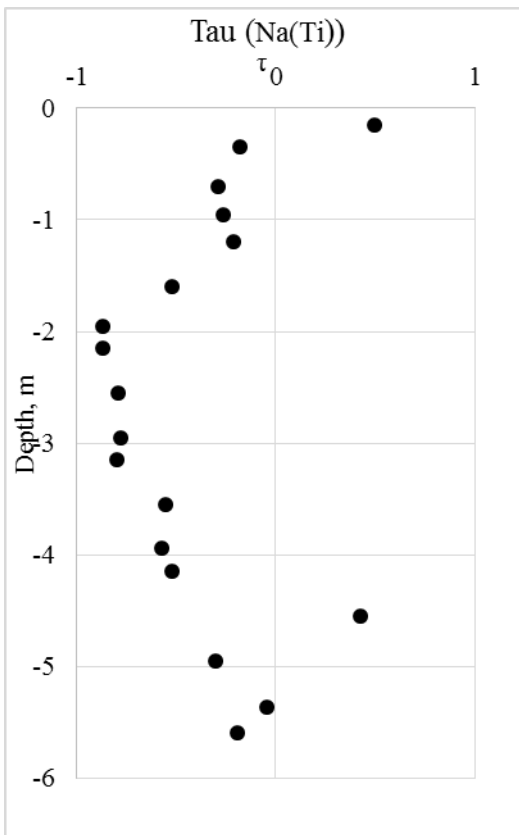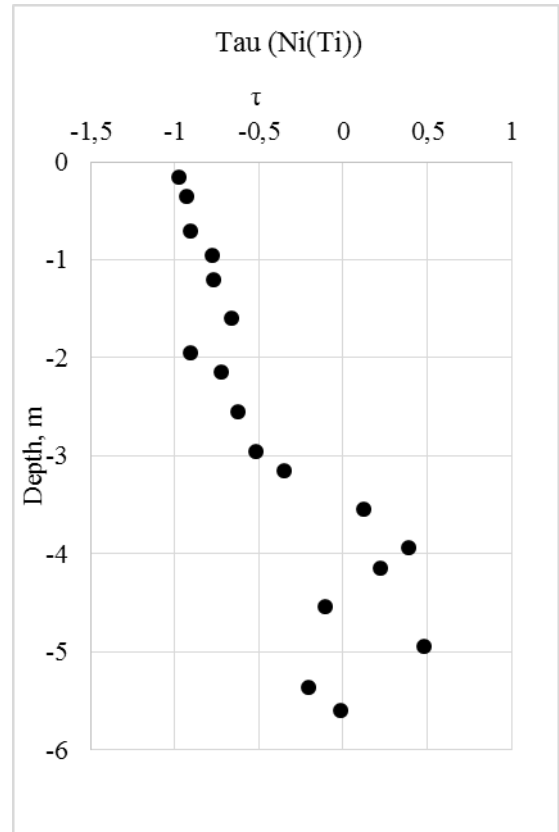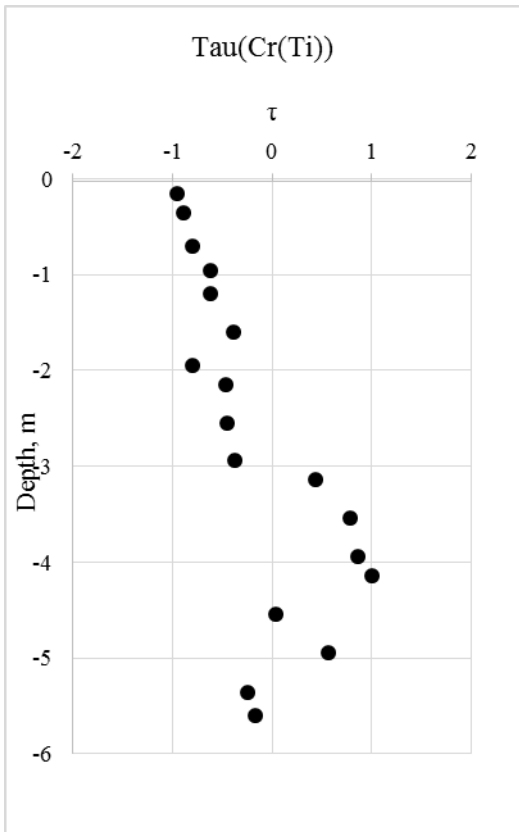
Figure 6 Mass gains or losses of specific elements (tau-values) due to the weathering processes, atmospheric deposition and/or biological uptake.

5. Discussion

The ICP-OES analysis allowed us to quantify concentrations of elements in the samples from different depths of the drill core, which made it possible to estimate more precisely lithological changes as a function of depth, and compare them to the visual field analysis and microscopic examination of petrologic and mineralogical characteristics done at the Czech Geological Survey. Though, we have evaluated results for as much as 10 elements, including Ca, Al, Ni, Cr, K, Li, Sr, Na, Mg and Ba, we have chosen five of them, namely three nutrient base cations (Ca, Mg and K) and two potentially toxic trace metals (Ni and Cr) for further discussion and interpretation. This choice is substantiated, firstly, by the importance in the biogeochemical processes, and, as they are more characteristic for determination of the rock-type, which is partly due to their letter solubility. From the whole list of the elements, we excluded Ba, as, according to the results from ICP-OES, the concentration values were negative, which meant that in our samples it was present in the amounts, which were below the determination limit of the machine and methodology used. Also, it should be noted, that Ti was chosen as immobile element due to its resistance against leaching and loss during weathering processes. As seen from the plots of our concentration data, both these methods (i.e. visual examination and geochemical analysis) showed consistent results in terms of lithological changes in the drill core. The same was stated by Brantley et al. (2007), who described Ti as a relatively unreactive element in such minerals as rutile and anatase, which commonly becomes enriched in regolith as more soluble constituents are depleted.

Namely, major changes in lithological composition at the study site (Pluhuv Bor) were observed, in general agreement with the study of Kram et al. (2009) that documented these major differences in rock types from the surface outcrops. Specifically, the following lithologies were observed: serpentinite, tremolite schist, actinolite schist and amphibolite, and the "end-member chemical compositions" of these rock types through our drill core could be plotted, in terms of concentration data that showed affinities of different parts of the drill core to certain "end-member" compositions. Based on the concentration data of Ca, K, Mg, Cr and Ni, it is seen that the first cca. 5.6 meters of the drill core are dominated by serpentinite. Then a major shift can be distinguished, where the representative rock–type changes to tremolite

schist composition, followed by actinolite schist, and finally, the deepest parts of the core can be characterized as amphibolite. Also, there was quite a notable change in a zone of the top 3.6 meters of the core, characterized be an increased degree of weathering of the bedrock.

At the second step the elemental gains and losses though the profile were calculated, following the Equation 5 (Methodology) and visualized (Figure 22, 23) to allow us to estimate the rate of weathering due to chemical, biological, physical and geological processes. Here, as the Tau-normalization approach, which we were using for this purpose, can only be applied to a monolithic profile, during our further investigation steps we were concentrating on the upper 6 meter-part of the core, represented by serpentinite rock type, which originally was of the main interest for the current research, and was monolythologic in comparison to the rest part of the core. According to the outcomes from Tau-analysis, the Ca geochemical trend shows a typical *depletion-enrichment* profile, also named as *biological* profile, which is characteristic for nutrient elements. This highlights that Ca in our systems actively participates in the biological processes in the plants tissues, indicating that more intensive uptake of Ca by plants roots and vegetation takes place, with the following deposition of Ca in the upper organic-rich soil layers.

On the other hand, Mg is much more abundant at our serpentinite site, compared to Ca so one would not expect such notable "biologically-driven" changes of its concentration as a function of the depth. Another interesting observation about Mg was that it is being leached out quite intensively from the soil profile, specifically from the Tau-Mg value from $\tau = 0$ (i.e., no leaching of an element) in the deeper parts of the serpentinite drill core (ca. 5.6 meters) to the Tau-Mg values of almost -1 in the topsoil, demonstrating that the large part of Mg is being lost. Hence, a possible explanation to the particular behavior of Mg at our serpentinite-dominated site could be that the drill core is being passively weathered, and at the same time, as Mg is presented in the large amounts in the bedrock and is thus not deficient, the forest ecosystem is not forced to store it in the forest's soil pools. Also, Mg is known to be more soluble in comparison to Ca and thus has higher affinities to form aqua-complexes, and so it is easier to be mobilized.

Another element that appeared to be interesting to analyze and investigate was K, as this element is also known to be a major nutrient. According to the results of our

study, the biogeochemical behavior of K at our site shows the same tendency as Ca in terms of the tau-normalized trends i.e. it also shows *depletion-enrichment* profile. At the same time Na shows to be more accumulated in the upper parts of the weathering soil profile, which is more likely to be from the atmospheric deposition rather than biological uptake, as Na is not known to be a major nutrient critical for plant growth. The primary source of Na could be actually seasalts, brought to the study site by the winds. However, this assumption could be checked only with some more explicit methods such as isotopic analysis, which is out of the frame of the current investigation.

For K, we could also observe high depletion in the stream, but the general picture of its' concentration changes could be explained by its' greater involvement in biological processes. K is known to be very sensitive to the vegetation type of the site, as it is intensively taken up by roots from the deeper mineral soils, and then it is recycled back from the needles of the trees and other deposition of organic material back to the soil. As a result K accumulates in the upper parts of the soil profile. It is notable, that for Pluhuv Bor this accumulation was shown to be quite deep (to the point of cca 120 cm below the surface), according to the concentration-depth plots, which might suggest that roots of the plants at this site reach these greater depths.

From the trace metals, the study was focused on Ni and Cr, which are both naturally enriched in this serpentinite-dominated site, and these metals are usually interrelated regarding their concentrations. The overall coupling of the concentration variations of Cr and Ni within the soil profile was confirmed also by the current study. To better estimate the this connection, the correlation between Cr and Ni concentration changes is represented in graph (Figure 24), which shows a high R^2 value of 0.8812, and importantly this high correlation coefficient is observed not only for the serpentinite part of the core, but actually for the whole length of the core. This observation documents that these two metals are biogeochemically coupled regardless the rock-type and not only during the rock formation processes, but also during weathering and soil formation processes. Hence, when Cr and Ni are affected by biological and soil-formation processes, they are affected in the very similar way.
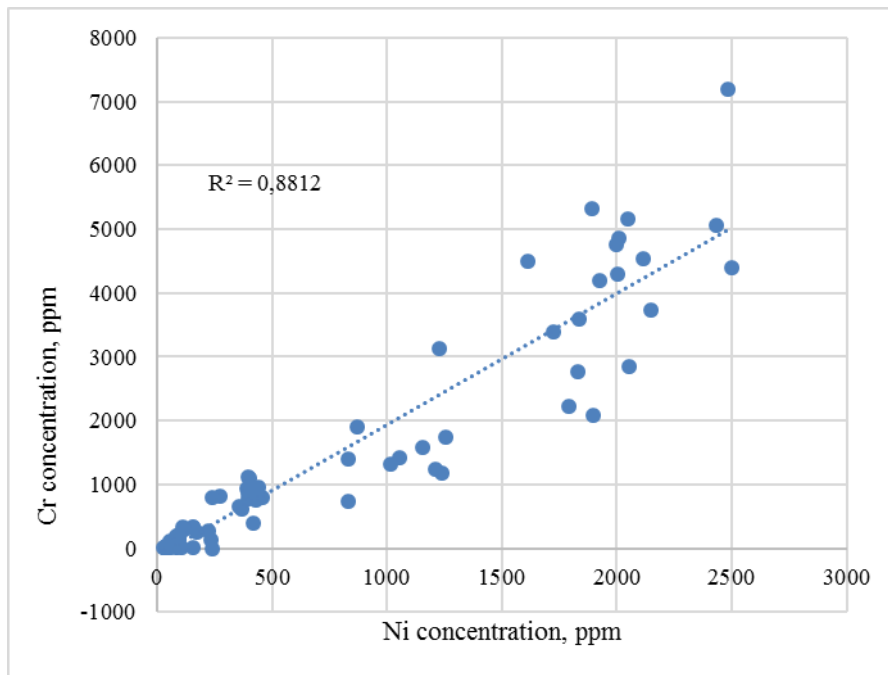
Figure 24 Correlation between Cr and Ni concentration changes by depth, aas determined for the drill core from Pluhuv Bor

As for the Tau-profiles for Ni and Cr, strong *depletion* profiles could be observed for both of these elements, and the data obtained indicate that up to 100% of Ni and Cr might have been lost during weathering processes in the top parts of the soil profile. Another argument is that these metals are not taken up, stored and/or recycled at a significant level by the vegetation. These results also do not show, that there is significant input of these metals from external sources such as atmospheric deposition, which is notable, as the site is situated close to a large coal-mining area, known as the Black Triangle which is the site of extensive surface coal mining operations (UNEP, 2014), meaning that the one could expect higher contribution to the deposition of these elements in the top-layers. This lack of evidence for significant accumulation of Cr and Ni from atmosphere in top soils could be explained by the content of these elements being so high in the soil and parent rock, that the atmosphere deposition becomes negligible in this case.

The observation that of Ni and Cr are being intensively leached and exported from the ecosystem, is in contrast to observations at the geochemically contrasting Lysina study site, located in the close vicinity of our Pluhuv Bor, but underlained by granite that is naturaly Cr and Ni poor rock type. At Lysina, Cr is actually being accumulated in the top organic rich soils. This can be partly attributed to the difference of drainage water pH (Krám et al., 1997) between these two geologically contrasting

catchments, which results in different speciation and thus solubility and mobility of these metals, especially Cr. More detailes on how different pH (and Eh) conditions can influence the redox state and solubility of chromium can be seen from a pH-Eh diagram (Figure 25) (Bonnand et al., 2013).
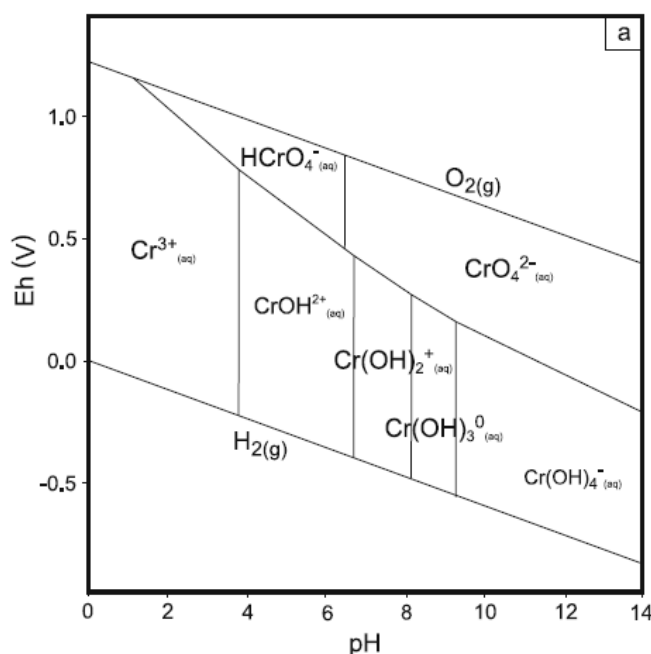

Figure 25 Speciation of Cr in sea water as a function of Eh and pH (Bonnand et al., 2013)

Thus, Cr is known to be in oxidized and hexavalent form (CrVI), which is more mobile, in alkaline and high pH environments. As seen from the diagram, in the acidic environment (with low pH of 3 to 4, which is characteristic true for the Lysina catchment) the dissolved Cr is mostly presented in the trivalent Cr (III) form, which is less soluble and bound to organic complexes. However, for alkaline environments, such as Pluhuv Bor with high pH of about 8 (Krám et al., 2013), Cr forms readily oxy-anions, which corresponds to the more soluble Cr(VI) form, and this form is very soluble. So, we suggest that the reason of the different mobility observed in the Cr-profiles at these geologicaly contrasting sites is reinforced by the higher loss rate of Cr at Pluhuv Bor due to its leaching in it's hexavalent-form. This form is also more toxic, however it is being exported from the soil pools more efficiently, in contrast to the acidic environments where Cr tends to be accumulated. Though it should be noted, that if the pH in this acidic soil-system will increase over time, which has been observed (Kram et al., 2013) and is expected, that Cr(III) which is stored in the organic-rich top

soils might become partly oxidized and thus more mobile and toxic, and accessible for uptake by plants.

7. Conclusion

The methods presented in this paper were designed to provide investigators with sufficient knowledge to assess the mobility and biogeochemical pathways of major base cations (Ca, Mg,K) and selected toxic metals (Ni, Cr) during weathering processes and biological uptake in sensitive forest ecosystems located in the Slavkov Forest, Czech Republic.

Concentration regolith profiles for the above elements were generated based on the analysis of soils and rocks from recently recovered the scientific drill core of 28 meters depth. Modern analytic technics, namely ICP-OES, was used for this purpose as a method, which is suitable for the elements under study and precise enough for the quantities, in which they were present in the samples. The net losses and gains of the elements accross the weathering profile were assessed by a simple normalization approach of tau-parametrization, with titanium (Ti) as the reference for the normalization.

The observations in terms of lithological changes in the drill core were consistent with visual field analysis and microscopic examination of petrologic and mineralogical characteristics. Lithologies such as serpentinite, tremolite schist, actinolite schist and amphibolite were observed, and the "end-member chemical compositions" of these rock types through our drill core could be plotted.

Tau-normalization was applied only to a monolithic profile of the upper 6 meter-part of the core, represented by serpentinite rock type.

Both trace metals, Ni and Cr, which are enriched in the serpentinite rocks and soils have shown similar concentration variation trends by depth, which allowed to see depletion profiles for both metals. Specifically, it was determined, that Ni was depleted to almost 100% in the topsoils, whereas K and Ca have shown inrichement to almost 100%, which confirms presence of a typical *depletion-enrichment* profile, or *biological* profile for these two cations. This outcome was expectable and should be attributed to the role of these elements as major nutrients for local vegetation, and their behavior, which would correspond to their involvement into biochemical processes. However, surprisingly, Mg, which, though is also major nutrient, have demostrated depletion profile which can be attributed to the facts that it is more than abundant at the study site and to its'higher solubility at the same time.

The behavior of trace metals, that could be observed in the run of experiment, corresponded to expectations, and can be explained by the role and cycling of these elements in connection to vegetation, as well as specific conditions of the study site, particularly by the level of soil acidity. However the contribution from atmospheric pollution could not be confirmed, which might be explained by naturally considerable amounts of these elements in the local rocks and soils.

References

Alexander, E.B., Coleman, R.G., Keeler-Wolf, T., and Harrison, S.P.. 2007. Serpentine Geoecology of Western North America: Geology, Soils, and Vegetation. Oxford University Press, New York, NY, USA. 512 pp., Brooks 1987

Alexander E.B,1988. Morphology, fertility and classification of productive soils on serpentinized peridotite in California.(U.S.A.). Geoderma 41:337–351

Alloway B.J.; Reimer T., 1999. Schwermetalle in Böden: Analytik, Konzentration, Wechselwirkungen. Springer Berlin: pp 540

Anderson, A.J., Meyer, D.R., Mayer, F.K., 1973. Heavy metal toxicities: levels of nickel, cobalt, and chromium in the soil and plants associated with visual symptoms and variation in growth of an oat crop. Aust J Agric Res 24: 557–571

Anderson, S.P., Dietrich, W.E., Brimhall Jr., G.H., 2002. Weathering profiles, mass-balance analysis, and rates of solute loss: linkages between weathering and erosion in a small, steep catchment. Geol. Soc. Amer. Bull. 114: 1143–1158

Anderson, R.S., and Humphrey, N.F., 1989. Interaction of weathering and transport processes in the evolution of arid landscapes. In: Cross, T., Quantitative Dynamic Stratigraphy: Englewood Cliffs, New Jersey, Prentice- Hall, pp. 349–361

Barnhart J., 1997, Occurrences, uses, and properties of chromium. Regulatory Toxicology and Pharmacology 26: 7-5

Becquer, T., Quantinb, C., Sicotc, M., Boudotb J. P., 2003. Chromium availability in ultramafic soils from New Caledonia. Science of The Total Environment 301 (1–3): 251–261

Bini Maleci, L.B., Gabbrielli, R., Gonnelli, C., Paolillo A., 1999. The effect of CrVI on the seedling development of two species of calendula (*C. arvensis* L. and *C. officinalis* L.). In: Wenzel, W.W., Adriano, D.C., Alloway, B., Doner, H.E., Keller, C., Lepp, N.W., Mench, M., Naidu, R., Pierzynski, G.M. (eds). Fifth International Conference on the Biogeochimistry of Trace Elements, Vienne, Austria: pp. 1146–1147

Blum J.D., Dasch A.A., Hamburg S.P., Yanai R.D., Arthur M.A., 2008. Use of foliar Ca/Sr discrimination and ^{87}Sr/^{86}Sr ratios to determine soil Ca sources to sugar maple foliage in a Northern hardwood forest. Biogeochemistry 87: 287– 296

Bonifacio, E., Falsone, G. & Catoni, M., 2012. Influence of serpentine abundance on the vertical distribution of available elements in soils. Plant Soil 368: 493–506

Bonifacio, E., Zanini, E., Boero, V., Franchini, A.M., 1997. Pedogenesis in a soil catena on serpentinite in Northwestern Italy. Geoderma 75:33–51

Bonnand P., James R.H., Parkinson H.J., Connelly D. P., Fairchild I.J., 2013. The chromium isotopic composition of seawater and marine carbonates. Earth and Planetary Science Letters 382: 10–20

Brantley, S.L., White, T. S., White, A. F.., Sparks, D., Richter, D., Pregitzer, K., Derry, L., Chorover, Chadwick, O., April, R., Anderson, S., Amudson, R., 2006, Frontiers in Exploration of the Critical Zone: Report of a workshop sponsored by the National Science Foundation (NSF), October 24-26, 2005, Newark, DE, 30p.

Brantley, S. L., Goldhaber, M. B., Ragnarsdottir, K. V., 2007. Crossing disciplines and scales to understand the Critical Zone. Elements 3: 307–314

Breemen, van, N., Driscoll, C. T. and Mulder, J., 1984. Acidic deposition and internal proton sources in acidification of soils and waters. Nature 307: 599–604

Breemen, van N. & Oeveren, van H., 1989. Calcium cycling in an oak-birch woodland on soils of varying CaCO3 content. Plant and Soil, Vol. 120**:** 253–261

Brimhall G.H., Dietrich W.E., 1987. Constitutive mass balance relations between chemical composition, volume, density, porosity, and strain in metosomatic hydrochemical systems: Results on weathering and pedogenesis. Geochimica et Cosmochimica Acta 51: 567-587

Brimhall, G.H., Chadwick, O.A., Lewis, C.J., Compston, W., Williams, I.S., Danti, K.J., Dietrich, W.E., Power, M.E., Hendricks, D. & Bratt, J., 1991. Defformational mass trasnport and invasive processes in soil evolution. Science 255: 695–702

Brooks, R.R. 1987. Serpentine and its Vegetation: A Multidisciplinary Approach. Dioscorides Press, Portland, OR, USA: pp. 514Burton, W., Morgan, E., 1983, The

influence of heavy metals upon the growth of Sitka spruce in South Wales forests, I. Upper critical and foliar concentrations. Plant and Soil, Vol. 73: 327-336

Burt, R., Filmore, M., Wilson, M. A, Gross, E.R., Langridge, R.W., Lammers, D.A., 2001. Soil properties of selected pedons on ultramafic rocks in Klamath Mountains, Oregon. Comm Soil Sci Plant Anal 32:2145–2175

Chardot, V., Echevarria, G., Gury, M, Massoura, S., Morel, J.L., 2007. Nickel bioavailability in an ultramafic toposequence in the Vosges Mountains (France). Plant Soil 293:7–21

Coleman, R.G. 1971. Petrologic and geophysical nature of serpentinites. Geological Society of America Bulletin 82:897–918

Davies, T., Fearn, T., 1996. Quality control of reference analytical data: How not to fool yourself. Spectrosc. Eur. 8: 36-39

Fendorf, S.E ., 1995. Surface reactions of chromium in soils and waters. Geoderma 67:1–2: 55–71

Frausto da Silva, J. J. R and Williams, R. J. P., 1991 The Biological Chemistry of the Elements: The Inorganic Chemistry of Life, Oxford University Press, pp. 575

Gasser, U. G., Juchler, S. J., Sticher, H., 1994. Chemistry and speciation of soil water from serpentinitic soils: importance of colloids in the transport of Cr, Fe, Mg and Ni. Soil Sciences 158:5: 314–322

Goldhaber, M.B., 2004. Sulfur-rich sediments. In: Mackenzie, F.T. (Ed.). Sediments, diagenesis, and sedimentary rocks. Treatise on Geochemistry. Elsevier, Amsterdam, pp. 257–288

Goldschmidt, V. M, 1937. The principles of distribution of chemical elements in minerals and rocks. J Chem Soc 140:655– 673

Heimsath, A.M., Dietrich, W.E., Nishiizumi, K., and Finkel, R.C., 1999. Cosmogenic nuclides, topography, and the spatial variation of soil depth. Geomorphology 27: 151–172

Hostetler, P.B., R.G. Coleman, F.A. Mumpton, and B.W. Evans. 1966. Brucite in alpine serpentinites. American Mineralogist 51:75–98.

Hruška, J., Krám, P., 2003. Modelling long-term changes in stream water and soil chemistry in catchments with contrasting vulnerability to acidification (Lysina and Pluhuv Bor, Czech Republic). Hydrol. Earth Syst. Sci. 7: 525–539.

Ilyin V.B.,1991. Heavy metals in the soil and plant system. Nauka, Sibir. Dpt., Novosibirsk:pp: 151 // Ильин В. Б., 1991. Тяжелые металлы в системе почва-растение.Наука. Сиб. отд-ние: 148 с.

Jobbagy E.G., Jackson R.B.. 2001. The distribution of soil nutrients with depth: global patterns and the imprint of plants. Biogeochemistry 53: 51-77 .

Jobbágy .EG., Jackson R.B., 2004. The uplift of soil nutrients by plants: biogeochemical consequences across scales. Ecology 85:2380–2389

Kabata-Pendias, A., and H. Pendias. 2001. Trace elements in soil and plants, 3rd ed. CRC Press, Boca Raton, Florida, USA: pp 671

Kazakou, E., Dimitrakopoulos, P.G., Reeves R.D., Baker, A.J.M., Troumbis, A.Y., 2008. Hypotheses, mechanisms, and trade-offs of tolerance and adaptation to serpentine soils: from species to ecosystem level. Biological Reviews 83:495– 508

Krám P., Oulehle F., Štedrá V., Hruška J., Shanley J. B., Minocha R., Traister E., 2009. Geoecology of a forest watershed underlain by serpentine in Central Europe. Northeastern Naturalist, 16, Spec. 5: 309–328.

Krám, P., Hruška, J. and Shanley J.B., 2012. Streamwater chemistry in three contrasting monolithologic Czech catchments. Applied Geochemistry 27: 1854-1863

Krám, P., Hruška, J., Wenner, B.S., Driscoll, C.T., Johnson, C.E., 1997. The biogeochemistry of basic cations in two forest catchments with contrasting lithology in the Czech Republic. Biogeochemistry 37: 173–202

Krám, P., Myška, O., Čuřík, J., Veselovský, F., Hruška, J., 2013. Drainage water chemistry in geochemically contrasting catchments. In: Stojanov R., Žalud Z., Cudlín P., Farda A., Urban O., Trnka M. (eds.) Global Change and Resilience From Impacts to Response Conference Proceedings, Global Change Research Centre of the Academy of Sciences of the Czech Republic, Brno, 173-177.

Krám, P., Čuřík, J., Veselovský, F., Myška, O., Lamačová, A., Hruška, J., Štědrá, V., 2014. Hydrologie a hydrochemie dlouhodobě zkoumaného ultrabazického povodí Pluhův bor. In: Šír M., Tesař M. (eds.) Sborník konference Hydrologie malého povodí 2014, Ústav pro hydrodynamiku Akademie věd České republiky, Praha, 238-245.

Larcher W., 2003. Physiological Plant Ecology. 4th Edition. Springer, Berlin: pp. 513

Liberatore, P.A., 1994. The determination of trace elements in geological samples by ICP-AES. Varian Instruments, ICP-AES Instruments at Work series ICP-16.

Lichtner P.C., 1988. The quasi-stationary state approximation to coupled mass transport and fluid-rock interaction in a porous medium. Geochimica et Cosmochimica Acta 52: 143-16

Majer, V., Krám, P., Shanley, J.B., 2005. Rapid regional recovery from sulfate and nitrate pollution in streams of the western Czech Republic – comparison to other recovering areas. Environ. Pollut. 135, 17–28.

Markert, B.A., Breure A.M., Zechmeister H.G., 2003. Bioindicators and Biomonitors. Principles, concepts and applications. Elsevier, Amsterdam: pp. 997

McBride, M.B., 1994. Environmental chemistry of soils. Oxford University Press, New York, pp. 406

McGaham, D. G., Southard, R.J., Claassen, V.P., 2009. Plant- available calcium varies widely in soils on serpentinite landscape. Soil Science Society of America Journal 73:2087–2095

McGrath, S P Smith, 1995. Chromium and nickel, Heavy metals in soils, 1995 V 7: 152-178.

McLennan, S. M. and Taylor S. R., 1999, Geochemistry of sediments. In Marshall c. P. and Fairbridge R. W. (eds.), Encyclopedia of geochemistry: Kluwer, Dordrecht, pp. 282-292

Menon M., Rousseva S., Nikolaidis N.P., van Gaans P., Panagos P., de Souza D.M., Ragnarsdottir K.V., Lair G.J., Weng L., Bloem J., Kram P., Novak M., Davidsdottir

B., Gisladottir G., Robinson D.A., Reynolds B., White T., Lundin L., Zhang B., Duffy C., Bernasconi S.M., de Ruiter P., Blum W.E.H., Banwart S.A.. 2014. SoilTrEC: A global initiative on critical zone research and integration. Environmental Science and Pollution Research 21: 3191-3195.

Navarre-Sitchler, A. and Brantley, S., 2007. Basalt weathering across scales. Earth and Planetary Science Letters 261: 321-334

Niskavaara, H., 1995. A comprehensive scheme of analysis for soils, sediments, humus and plant samples using inductively coupled plasma atomic emission spectrometry (ICP-AES). Geological Survey of Finland, Special Paper 20, 167–175

Nolte, J., 2003. ICP Emission Spectrometry: A Practical Guide. Wiley-VCH, Weinheim, Germany: pp. 281, pages

Oze, C., Skinner. C., Schroth, A.W., Coleman, R.G., 2008. Growing up green on serpentine soils: biogeochemistry of serpentine vegetation in the Central Coast Range of California. Appl Geochem 23: 3391–3403

Rad, S., Cerdan, O., Rivé, K., Grandjean, G., 2011. Age of river basins in Guadeloupe impacting chemical weathering rates and land use. Appl. Geochemistry 26: 123–126

Pape, T., van Breemen N, van Oeveren, H., 1989. Calcium cycling in an oak-birch woodland on soils of varying $CaCO_3$ content. Plant Soil 120: 253–261

Raymo, M.E., Ruddiman, W.F., and Froelich, P.N., 1988. Influence of late Cenozoic mountain building on ocean geochemical cycles. Geology 16: 649–653.

Raymo, M.E., and Ruddiman, W.F., 1992. Tectonic forcing of late Cenozoic climate. Nature 359: 117–122

Reynolds, R., Neff, J., Reheis, M., Lamothe, P., 2006. Atmospheric dust in modern soil on aeolian sandstone, Colorado Plateau (USA): variation with landscape position and contribution to potential plant nutrients. Geoderma 130: 108–123

Reimann C, de Caritat P., 1998. Chemical elements in the environment—factsheets for the geochemist and environmental scientist. Springer-Verlag, Berlin, Germany pp. 397;

Reimann C., 2005. Sub-continental-scale geochemical mapping: sampling, quality control and data analysis issues. Geochem Explor Environ Anal 5: 311-323

Rosenbloom, N.A., Anderson, R.S., 1994. Hillslope and channel evolution in a marine terraced landscape, Santa-Cruz, California. Journal of Geophysical Research 99B: 14013–14029

Ure, A. M. and Berrow M. L., 1982. The elemental constituents of soils. In Bowen H.J.M. (ed.), Environmental Chemistry, Vol. 2, Royal Soc. Chem., London: pp. 94-204.

Schaetzl R, Anderson S., 2005. Soils: genesis and geomorphology. Cambridge University Press, New York, 817 p.

Sharma, D. C.; Chatterjee, C. and Sharma, C. P., 1995. Chromium accumulation by barley seedlings (Hordeum vulgare L,). Journal of Experimental Botany 25: 241-251.

Singh, H.P. , Mahajan, P., Kaur, S., Batish, D.R., Kohli, R.K., 2013. Chromium toxicity and tolerance in plants (Review). Environmental Chemistry Letters: 11: 3: 229-254

Sleep, N.H., A. Meibom, T. Fridriksson, R.G. Coleman, and D.K. Bird. 2004. H_2-rich fluids from serpentinization: Geochemical and biotic implications. Proceedings of the National Academy of Science USA 101:1218–1223

Soane, B.D., Saunder, D.H., 1959. Nickel and chromium toxicity of serpentine soils in Southern Rhodesia. Soil Sciences 88: 322–330

Somerfield, P. J, Ge, J. M., Warwick R. M.,1994. Soft sediment meiofaunal community structure in relation to a long-term heavy metal gradient in the Fal estuary system, Marine Ecology Progress Series, 105: 79-88

Stallard, R.F., 1985. River chemistry, geology, geomorphology, and soils in the Amazon and Orinoco basins. In: Drever, J.I. (ed.), The chemistry of weathering: Dordrecht, Netherlands, D. Reidel Publishing Company, pp. 293–316

Suzuki, S., Mizuno, N, Kimura, K.,•1971. Distribution of heavy metals in serpentine soil. Soil Science and Plant Nutrition 17:5: 37–41.

Turner, M.A. and R.H. Rust. 1971. Effects of Cr on growth and mineral nutrition of soybeans. Soil Science Society of America Journal 35: 755-758.

Warda, A. F., Marcielloa, L. F., Carraraa, L. and Lucianoa, V. J., 1980. Simultaneous determination of major, minor, and trace elements in agricultural and biological samples by Inductively Coupled Argon Plasma Spectrometry. Spectroscopy Letters: 13: 803-831

Wedepohl, K. H., (Ed.) 1978. Handbook of geochemistry, elements Cr (24) to Br (35), v. II/3: New York, Springer-Verlag, 70 p

Weeks, M. E., 1932. The discovery of the elements. III. Some eighteenth-century metals. J. Chem. Educ., 9 (1): 22

White AF, Brantley SL (eds), 1995. Chemical Weathering Rates of Silicate Minerals. Mineralogical Society of America Reviews in Mineralogy 31; 584 pp

Internet sources

CHEMIASOFT, 2014, online: http://www.chemiasoft.com/chemd/node/52

de la Roche, H., Govindaraju K., 1967. Rapport sur deux roches diorite DR-N et serpentine UB-N proposées comme étalons analytiques par un groupe de laboratoires français. Centre de Recherches Petrographiques et Geochimiques CNRS B.P. Bulletin de la Société Française de Céramique 85. Online: http://georem.mpch-mainz.gwdg.de/sample_query.asp

De Vos W., Tarvainen T., 2006, Geochemical Atlas of Europe, Part 2: Calcium, online: http://weppi.gtk.fi/publ/foregsatlas/text/Ca.pdf

De Vos W., Tarvainen T., 2006, Geochemical Atlas of Europe, Part 2: Chromium, online: http://weppi.gtk.fi/publ/foregsatlas/text/Cr.pdf

De Vos W., Tarvainen T., 2006, Geochemical Atlas of Europe, Part 2: Potassium, online: http://weppi.gtk.fi/publ/foregsatlas/text/K.pdf

De Vos W., Tarvainen T., 2006, Geochemical Atlas of Europe, Part 2: Magnesium, online: http://weppi.gtk.fi/publ/foregsatlas/text/Mg.pdf

De Vos W., Tarvainen T., 2006, Geochemical Atlas of Europe, Part 2: Nickel, online: http://weppi.gtk.fi/publ/foregsatlas/text/Ni.pdf

De Vos W., Tarvainen T., 2006, Geochemical Atlas of Europe, Part 2: Potassium, online: http://weppi.gtk.fi/publ/foregsatlas/text/K.pdf

I-Think, 2013, Chromium, online: http://www.i-think.ru/wikimet/?type=metall&section_id=301

I-Think, 2013, Nickel, online: http://www.i-think.ru/wikimet/?type=metall&section_id=373

Nickel Institute, 2013, online: http://www.nickelinstitute.org/NickelUseInSociety/AboutNickel/NickelMetaltheFacts/DidYouKnowCartoons/Cartoon2.aspx]

Robertson, S. 1999: BGS Rock Classification Scheme, Volume 2: Classification of metamorphic rocks. British Geological Survey Research Report, RR 99-02. online: https://www.bgs.ac.uk/downloads/start.cfm?id=8

Thesaurus of Cultural Heritage Computing at the University of Salzburg, 2014, Simplified Petrography, online: http://chc.sbg.ac.at/sri/thesaurus/node.php?id=42

Salminen. R., 2005, Geochemical Atlas of Europe, Part 2, Sample preparation and analysis. online: http://weppi.gtk.fi/publ/foregsatlas/article.php?id=3

Stefan Smidt, Robert Jandl, Heidi Bauer, Alfred Fürst, Franz Mutsch, Harald Zechmeister and Claudia Seidel, 2012. Trace Metals and Radionuclides in Austrian Forest Ecosystems, The Biosphere, Dr. Natarajan Ishwaran (Ed.), ISBN: 978-953-51-0292-2, InTech, online: http://www.intechopen.com/books/the- biosphere/trace-metals-in-austrian-forest-ecosystems

Stoffer and Messina, 2002, Field-Trip Guide to the Southeastern Foothills of the Santa Cruz Mountains in Santa Clara County, California, USGS/NPS Geology in the Parks Website: USGS Open-File Report 02-121, online: http://vulcan.wr.usgs.gov/LivingWith/VolcanicPast/Notes/serpentine.html

UNEP, 2014, The Black Triangle, online: http://na.unep.net/atlas/webatlas.php?id=7Weigel H.J., Helal H.M., 2001., Schwermetalle. In: Guderian R., (Ed.), Terrestrische Ökosysteme. Wirkungen auf Pflanzen, Diagnose und Überwachung, Wirkungen auf Tiere: 101-148 online: http://bfw.ac.at/peter/wlv.txt?keywin=1565

WHO (World Health Organization), 1996. A Model for Establishing Upper Levels of Intake for Nutrients and Related Substances, online: http://www.who.int/ipcs/highlights/full_report.pdf?ua=1

Other sources

Agilent Technologies, Inc., 2010. Technical description: Flexible. Productive. Robust.AGILENT 720/730 SERIES ICP-OES Agilent Technologies, Inc. Printed in U.S.A. 5990-6497EN

Anonymous. 2008. Directive 2008/105/EC of the European Parliament and of the Council of 16 December 2008 on environmental quality standards in the field of water policy. Offi cial Journal of the European Union L 348:84–97

Garofalo, P., 2014. Lectures for **Petrography (00799),** BiGeA Department, of the BiGeA Department, Bologna university

Gribovsky Yu. G./Грибовский Ю.Г., 2000. Научное обоснование комплекса мероприятий по снижению отрицательного влияния никеля на организм домашних животных и санитарное качество продуктов животноводства в природно-техногенных провинциях Урала: Doctoral Dissertation, Troitsk, УГИВМ/Troitski University of Veterinary: pp. 344.

Hoobin D. and Vanclay, E., 2011. Ultra-fast ICP-OES determinations of soil and plant material using next generation sample introduction technology, Application note, Agriculture, Agilent Technologies, Inc. Melbourne, Australia Publication number: 5990-7917ENAgilent Technologies
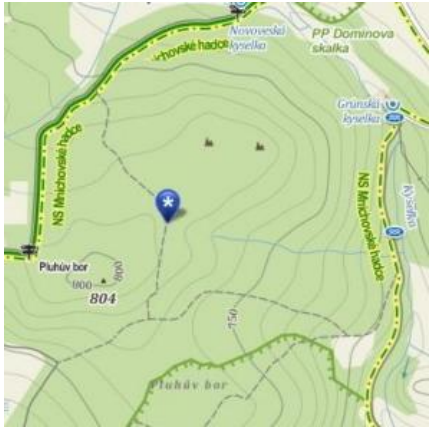
Pavlov, V.A., 1988. Territorial Geological Fund № 5214: Report on the results of ecological and geological mapping of the western part of the Murmansk region in the area 82,570 square kilometers at 1:1000000 scale in 1995-97 yy. JSC "Central Kola Expedition" Monchegorsk, Murmansk region., 1998/ Павлов, В.А, 1988, № ТГФ

(Территориальный геологически фонд) 5214: Отчет о результатах эколого-геологического картирования мас-штаба 1:1000000 западной части Мурманской области на площади 82570 кв.км в 1995-97 г.г. ОАО "Центрально-Кольская экспедиция" г. Мончегорск Мурманской обл.

Solovyov A. I., 2003. Technologenny ad. Zerkalo nedeli 40: 465 Kyiv/Соловьёв А. И. Техногенный ад. // Зеркало недели 40/465-2003. Киев]

Suarez Bilbao, S., Garcia F. N., Roldan, F. V., 2008. Serpentine As a Natural Nickel scavenger in Weathering Profiles of the Aguablanca Ni-Cu-(PGE) Deposit (Spain). A SEM and HRTEM Study. In Suárez et al., Macla 10 (ed.), Resumen WORKSHOP 2008: 142-144

Appendix

<table>
<tr>
<td rowspan="2" colspan="2">**ČGS**</td>
<td colspan="4">Preliminary geological documentation of drill
Project: **SoilTrEC č. 667500**   Name of the drill core: **PB-V1**
List: **1**</td>
</tr>
</table>

Loction	Inlet of the shaft	Yield of the core	List mapy: 11-233
Pluhův Bor, ML	**X** 50°03.778´N	99 %	**Schematic location**
Executor	**Y** 12°46.619´E	**Outflow of water**	
SG IGHG Tachlovice	**Z** 801 m	No	
Type of technical means used	**The diameter of the borehole (mm)**	**The loss of water**	
ADBS, Mercedes Benz Atego	175 for the upper part of borehole, 89 mm for the lagging, 76 mm for the rest of borehole	No	
Dates, start-end	**borehole type:**	**The depth of the borehole:**	
29.-30.8.2012	vertical core	26.14 m	
Responsible	**Documented by**	**Date of photodocumentation**	
Marek Topinka	Veronika Štědrá	29.-30.8.2012	

Photo of core (cca 1 : 10)	Depth from(m)	Field description	Petrology, mineralogy	Samples
	0,0 ◉ 170 mm	Organic soil and brown-gray soil	Organic matter + soil,	
	0,10	residual clays with soil and serpentinite fragments, heterogeneous mixture	Serpentinite + soil + reziduum	
	1,20	grey green clayei to snady residuum with fragments of S	clayey serpentinite + residual mixture	
	1,90	Stony residuum	stony residuum of serpentinite	N 2,59
	3,60	in situ weathered fragments of S	fully serpentinized peridotite with grains and veinlets of secondary magnetite	►4,50 GCH 4,50 N 4,04+ H 3,73

106

	Description	Rock type	
5,0 ◙76mm	fragments of altered S, with yellowish alterations with chlorite, possibly also talc	altered serpentinite in fragments	
5,20	core enriched in Fs	Serpentinite	
5,45	fragments and pieces of brecciated amphibolized serpentinite matrix	Serpentinite	
5,65	intensely altered shear zone light creamy colour, chloritized	Def./shear zone	
5,80	homogeneous S, core and pieces, chloritized, black matrix	Serpentinite	
6,10	gragments and melt of Amphibolite with Fs	Fs melt	
6,22	light alterexd layer Fs-Tc, dip 20–25° with Fs band up to 2,5 cm	Fs melt	
6,43	Serpentinite of light greenish colour of crashed rock, sheared, deformed, brecciated with ultramafic alterations, loss of core.	Serpentinite	
7,0	black amphibolite, Act schist with rare bands of white Fs, vertical veinlet with white Fs up to 1,5 cm.	AMF	H 7,33
7,37	Crashed rock and fragments, Fs-Chl-Tc shear zone.	Def./shear zone	
7,57	Core: fine grained dark black to gray rock with fine layering, up to 11 mm, discrete lenticular Fs.	AMF	
7,65	transition of finegrained blackish Amphibolite (Actinolite schist) to medium grained recrystalized mobilisate with Chl and altered Fs	Tremolite schist with Mg-rich minerals and Mg-Chl (tremolitite)	►7,80 GCH 7,85

8,0	def. altered rock, with pseudomorph aggregates after precursor mineral up to 2 cm in size, average up to 8 mm, clastic fabric. with Fs and Chl, light green to creamy	AMF	
8,15	green to black dark rock with Chl/Serp flakes up to 5 mm	metabasite	
8,80	a band with Fs augens in dark matrix, cross vein with Fs dipping 65° and thick up to 2 cm, light whitish to creamy colour.	Fs melt	
8,86	homogeneous black core	homogeneous dark metabasite	
9,27	crashed rock with yellow to rusty Fe alteration	Def./shear zone	
9,35	in places banded amphibole-rich rock with Fs veinlets, in parts fine-grained lenticular Fs in the matrix	AMF	
9,84	homog. black hazely banded ultrabasic rock	AMF	
10,09	pale green altered vein of recrystallized pyroxenite to tremolite schist, with younger deformed with dip 20°	Tremolite schist (metabazite)	►10,15 GCH 10,20 N 10,60
10,21	blackgreen core with irregular Fs veinlets	Actinolite schist (metabazite)	►11,60 GCH 11,65
11,67	heavily crashed	metabasite	
11,90	core, dark fine-grained blackish rock	metabasite	
12,0	crashed, altered white-yellow fine to medium-grained, foliated under angle 10°	Def./shear zone	
13,05	core, black-green fine-grained rock	metabasite	
13,75	core folded with small lentils of Fs and flaky dark Chl-Serp aggregates	Def./shear zone	

	14,50	crashed core with Act, Amph and Fs lenticular aggregates up to 1 mm in thickness	Def./shear zone	
	14,60	Serpentinite, core	metabasite	
	14,80	crashed zone	Def./shear zone	
	14,85	core, blackish coloured rock	metabasite	
	15,15	cca 2 cm thick irregular vein of Fs-Qtz, dip up to 10°	Fs melt	
	15,17	core, blackish coloured rock	Tremolite schist (Mg-rich metabazite)	>15,40 GCH 15,30
	16,08	Lighter, with lenses of pink feldspar aggregates of the size about 1.5 cm, matrix with gray-green colouring	intermediate AMF with younger Act in the melt	
	16,18	Greenish „meta-dolerite"	greenish amphibolized metadolerite	
	16,30	Shear zone with feldspar vein (5 mm), inclination of 10 degrees, composition dominated by chlorite, talc, actinolite; transition to amphibolitic zones with feldspar, chlorite and serpentine	Def./shear zone	
	16,85	deformed zone	Def./shear zone	
	16,90	recrystalized deformed metabasic rock	Actinolite schist METABASITE	►17,10 GCH 17,05
	17,15	Fs vein dipping under 45°, thickness up to 1 cm, younger and discordant with respct to alignment and refoliation	Fs melt	
	17,18	Augen-textured amphibolite	AMF (or metagabbro) with Pl phenocrysts and younger cracks	►17,60 GCH 17,50 N 17,58

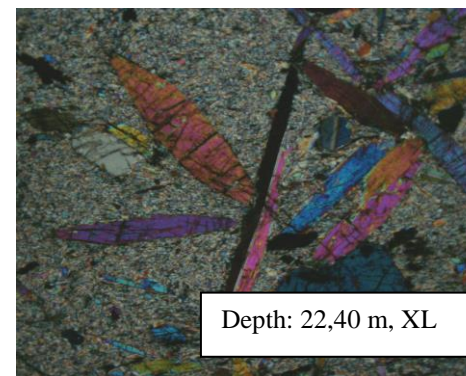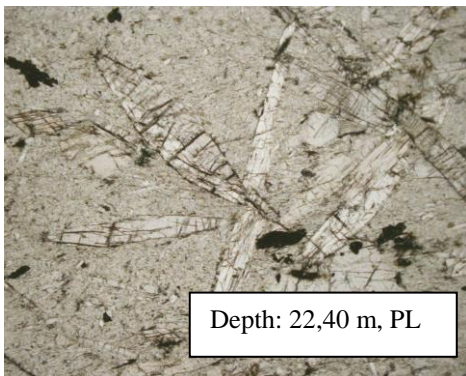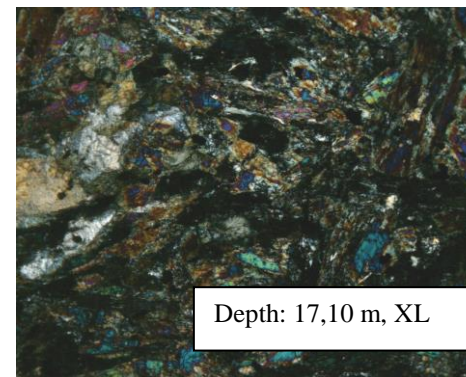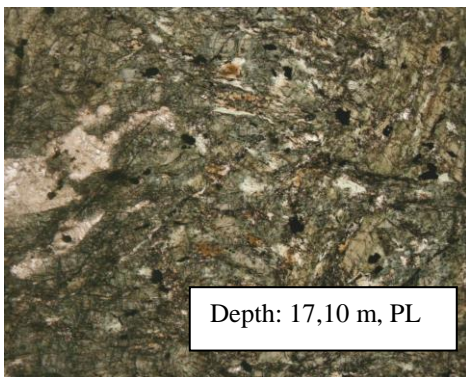|	Depth	Description	Interpretation	Marker
	17,85	strongly deformed laminated layer with limonitization, terminated by Ep-Act aggregate of green-schist type	Def./shear zone	H 18,10
	18,18	core, massive dark rock with Fs veinlets	ULTRA/METABASITE	
	18,90	def. laminated zone with greenish white Fs-Ep vein dipping under 60°	AMF with a vein	
	19,17	Augen-like layers of pinkish Fs in finely laminated amphibolite	laminated AMF with felsic schlieren	
	19,53	well expressed shear zone with coarse.grained flakes of Mg-rich micaand crystals of black Act, with brown limonite spots, possibly with orthoamphibole and talc (Tc)	UB: Def./shear zone, strongly deformed tremolite-rich filling of the shear zone (Tr-Tc schist)	►19,60 GCH 19,55
	19,64	soft tectonic clay, Tc + micas + Chl	Def./shear zone	
	19,69	blackish ultramafic rock	METABASITE	
	19,82	clay crack at 19,74 m, dark rock	clay tectonic zone in dark metabasite	
	19,85	dark rock, with lenticular porphyroclasts of Fs up to 0,5 cm	black metabasite with Fs lenticular augens	
	20,16	finely banded Amphibolite with ptygmatic folds in Fs veinlets up to 1 mm	coarse-grained Amp-rich melt, with Ru inside the Ilm aggregates,	►20,25 GCH 20,30
	20,65	homogenneous coarse-grained amphibolite	metabasite	
	20,90	Amphibolite with Fs bands, deformed: folding plus fine ptygmatic deformation along fold cleavage planes, dip of cleavage approx. 30°	fine-grained banded AMF	►21,30 GCH 21,35
	21,88	irregular Czo-Trem creamy veinlet, with cleavage up to 30° and thickness 2,5 cm	Def./shear zone	

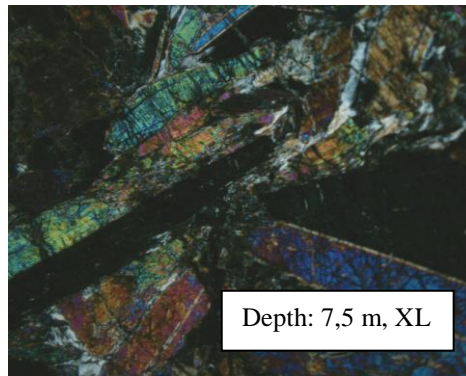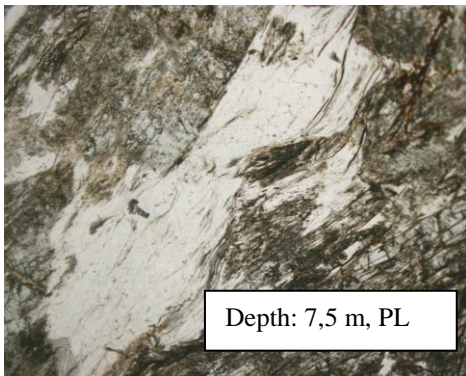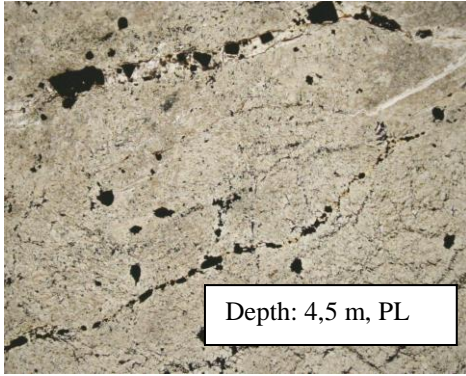|			
21,90	schlieren-like dark blackish amphibolite or ultrabasic rock	METABASITE	
22,26	! discontinuity of oblique foliation planes with clear banding - to horizontal banding with laminar banding in fine-grained gray rock. Weak yellowish alteration towards the contact.	Discontinuity with alteration	
22,32	sudden transition to the homogeneous dark medium to coarse-grained rock	metabasite: talc-rich schist with porphyritic texture and Mg-silicates (metabazite)	►22,40 GCH 22,45
22,44	Fs-Chl layer, dip up to 10°	Fs/Zo-Chl melt	>22,50
22,55	irregular toren contact with medium-grained dark rock, 6 cm lighter, and dark again with flakes of Mg-rich mica	metabasite	
22,76	sharp contact with pale green metamorphosed vein (metapyroxenite)	metapyroxenite Tremolite-chlorite schist with magnetite	►23,10 GCH 23,10
23,17	darker part of the metapyroxenite probably with OAmp and Act	talc-rich metabasite with Mg-amphibole (tremolite/anthophyllite)	>23,22
23,45	almost homogeneous pale green metapyroxenite with black grains of magnetite, remnants of hazy banding, heterogeneous mixture of Ultrabasic rocks and metapyroxenite	metapyroxenite (Tr green schist)	N 23,62 H 23,80
24,15	dark green Mg-amphibolite	AMF	
24,55	micaceous transient zone	talc-rich AMF	
24,72	dark blackish amphibolite	metabasite	
24,78	a shearzone with alteration yellow-green, possibly Chl-Serp	Def./shear zone	
24,90	light green Serp-Chl. mixture	Def./shear zone	

25,0	light green rock with steep 75° refoliation in the secondary minerals, metapyroxenite without magnetite, ends with white band. The colour tint to apple green indicating higher Cr content.	talc-rich tremolite/anthophyllite schist (hornblendite)	>25,10 GCH 25,15
25,17	heterogeneous mixture of micas of dark green colour with amphiboles	Def./shear zone	
25,42	core homogeneous blackish, weakly banded and augen-textured rock, with amphibole	Recrystallized mylonitized amphibolite (metabazite) Hbl-Pl amphibolite with perfect plan-parallel schistosity	►25,50 N 27,58 ►27,70 GCH 27,75
28,00	End of the borehole		

Appendix 1 The detailed description of the conditions of the drill core procedure and the outcomes of visual examination of the mineralogical and petrological characteristics, as provided by Czech Geological

(Abbreviations: *S – serpentinite, Serp – serpentine, Tlc – talc, Act- actinolite, Amph (or Amp) –amphibole, Chl – chlorite, Flds- feldspar, Ep-Epidote, UB-ultrabasic, Ru-rutile, Ilm – ilmenite, Trem-tremolite, Zo-zoisite, Hbl – hornblende, Plag – plagioclase, Orth- orthoclase, Czo - clinozoisite)*

Depth: 4,5 m, PL

Depth: 7,5 m, PL

Depth: 7,5 m, XL

Depth: 17,10 m, PL

Depth: 17,10 m, XL

Depth: 22,40 m, PL

Depth: 22,40 m, XL

Appendix 2 Thin-sections of the samples from the Pluhuv Bor drill core in plane-polarized light (PL) and cross-polarized light (XL)